CANADIAN THESES ON MICROFICHE

I.S.B.N.

THESES CANADIENNES SUR MICROFICHE

National Library of Canada
Collections Development Branch

Canadian Theses on
Microfiche Service

Ottawa, Canada
K1A 0N4

Bibliothèque nationale du Canada
Direction du développement des collections

Service des thèses canadiennes
sur microfiche

NOTICE

The quality of this microfiche is heavily dependent upon the quality of the original thesis submitted for microfilming. Every effort has been made to ensure the highest quality of reproduction possible.

If pages are missing, contact the university which granted the degree.

Some pages may have indistinct print especially if the original pages were typed with a poor typewriter ribbon or if the university sent us a poor photocopy.

Previously copyrighted materials (journal articles, published tests, etc.) are not filmed.

Reproduction in full or in part of this film is governed by the Canadian Copyright Act, R.S.C. 1970, c. C-30. Please read the authorization forms which accompany this thesis.

THIS DISSERTATION
HAS BEEN MICROFILMED
EXACTLY AS RECEIVED

AVIS

La qualité de cette microfiche dépend grandement de la qualité de la thèse soumise au microfilmage. Nous avons tout fait pour assurer une qualité supérieure de reproduction.

S'il manque des pages, veuillez communiquer avec l'université qui a conféré le grade.

La qualité d'impression de certaines pages peut laisser à désirer, surtout si les pages originales ont été dactylographiées à l'aide d'un ruban usé ou si l'université nous a fait parvenir une photocopie de mauvaise qualité.

Les documents qui font déjà l'objet d'un droit d'auteur (articles de revue, examens publiés, etc.) ne sont pas microfilmés.

La reproduction, même partielle, de ce microfilm est soumise à la Loi canadienne sur le droit d'auteur, SRC 1970, c. C-30. Veuillez prendre connaissance des formules d'autorisation qui accompagnent cette thèse.

LA THÈSE A ÉTÉ
MICROFILMÉE TELLE QUE
NOUS L'AVONS REÇUE

NL-339 (r. 82/08)

Canada

0-315-09051-0

National Library of Canada
Canadian Theses Division
Ottawa, Canada
K1A 0N4

Bibliothèque nationale du Canada
Division des thèses canadiennes

169

56968

PERMISSION TO MICROFILM — AUTORISATION DE MICROFILMER

- Please print or type — Écrire en lettres moulées ou dactylographier

Full Name of Author — Nom complet de l'auteur

CECILIO JAVIER REBOLLAR BUSTAMANTE

Date of Birth — Date de naissance: NOV 26 1946

Country of Birth — Lieu de naissance: MEXICO

Permanent Address — Résidence fixe

ESPINOZA 843, ENSENADA, BAJA CALIFORNIA, MEXICO

Title of Thesis — Titre de la thèse

EARTHQUAKE SOURCE PARAMETER ESTIMATES USING LIMITED DIGITAL SEISMIC DATA

University — Université: UNIVERSITY OF ALBERTA

Degree for which thesis was presented — Grade pour lequel cette thèse fut présentée: Ph.D

Year this degree conferred — Année d'obtention de ce grade: SPRING 1982

Name of Supervisor — Nom du directeur de thèse: EDO NYLAND

Permission is hereby granted to the NATIONAL LIBRARY OF CANADA to microfilm this thesis and to lend or sell copies of the film.

The author reserves other publication rights, and neither the thesis nor extensive extracts from it may be printed or otherwise reproduced without the author's written permission.

L'autorisation est, par la présente, accordée à la BIBLIOTHÈQUE NATIONALE DU CANADA de microfilmer cette thèse et de prêter ou de vendre des exemplaires du film.

L'auteur se réserve les autres droits de publication; ni la thèse ni de longs extraits de celle-ci ne doivent être imprimés ou autrement reproduits sans l'autorisation écrite de l'auteur.

Date: APRIL 5, 1982

Signature

NL-91 (4/77)

THE UNIVERSITY OF ALBERTA

EARTHQUAKE SOURCE PARAMETER ESTIMATES USING LIMITED DIGITAL SEISMIC DATA

by

© CECILIO JAVIER REBOLLAR BUSTAMANTE

A THESIS

SUBMITTED TO THE FACULTY OF GRADUATE STUDIES AND RESEARCH

IN PARTIAL FULFILMENT OF THE REQUIREMENTS FOR THE DEGREE

OF DOCTOR OF PHILOSOPHY

IN

GEOPHYSICS

DEPARTMENT OF PHYSICS

EDMONTON, ALBERTA

SPRING 1982

THE UNIVERSITY OF ALBERTA

RELEASE FORM

NAME OF AUTHOR CECILIO JAVIER REBOLLAR BUSTAMANTE

TITLE OF THESIS EARTHQUAKE SOURCE PARAMETER ESTIMATES USING LIMITED DIGITAL SEISMIC DATA

DEGREE FOR WHICH THESIS WAS PRESENTED DOCTOR OF PHILOSOPHY

YEAR THIS DEGREE GRANTED SPRING 1982

Permission is hereby granted to THE UNIVERSITY OF ALBERTA LIBRARY to reproduce single copies of this thesis and to lend or sell such copies for private, scholarly or scientific research purposes only.

The author reserves other publication rights, and neither the thesis nor extensive extracts from it may be printed or otherwise reproduced without the author's written permission.

(SIGNED) ....

PERMANENT ADDRESS:

CICESE

Espinosa 843

Ensenada Baja Cal. Mexico

DATED March 12 1982

THE UNIVERSITY OF ALBERTA

FACULTY OF GRADUATE STUDIES AND RESEARCH

The undersigned certify that they have read, and recommend to the Faculty of Graduate Studies and Research, for acceptance, a thesis entitled EARTHQUAKE SOURCE PARAMETER ESTIMATES USING LIMITED DIGITAL SEISMIC DATA submitted by CECILIO JAVIER REBOLLAR BUSTAMANTE in partial fulfilment of the requirements for the degree of DOCTOR OF PHILOSOPHY in GEOPHYSICS.

Ed. Nyland

Supervisor

H.A.K. Charlesworth

E. R. Kanasewich

Shri Krishna Singh

External Examiner

Date March 12, 1982

TO MY GRANDFATHER, JOSE BUSTAMANTE ALVAREZ

Abstract

Theoretical models of seismic sources are developed for digital data collected mainly at Edmonton and Mexico city. This thesis uses the first digital data ever recorded for a major earthquake sequence in Mexico and is the first attempt to do a study of source parameters in South West Alberta.

First, source theory and some empirical relationships in seismology are reviewed. Then the source parameters of the aftershocks of the Oaxaca, Mexico earthquake of November 29, 1978, are discussed. The digital data used here was recorded at an epicentral distance of approximately 500 km and is the first to be recorded in a set of permanent telemetering digital seismic stations in central Mexico (RESMAC). These source parameters are compared with those calculated using data recorded by digital stations located above the source region.

The source parameters of the Rocky Mountain House earthquake swarm were studied using data recorded by the Edmonton (EDM) digital station. Even though a typical RESMAC station, and Edmonton station have different amplitude response curves, and the epicentral distances of the events were different, the bandwidth of useful information in both systems was between 0.5 and 7 Hz.

Some events of the Rocky Mountain House earthquake swarm were also studied with a portable digital seismic station. The data obtained from this station was of much higher quality than the data from RESMAC or the Edmonton

digital station. Finally, seismic data related to the local seismicity of South West Alberta recorded at Edmonton since 1970 are used to make tentative conclusions about the present day dynamics of this area.

Acknowledgements

Edo Nyland supervised this work, E.R. Kanasewich provided the data analyzed in chapter four, and contributed considerable much appreciated criticism. T. Garza and C. Lomnitz of IIMAS at UNAM made available the installations at IIMAS, J. Brune, Alfonso Reyes, and Luis Munguia provided access to CICESE-UCSD data. R. J. Wetmiller and the Earth Physics Branch, Department of Energy, Mines and Resources, Ottawa gave advance access to their data on the Rocky Mountain House Earthquake swarm. I am grateful to them all.

I wish to acnowledge the invaluable assistence provided by Bruce McGavin in my search for records of seismicity and for permission to use the fruits of his labor at the Department of Physics of the University of Alberta. He and Panos Kelamis did the field work for chapter four. Charles McCloughan's patient help in decoding Edmonton station data tapes is much appreciated.

I would like to express my gratitude to the staff of the Department of Physics who made my stay as a graduate student a pleasure. Especially I thank my good friend and fellow student Luis Munguia Orosco who helped me with innumerable discussions during the course of this study. I also wish to acknowledge my wife, Margarita (Mayo), for her invaluable understanding and encouragement during this part of our life.

My grandather, Jose Bustamante Alvarez, to whom this thesis is dedicated, has given me financial and emotional support during my career.

This work has been supported by research grants from the Natural Sciences and Engineering Reseach Council of Canada. I acknowledge the support by El Consejo Nacional de Ciencia y Tecnologia de Mexico (CONACYT) by means of a scholarship, and the University of Alberta in the form of a teaching assistanship.

List of Figure Captions

Figure 1....Morphotectonic provinces of Mexico. page 32

Figure 2....The response curve for RESMAC and UCSD-CICESE stations and an index map of the area showing stations in 1978 page 34

Figure 3....Examples of Oaxaca seismograms. page 36

Figure 4....Variation of the spectra with increasing sample length. page 40

Figure 5....Two examples of spectra for events recorded both by CICESE-UCSD and RESMAC stations. page 42

Figure 6....Spectra of the main shock and the first two aftershocks recorded at RESMAC page 46

Figure 7....The two upper spectra show well defined corner frequencies and the two lower spectra are not well defined. page 47

Figure 8....Comparison of the Oaxaca seismic moments with the seismic moments of the Rocky Mountain House earthquake swarm page 50

Figure 9....Seismicity of Western Canada. page 54

Figure 10....Geologic provinces of the Southern Rocky Mountains and locations of some seismic events recorded at EDM, SES, and PNT. page 56

Figure 11....Magnification curve of the short period seismic station, vertical component. page 58

Figure 12....Histogram of number of events from the Rocky Mountain House earthquake swarm recorded at EDM against time with no apparent frequency magnitude relation. page 59

Figure 13....Local events (S-P times of less than 60 sec) recorded at Edmonton station since 1970 page 60

Figure 14....Events recorded at Edmonton from the Rocky Mountain House earthquake swarm, left - complex event, right - simple event. page 61

Figure 15....Theoretical travel time curves for the Alberta model at different depths.The best match of Pg, Sn, and Sg with the theoretical travel time curves was for a source depth of 20 km. page 69

Figure 16....Spectra of typical events. The amplitude of radial and tangential components has been increased in order to plot them together. The spectra were smoothed with a Daniel window -DW- of .2 Hz page 74

Figure 17....Plot of local magnitude, source radii and stress drop. page 77

Figure 18....Comparison of theoretical relationships between M_0 and M_L for a circular fault with our experimental relationship, squares are the moments calculated using Thatcher and Hanks (1973) relation page 79

Figure 19....The location of the Rocky Mountain earthquake swarm. The dash square indicates the seismic locations reported by Wetmiller 1981 an the locations of the digital station. Almost all the locations were near the gas wells page 87

Figure 20....Magnification curves of the digital station at 60 and 120 db. The station was operated at 66 db. page 89

Figure 21....Travel time curves for different depths using Richards and Walker model 1959. Arrows show S-P times of approximately .5 and 1 seconds of typical events. b) Possible deep event c) typical event page 90

Figure 22....Similar events and the spectra of the transverse T and radial component R of the S wave. PZ is the P-wave spectrum calculated from the vertical component, arrows show corner frequencies. page 92

Figure 23....Similar events and the spectra of the transverse T and radial component R of the S wave. PZ is the P-wave spectrum calculated from the vertical component, arrows show corner frequencies. page 93

Figure 24....P-wave spectra of the events of figures 25 and 26. These events show a possible path effect in the corner frequencies; P-wave corner frequencies were usually higher than S-wave corner frequencies page 97

Figure 25....Spectra of the vertical Z, radial R, and transverse T component of the S-wave of the events used in this analysis. Arrows show corner frequencies. Some spectra show possible path inhomogeneities. page 98

Figure 26....Spectra of the vertical Z, radial R, and transverse T component of the S-wave of the events used in this analysis. Arrows show corner frequencies. Some spectra show possible path inhomogeneities. page 99

Figure 27....A comparison of the relation of local magnitude versus seismic moment for deep events detected at EDM and shallow events recorded with the portable digital station. Heavy line is $\log M_0 = 1.3M_L + 16.6$. page 102

Figure 28....Plot of local magnitude versus log of radiated seismic energy. GR is the Gutenber and Richter relationship and TH is the Thatcher and Hanks relationship. page 105

Figure 29....Plot of apparent stress versus stress drop . The heavy line shows Hartzell and Brune 1977 relation for the Imperial Valley. Similar events have a relation of page 110

Figure 30....Location of Snipe, Willmore and McNaughton events and some events located by EPB from the Rocky Mountain House earthquake swarm. Dash are depict maximum S-P time recorded ar EDM equivalent to 120 km page 120

Figure 31....a)Histogram of local seismicity recorded at EDM including RMH earthquake swarm. b) Without RMH earthquake swarm. c) Histogram of some well defined S-P times ar EDM page 130

Figure 32....Local events recorded at EDM. Right, it is an event with S-P=12 sec. Left, it is an event with Sg-Pg=27.3 and Pg-Pn=2.4 and was located by EPB at 51.95N and 115.76W. page 133

Figure 33....Example of the Rocky Mountain House events detected in the analog stations at EDM, SES, and PNT. Some of those seismograms do not show clear phases. page 135

Figure 34....Events with S-P times greater than 40 sec probably coming from the McNaughton lake area. Right event has Sg-Pg=44, Sg-Sn=11.5, and Pg-Pn=7.7 sec. Left event has Sg-Pg=46 and Pg-Pn=11 seconds. page 136

Figure 35....Energy release, cumulative energy release, and strain release from the Rocky Mt. earthquake swarm calculated at EDM since 1976 to 1980 page 139

Figure 36....Evaluation of the b value for the Rocky Mountain House earthquake swarm page 141

Figure 37....A plot of ten first motions in an equal-area projection of the focal sphere showing probable fault orientations (D=Dip and DD=Dip Direction) page 145

Figure 38....Seismograms and spectra of Willmore (Ms=3) and McNaughton (M_1=4.8) events. Upper (Willmore) event show EW and NS saturated components. Bottom (McNaughton) shows the vertical component at EDM page 147

List of Tables

Table 1....Source parameters derived from RESMAC data recorded at Cerrillo. page 37

Table 2....Events recorded at RESMAC and SISMEX stations fifty two hours after the Oaxaca event. page 39

Table 3....RESMAC spectral parameters for diferent values of Q compared with the results from the CICESE-UCSD nearby stations. page 44

Table 4....RESMAC source parameters for Q=500 compared with CICESE-UCSD results. page 45

Table 5....Pg-Pn, Sg-Sn and Sg-Pg phase differences recorded at Edmonton station (N North South and E East West Components) page 62

Table 6....The velocity structure (Richards and Walker 1959) page 66

Table 7....A modified version of the Richards and Walker velocity structure page 68

Table 8....A selection of predicted differential travel times for the modified Richard and Walker model page 68

Table 9....The bounds on the search for feasible models of the velocity structure page 71

Table 10....The only satisfactory models in a suite of 1000 reasonable ones page 71

Table 11....Seismic moment, source dimension, stress drop, and local magnitude of some events of the Rocky Mountain House earthquake swarm page 76

Table 12....Spectral parameters for the events recorded in the portable digital station page 104

Table 13....Comparison of minimum strain energy according to Kanamori 1977 and Radiated seismic energy by Hanks and Thatcher 1972 page 108

Table 14....Active seismic stations in British Columbia and Alberta page 117

Table 15....Events located by Earth Physics Branch of Canada from the Rocky Mountain House area since 1976. page 119

Table 16....Table of all the events recorded at Edmonton from the Rocky Mt. House earthquake swarm page 129

Table 17....Events from the Rocky Mountain earthquake swarm detected at CUM page 132

Table 18....Events recorded at Edmonton with clear S-P times, that fall in the definition of local activity i. e. S-P times of less than 60 sec page 137

Table 19....Table of the seismic stations used in the plot of the equal-area projection of the Willmore earthquake page 142 page 144

Table of Contents

Chapter Page

1. Introduction 1

1.1 The Data Used 4

1.2 Seismic Source Models 6

1.2.1 Studies related to Brune Model 15

1.3 Empirical Relations in Seismology 20

2. Spectra of some Oaxaca Earthquake Aftershocks from RESMAC 28

2.1 Tectonic Background of the Oaxaca Earthquake 30

2.2 The Oaxaca Data Set 31

2.3 Instrumentation 33

2.4 Data Analysis 35

2.5 Source Parameters 43

2.6 Seismic Moment and Local Magnitude Relationship of the Oaxaca Aftershocks 49

2.7 Conclusions 49

3. Focal Depths and source Parameters of the Rocky Mountain House Earthquake Swarm from the digital data at Edmonton 52

3.1 Introduction 53

3.2 Analysis of the Data 55

3.3 Analysis of Refracted Phases 62

3.4 Spectral Analysis 71

3.5 Seismic Moment and Local Magnitude 77

3.6 Conclusions 81

4. Source parameters from shallow events in the Rocky Mountain House earthquake swarm 84

4.1 Digital Recorder 87

4.2 Event Locations 87

4.3 Calculation of the Spectra 93

4.4 Source Parameters and Discussion of the Spectra ...95

4.4.1 Further Field Work 109

4.5 Conclusions 111

5. Other seismicity of South West Alberta and Conclusions 114

5.1 Previous Studies 116

5.1.1 Seismicity in South West Alberta as Seen by Edmonton 121

5.1.1.1 Relation to the Mica Array 129

5.1.2 Summary 130

5.1.3 Energy release and b value of the Rocky Mountain Earthquake swarm 135

5.1.4 The Willmore Earthquake 141

5.2 On the relation of Source Parameters to Tectonics 147

5.2.1 Speculations on Tectonic Implications 148

5.2.1.1 Comments on Quantitative Aspects of Plate Dynamics 151

5.2.2 A Speculation on the Cause of the Rocky Mountain House Earthquake Swarm 153

5.2.2.1 Is There a Relationship to the Athabasca Axis? 156

5.3 Summary of Conclusions 158

6. References 160

7. Appendix 1 177

8. Appendix 2: Program listings 190

1. Introduction

Geophysical data, such as observations made on earthquakes, have been described, only partly facetiously, as of type III; Inaccurate, Incomplete, and sometimes Incorrect. The reason for this lies in the fact that a controlled experiment in earthquake seismology is impossible and that the configuration of observing equipment is only partly designed with basic research in mind. The underlying problem in earthquake seismology is then to analyse Type III data sets and to extract from them scientifically valid conclusions. In this work I investigate 3 such data sets, show that limited conclusions about the nature of the mechanism that generates the events are possible, and that these conclusions have geological implications.

With the exception of California and Japan, earthquakes do not often happen in areas well instrumented to study the response of the earth to this stimulus. Much of our knowledge of these phenomena is thus derived from observations made at a distance combined with models of processes at the source. The verification of the legitimacy of these models and the determination of their free parameters is the concern of observational seismology. The data on which such investigations are based are the records of vibrations induced at various seismic stations around the world by the earthquakes.

Effective analysis of these records is limited by the means available to process the data. Until recently the recording medium for the data was photographic paper. Although it was relatively easy to determine the time of arrival of the wave on such a record a systematic study of the spectral content of the signal was truly painful. Even computer aided digitization schemes required numerous corrections for unfortunate properties of the data recording scheme. Surprisingly, modern versions of the original seismograph, a sharp stylus scratching smoked paper, are still in fairly common use.

The appearance of technology which allowed digital recording of seismic data (see Aki and Richards Section 11.1.2 1980) changed the nature of seismic investigations dramatically. It now became possible to manage, with the aid of computers, very large sets of data. In particular the spectral characteristics and the nature of the radiation pattern from earthquakes could be investigated. The work done on the LASA network (see for example Engdahl et al 1970) is one example of the processing that evolved. Recently the appearance of cheap digital technology has lead to the spread of these techniques from large expensive installations to smaller research operations.

In spite of the developement of technology, the distribution of seismic stations in many parts of the world is far from optimal for investigation of the spectral characteristics of the radiation pattern of seismic events. This does not mean data acquired at such installations is useless, merely that there are limitations to its value.

Since many such installations now exist in the world it is useful to ask not only what observations on these installations tell us about the spectral characteristics of the seismic source, but also to what degree the limited scope of the installation limits the value of its data for such investigations.

I discuss here the analysis of 3 sets of such data. The first objective of the work was to determine in so far as was possible the nature of the source that gave rise to the seismic signal. Clearly understanding of this source must have implications for the physical process causing earthquakes and a second objective was to connect the measured characteristics of the signal to acceptable models of the source. The parameters of these models hopefully will cast some light on the exceedingly complicated process generating seismic events. As a byproduct of the study I came to some conclusions about the relationship between the capabilities of the observing system and the resolution in the source that could be achieved.

Studies of source parameters, such as those reported here, are of great importance in seismology because they can show regional differences in the earthquake generation process. In other words, regional tectonic processes can give rise to variations in the source related parts of the spectra of seismic signals. Evidence of such changes is contained in the radiated elastic wave energy.

One of the more powerful techniques for such studies is the analysis of the spectra of body and surface waves in the near and far field. Study of the spectra in the far-field give us average properties of the source, such as seismic moment (strength of the fault), and average stress drop. On the other hand, the study of near-field spectra gives us details about the rupture process. Such details include complexities of the rupture process, energy focusing, maximum and minimum displacements, and velocities and acelerations as a function of azimuth.

1.1 The Data Used

The data sets I used are

1. The aftershocks of the Oaxaca (November 29, 1978) earthquake as recorded on a digital station 500km from the epicentral zone.
2. The events of a swarm of small magnitude earthquakes near the Canadian Rockies as recorded on a digital/analogue station 180km from the epicentral area.
3. And the records of this same swarm recorded on portable digital seismic recorders above the swarm.

This data constituted a substantial, unexploited digital seismic data set. It originated from **RESMAC** in Mexico and Edmonton station in Canada.

At the end of 1978, when the Oaxaca earthquake occurred, **RESMAC** had only three stations in operation, Cerrillo (CRX), Mexico city (MEX), and Acapulco (ACR). In addition to the RESMAC stations, the SISMEX stations Tonantzintla (IIT), Santa Rita (IIC), and El Pino (IIP), provided additional information. Typically with a limited network of stations, such as this, epicentral locations near the shock cannot be significantly improved. It is possible; however, to do spectral analysis of body waves of the aftershocks of the Oaxaca earthquake, and compare our results with the spectral analysis from the portable digital stations deployed by others above the aftershock area. The results of this study are described in chapter two.

Edmonton is the only permanent station in Alberta that records in analog and digital format in its six components (short and long period), and the only one in Western Canada that records in digital format. It was designed to record teleseismic data (McCloughan and Kanasewich 1974), it records 18 samples per second in the short period and three samples per second in the long period signal. It has an amplitude response curve typical of the World-Wide Standard Seismograph Network.

All useful information from this station is archived on magnetic tapes at the Department of Physics of the University of Alberta. The information recorded at Edmonton from the South West Alberta of the Rocky Mountains and particularly from the Rocky Mountain House earthquake swarm allows a study of this activity. Epicentral locations are generally done by Earth Physics Branch, Department of Energy

Mines and Resources in Ottawa, consequently, in order to improve those epicentral locations a network of stations above the epicentral area is desirable.

I did the spectral analysis of the body waves of the Rocky Mountain House earthquake swarm as observed at Edmonton, in order to investigate the earthquake source, and the analysis of the refracted shear wave Sn in order to calculate focal depths of those events showing clear Sn phases in the digital records.

In chapter four I analyse a fraction of the Rocky Mountain House earthquake swarm recorded on a Spregnether DR-100 digital instrument. The results obtained are far better, and the source parameters are more representative of the active area; However, in order to improve this information more than one station above the earthquake source is necessary. Then it would be possible to obtain fault plane solutions and determine principal stress orientations in this area.

1.2 Seismic Source Models

All these studies explicitly or implicitly require a model of the earthquake source. In general the source model consists of the intuitively reasonable assumption that over a finite surface, the fault plane, within the earth (modelled as perfectly elastic) there exists a discontinuity in displacement. By analogy with usage in solid state physics this is generally known as a dislocation even though the scale of the processes in seismology is much larger and pays no heed to atomic structure. In the more general case there can also be a discontinuity in the traction on the fault plane. The resulting displacements in the model can be calculated using the representation theorem (Aki and Richards 1980 equation 2.41)

$$u_n(\overline{X},t) = \int_{-\infty}^{\infty} d\tau \iiint_V f_i(\overline{\xi},t) G_{in}(\overline{\xi},t-\tau;\ \overline{x},0)\, dV(\overline{\xi})$$

$$+ \int_{-\infty}^{\infty} d\tau \iint_S \Big\{ G_{in}(\overline{\xi},t-\tau;\overline{X},0)\, T_i(\overline{u}(\overline{\xi},\tau),\overline{n})$$

$$- u_i(\xi,\tau) c_{ijk\ell}(\overline{\xi}) n_j G_{kn,\ell}(\overline{\xi},t-\tau;\overline{x},0) \Big\}\, dS(\overline{\xi}).$$

If the size of the fault plane is small compared with the epicentral distance to the detector the displacements can be separated into terms that decay like r^{-1} and terms that decay as higher powers of r (r is the epicentral distance). Displacements that decay like r^{-1} are called far field displacements and terms that decay at higher powers of r are called near field (see Aki & Richards 1980 page 73). One characteristic of the far field is that it can be separated into P and S displacements. In the near field (distances of the order of the fault length) we have mixed P and S body waves.

The problem in source studies is to characterize the time evolution of the discontinuities on the fault plane. Obviously additional physics is needed for there is nothing in the theory that indicates when a discontinuity will appear (an earthquake will start) or when it will stop. Since the physical properties of faults are largely unknown seismologists assume time histories and fit them to spectral properties of the radiated elastic energy or to the actual signal shape as observed on seismographs.

There is a useful simplification of the representation theorem. If we introduce the concept of a moment tensor to describe the source, the representation theorem acquires the form (Aki and Richards 1980 equation 3.22)

$$u_n(\overline{x},t) = \iint_{\Sigma} m_{pq} * G_{np,q} \, d\Sigma$$

In general nine couples (called vector dipoles) are required to obtain equivalent forces for an arbitrary displacement discontinuity in an anisotropic medium. In other words, the equivalent forces corresponding to an infinitesimal dislocation can be represented as a combination of those nine vector dipoles. Those nine dipoles together constitute the seismic moment tensor and have units of moment per unit area (dynes-centimeter). The components of the seismic moment tensor for a constant slip on an infinitesimal fault in cartesian coordinates are given by:

$$M_{xx} = - M_o (\sin \delta \cos \lambda \sin 2\phi_s + \sin 2\delta \sin \lambda \sin^2 \phi_s),$$

$$M_{xy} = M_o (\sin \delta \cos \lambda \cos 2\phi_s + \tfrac{1}{2} \sin 2 \delta \sin \lambda \sin 2\phi_s) = M_{yx},$$

$$M_{xz} = - M_o (\cos \delta \cos \lambda \cos \phi_s + \cos 2\delta \sin \lambda \sin \phi_s) = M_{zx},$$

$$M_{yy} \quad M_o (\sin \delta \cos \lambda \sin 2\phi_s - \sin 2\delta \sin \lambda \cos^2 \phi_s),$$

$$M_{yz} = - M_o (\cos \delta \cos \lambda \sin \phi_s - \cos 2\delta \sin \lambda \cos \phi_s) = M_{zy},$$

$$M_{zz} = M_o \sin 2\delta \sin \lambda$$

Where M_o is the seismic moment, ϕ_s is the strike of the fault, λ is the rake (rake is the angle between strike direction and slip), δ is the dip, and M_{pq} are the components of the seismic moment tensor. The constant term M_o is the static seismic moment and gives us the strength of the fault. The dislocation is a function of time, therefore the seismic moment tensor is also a function of time since it depends directly on the average dislocation along the fault.

The problem of observation interpretation then becomes the calculation of properties of the moment tensor and the further interpretation requires connection of this moment tensor to models of the discontinuities. Steketee (1958), Maruyama (1963), Burridge and Knopoff (1964), Brune (1970,1971), among others developed a general theory for the faulting process in an elastic medium. They assumed that the rebound theory is valid for shallow earthquakes, and calculated the displacements using the representation theorem. Although their work preceeded the formal statement of the moment tensor representation it is easy to derive formulas to connect moments with discontinuities. Excellent reviews of source theory can be found in Archambeau (1968,1975), Ben-Menahem and Singh (1972), Johnson (1979), and Sahay (1980).

Seismologists usually follow either a kinematic or a dynamic approach. In the kinematic approach the earthquake process is specified by the starting size of the discontinuity, the velocity at which slip spreads over the fault, and final dimensions of the region over which the slip has occurred. In the dynamic approach to the earthquake process, the earthquake is modelled as a shear crack. The crack nucleate in a preexisting stress field which causes stress concentrations around the tip of the crack which in turn cause the crack to grow. Time history of the rupture velocity of the crack as well as self-similarity are assumed (If a function $u(x,t)$, the solution of the shear dislocation for example, is a homogeneous function of x, t of degree 1, we say that we have a self-similar solution).

Given such assuptions the wave equation with appropiate boundary conditions outside the source region can be solved by developing a Green's function (see Aki & Richards 1980 sec 4.2). This Green's function can be convolved with the source term in order to obtain P and S displacements.

Clearly such displacements carry information about fault orientation, source strength (seismic moment), and have a directivity pattern or radiation pattern.

Seismologists do not usually have sufficient data to calculate all properties of the seismic moment tensor. Often they are restricted to determining M_0, the seismic moment. Several methods can be used to calculate the seismic moment. Geodetic measurements estimate the average dislocation at infinite periods (D), hence knowing the fault surface, A, (for example from the aftershock area) and assuming the shear modulus (μ), the moment is given by $M_0=\mu DA$. However, a more common method for calculating the seismic moment is from the spectra of the far-field displacement of body waves, surface waves or free oscillations of the earth.

The spectrum of the body waves gives the moment at periods of the order of seconds. Therefore this moment is more affected by anomalies in the spectrum resulting from local complexities of the earth structure which give rise to scattering related energy losses. The moment calculated with long-period surface waves or free oscillation data is less affected by structure complexities, since it is calculated at periods of minutes and hours. Values of M_0 range from about 10^{30} dyne-cm for very large earthquakes to 10^{12} dyne-cm for micro-earthquakes, and 10^{8} dyne-cm for microfractures laboratory experiments in rocks (Aki & Richards page 49).

Observational studies are directed primarily at obtaining the data necessary to either check the theoretical studies or investigate the consequences of interpreting earthquakes in terms of a specified model. This process can be done in two different ways; in the time domain, by adjusting the source parameters until a reasonable agreement is achieved between synthetic and observed seismograms, and in the frequency domain by inferring those characteristics of the spectra such as the long period level, high-frequency asymptote, and corner frequencies, that can be directly related to the source properties.

Brune's model (1970, 1971) follows this last approach. It illustrates both the virtues and difficulties of this problem. The Brune model is simple enough to be a reasonable and tractable representation of some properties of an earthquake. It is in fact remarkably successful. Nevertheless it is by no means a complete description. The properties of an earthquake derived by assuming Brune's model to be correct are best thought of as a more compact and transparent representation of the seismic observations. Their connection to real processes requires further analysis. Perhaps the current state of this science is best illustrated by the undoubted fact that most observations can be fit to such a simple model in spite of its obvious physical deficiencies.

An earthquake source can be modelled (Brune 1970,1971) as a tangential stress pulse applied instantaneously to the interior of a dislocation surface (this implies a nonphysical infinite rupture velocity). The total shear stress available to accelerate the two sides of the fault is the difference between the initial stress and the dynamic frictional stress which is of the opposite sense to the initial stress and always acts to resist the fault slip. If the movement across the fault is such that the shear stress acting across the fault has decreased to the value of the frictional stress (Orowan 1960 see also Pilant 1979 page 392), then the stress drop is equal to the total or effective stress drop, otherwise we have a fractional stress drop. The fractional stress drop is defined by Brune as:

$$\varepsilon = \frac{\sigma_1-\sigma_2}{\sigma} = \frac{\sigma_1-\sigma_2}{\sigma_1-\sigma_f}$$

where σ_1 is the initial stress, σ_f is the dynamical frictional stress, σ_2 is the final stress ($\sigma_2 \geq \sigma_f$) and is the total or effective stress drop.

The moment, source dimension, and fractional stress drop for the proposed model can be related to the spectra of the far-field displacement of an SH body wave. The long period level of the spectrum is proportional to the seismic moment, and the intersection of the long period level and the asymptote at high frequencies defines the corner frequency which is related to the size of the fault. This spectrum corresponds to total stress drop. If we do not have a total stress drop ($\varepsilon < 1$), the long period level of the spectrum is reduced to ε times its value for a total stress drop.

Brune obtained the corner frequency by considering a balance of energy around the dislocation surface. This corner frequency in the spectrum can arise from finite energy flow away from the dislocation surface, from finite rupture velocities or from finite length of the fault. Later, Hanks and Wyss (1972) extended Brune's theory empirically to include P-wave spectra for non-circular faults.

The decrease in the amplitude spectra at high frequencies proportional to ω^{-2} and ω^{-3} was first proposed by Aki (1967). In the Haskell (1964) model falloff is as ω^{-3}. In kinematic models the effect of finiteness and rupture velocity of the source time function introduces a smoothing factor of ω^{-1} at "intermediate" frequencies given by the envelope of sin(X)/X (see Aki and Richards 1980 sec 14.1.5). The effect of finite rise time introduces another factor proportional to ω^{-1}. Thus, the spectra have a flat part at low frequencies, a corner frequency, an ω^{-1} dependence at "intermediate" frequencies, and a ω^{-2} decrease at high frequencies. Asymptotes in the spectra at high frequencies have been observed in the range from 1 to 4.

The spectrum of SH reflects source properties since SH does not suffer conversion of phases at sharp interfaces. However, we need to rotate the horizontal components (NS and

EW) in order to obtain the horizontal components of motion transverse to the azimuth from the epicenter to the station. Corrections applied to SH spectra are: free surface amplification, (for SH this is 2 and for SV it should be calculated, see for example Nutlli 1961), radiation pattern, instrument response, and attenuation, Q (generally taken as independent of frequency).

Other earthquake source models (Haskell 1964, Savage 1972, Dahlen 1974, Burridge 1975) are discussed in the next section, and compared with the observed results obtained with Brune's model.

1.2.1 Studies related to Brune Model

Theoretical models which assume a rupture velocity predict corner frequencies as a function of azimuth (Madariaga 1976, Vargas et al 1980). Theoretical models of long narrow faults predict similar corner frequencies for P and S wave spectra. Models of equidimensional faults predict greater corner frequencies for P waves than those for S waves. Molnar, Tucker and Brune (1973) analysing the spectra of P and S-waves of the aftershocks of the San Fernando earthquake, concluded that their observations were consistent with a model which treats earthquakes as approximately equidimensional.

Savage (1972) comparing the spectra of the Haskell model (1964) with Brune's model found that they have similar relations between the fault dimension and the corner frequency in the displacement spectrum. One of the characteristics of the spectra derived from the Haskell model is that P and S-wave corner frequencies are similar as long as the rupture velocity is subsonic, i. e. with a dislocation velocity less than the S-wave velocity. Later Savage (1974) explained that the Haskell model he considered in 1972 can predict that P-wave corner frequency may exceed the S-wave corner frequency if near-sonic or supersonic rupture velocities are considered. Laboratory experiments along pre-existing shear faults show rupture velocities from 0.25 to slightly excceding shear velocities (Shamina et al 1978, Vinogradov 1978).

Dahlen (1974) also considered a kinematic model in order to explain the observed ratio of P to S corner frequencies obtained using Brune model and later empirically extended by Hanks and Wyss. He assumed that the rupture nucleates at a single point on the fault surface and spread subsonically. He found that the ratio of P to S corner frequencies is less than unity at all points of the focal sphere.

Burridge (1975) modified Dahlen's model for shallow earthquakes in order to analyse the controversial frequency shift of the corner frequency. He considered that the rupture nucleated at some point and began to propagate at the P speed, slowing down in such a way that the initial break governs the high-frequency content of the spectrum. This model predicts that in 70 per cent of the focal sphere the P corner frequency is higher than that of S while in the remaining 30 per cent, S corner frequencies are higher than P corner frequencies. This is more or less in agreement with the observations, see for example Molnar Tucker and Brune (1973).

Brune et al (1979) analysed the effects of bilateral and unilateral dislocation ruptures on the far-field displacements. They found that the pulse shapes are strongly dependent on the azimuth. This is equivalent to different corner frequencies at different azimuths

Tucker and Brune (1977) analysed the spectra of the aftershocks of the San Fernando earthquake using a great variety of instruments at different hypocentral distances. They found events with one and two corner frequencies. Events with a single corner frequency were consistent with faulting confined to about 0.1 sec in time or 500 m in space. About half of the larger events had two corner frequencies which are consistent with an initial rupture that grows during about 2 sec and to about 6 km. They explain the events with two corner frequencies as fore-slip with a high dislocation velocity followed by afterslip with a low dislocation velocity. The calculated stress drops for those events lie between 1 to 300 bars.

Hanks (1981) in a review of 36 source mechanism studies comments,

> "The corner frequency shift is a very common condition of the far-field body wave of earthquakes, with no discernible dependence on earthquake source strength, hypocentral distance, depth, or recording device; and the frequency shift is the manifestation of an intrinsic property of earthquakes, source finiteness."

His conclusions constrain theoretical earthquakes source models. Greater P-wave corner frequencies than S-wave corner frequencies are in general observed. However, there have been some cases of smaller P corner frequencies. This may be due to the analysis of data from a single station which can be affected by complicated local effects (see for example Bakun et al 1976, Rebollar et al 1981).

Fault slips for small events obtained using spectral analysis have been found to vary substantially with the distance at which observations are made. In deep mines they can be several orders of magnitude less than those measured directly (McGarr et al 1979). However, fault slip calculated from spectra of large events usually agrees with geological observations.

Stress drops of the order of kilobars have been found in laboratory experiments on brittle fracture of rocks, while stress drops of natural earthquakes lie in the range of a few bars (1-100). McGarr et al (1979), found that tremors in deep mines appear to be associated with stress drops of the order of 1 kilobar. Consequently, they postulate that a certain amount of stress inhomogeneity is required before failure occurs. This may imply large concentrations of stress in localized regions.

Miyatake (1980a) investigated a three-dimensional dynamic crack model in infinite and semi-infinite homogeneous elastic model using the finite difference method. He considered different strength distributions on the fault and investigated the effect of fault strength on crack propagation. For low strength the shape of the rupture front is elliptic, with a rupture velocity of the order of P along the major axis and with a rupture velocity close to S along the minor axis. Relatively high strengths produce a nearly circular rupture front with a rupture velocity nearly equal to S. For a line barrier in the fault (like that proposed by Das and Aki 1977), he found that the rupture propagated backwards, generating multiple shocks. In the case of random strength distributions on the fault, highly irregular rupture propagation is generated and in some cases unfractured regions remain.

Miyatake (1980b) analysed the near and far field displacement as well as the shape of the spectrum due to different distributions of strength on the fault. He found that complex seismic waves including multiple shocks are generated more by irregular propagation of the rupture than by a complex source time function. The analysis of the spectrum in the near-field shows a variable slope at high-frequencies with almost the same corner frequency for uniform strength, line barrier, block barrier, or random barrier. Far-field spectra also show a variable slope at high-frequencies.

1.3 Empirical Relations in Seismology

It is an implicit assumption in seismology that earthquakes which occur in the same region will have similar source properties. This is true in spite of the fact that there can be a large range of magnitudes in a particular region. This similarity assumption (Aki 1967) implies that relationships might exist between various aspects of the source in the population of all earthquakes in a region. These can be investigated by analysis of statistical distributions of source properties. Various authors have proposed various such relationships. Since the use of larger populations may allow average statements about a source region, and since I use this device in the work that follows, I now review these relationships.

Originally (Richter 1935) the magnitude of an earthquake was empirically related to the maximum amplitude measured in a standard seismograph, the epicentral distance and depth of a local earthquake in California. Evidently this magnitude was related to the energy radiated from the earthquake source. The first attempts to relate local magnitude and energy were given by Gutenberg and Richter (1942, 1956), they also proposed what they called a unified magnitude mb, that is derived from body waves recorded at teleseismic distances.

The usually accepted relationship between local magnitude and energy is $\log(Es)=1.5(Ms)+11.8$, where according to Richter (1956), Ms (surface wave magnitude) is an approximation to local magnitude for shallow earthquakes. (An excellent treatment of the definition of earthquake magnitude is given by Pilant 1979 page 385). Another independent relation given by Bath (1958) is

$$\log(Es)=1.44(Ms)+12.24.$$

Equations that have been used in energy calculations are those obtained by Starr (1928 equation 18) and Knopoff (1958 equation 33). Tsuboi (1956), assuming that shallow earthquakes have a certain voluminal upper limit to support concentrations of stresses, calculated a relation between energy and fault area (cm^2) given by $E=600xA^{1.5}$ (ergs). Pilant (1979), using simple physical considerations, calculated the energy necessary for a crack to return to its original position before rupture, and obtained $Es=(M_0/\mu)\times\eta\bar{\sigma}$, where η is the seismic efficiency $\eta\bar{\sigma}$ is the apparent stress, and μ is the shear modulus.

A theoretical relation between energy and source dimension was calculated by Gibowics (1975), using Randall (1972) expression for the seismic energy $Es=(1/2)\Delta\sigma M_0/\mu$ and Keilis Borok (1959) expression for the seismic moment, $M_0=(16/7)\Delta\sigma r^3$, that is given by

$$\log(Es)=2\log(M_0)-3\log(r)-27.14 \text{ (cgs units)}.$$

With new data and improvement in the understanding of earthquake sources, new empirical relationships between source parameters (seismic moment, source dimension, stress drop) and local magnitude, surface wave magnitude, body wave magnitude and a new earthquake magnitude (M_ω) proposed by Kanamori (1977), have been developed.

The first attempt to relate seismic moment to earthquake magnitude was made by Brune (1968). He also gave a method for calculating the average slip along faults. Wyss and Brune, 1968, analysed the surface waves of thirteen earthquakes in California with local magnitudes ranging from 3.2 to 5.5. They found the relationship: $\log M_0 = 1.4 M_l + 17$.

Thatcher and Hanks (1973) systematically studied source characteristics of Southern California earthquakes with local magnitudes in the range between 2 and 7. They found empirical and theoretical relationships between local magnitude and source parameters. The relationship of seismic moment and local magnitude ($\log M_0 = 1.5 M_l + 16$) was similar to that found by Wyss and Brune (1968). They also showed:

$$M_l = \log(M_0) - 2/3(\log(r)) - 17.8,$$

$$\log(M_0) = 2(M_l) + 14.2 - \log \Delta\sigma \ ,$$

$$\log(2r) = (2/3)M_l + 2.9 - (2/3)\log \Delta\sigma \ , \text{ (cgs units)}$$

for earthquakes with magnitudes from 3 to 7. Here, M_0 (seismic moment) is in dynes centimeters, r (source dimension) is in kilometers and $\Delta\sigma$ is stress drop in bars.

Source dimensions of these events lie between 0.6 to 25 km and stress drops between 0.3 and 200 bars. There is some scatter in their data, therefore, these relationships should be used with caution in other tectonic settings. They are useful in the sense that they can be compared with similar empirical relationships from other tectonic settings.

Randall (1973) combined the spectra of the far-field displacement and the response of the Wood-Anderson seismograph, in order to calculate a set of relations between source parameters and local magnitude. Gibowics (1975) following a similar approach, plotted different theoretical curves of local magnitude against seismic moment as a function of source radius and stress drop. Knowing a given event with M_0 and M_l it is possible to estimate the source radius and stress drop from those curves. As the source radius decreases so does the seismic moment. From the graphical relations of Randall (1973) Gibowics calculated $\log M_0 = M_l + 17.16$, for events with source dimensions less than 500 meters. This relation is similar to that calculated by Rebollar et al (1982a), using Sato-Hirasawa model, for similar source dimensions. Bakun and Bufe (1975) found

$$\log M_0 = (1.52 \pm 0.05) M_l + (16.2 \pm 0.1)$$

for events with magnitudes in the range from 1 to 5 in Central California.

Kanamori and Anderson (1975) found theoretical relations between seismic moment and surface wave magnitude using the Haskell model and assuming similarity conditions, i. e. the ratio of length to the width of the fault (aspect ratio), the ratio of average dislocation to the length of the fault (constant strain drop), and the ratio of the product of risetime and rupture velocity to fault length (constant effective stress or dynamic similarity). Those relationships are: $Ms=\log M_o$ for small earthquakes and short risetimes, $Ms=(2/3)\log M_o$ for earthquakes with magnitudes between 6 and 8, and $Ms=(1/3)\log M_o$ for great earthquakes. Further similarity conditions have been investigated by Ben-Menahem (1976, 1977), and implicitly by Iida and Aki (1972), who included the Mach number, i. e., the ratio of rupture velocity to phase velocity. They also obtain a relation between seismic moment and source area given by

$$\log M_o=(3/2)\log S+\log(16\Delta\sigma/7\pi^{3/2})$$

This is a linear relationship for a constant stress drop. A plot of seismic moment against fault area for published data indicates a constant stress drop between 10 and 100 bars for inter- and intra- plate earthquakes. However, inter-plate earthquakes seems to have stress drops around 30 bars and intra-plate plate events around 100 bars.

Geller (1976) assuming a stress drop of 50 bars obtained

$\log M_0 = Ms + 18.89$ for $6.76 \geq Ms$

$\log M_0 = (3/2)Ms + 15.51$ for $8.12 \geq Ms \geq 6.76$

$\log M_0 = 3Ms + 3.33$ for $8.22 \geq Ms \geq 8.12$

$Ms = 8.22$ for $\log M_0 \geq 28$

However Sato (1979) argues that such detailed relations cannot hold due to the uncertainity of the data. Ohnaka (1978) implicitly assumed the constant strain drop similarity and calculated a linear relation between $\log(M_0 D/L)$ and local and surface wave magnitude for world-wide and California earthquake data (D is average dislocation and L fault length); he obtained

$\log(M_0 D/L) = (1.089 \pm 0.1)Ms + (8.82 \pm 2.05)$ $Ms \geq 5.5$

$\log(M_0 D/L) = (1.88 \pm 0.08)M_L + (9.07 \pm 1.49)$ for $2.0 \leq M_L \leq 6.8$

In fact $M_0 D/L$ is the seismic energy. He defines the "total force drop" as the product of stress drop times the fault area (ΔF), and calculates

$\log \Delta F = (1.07 \pm 0.03)M_L + (12.81 \pm .64)$

Following a different approach Sato (1979), theoretically re-examined the empirical relationships obtained by other investigators, and suggested

$\log S(km^2)=M-4.07$

$\log D(cm)=0.5M-1.4$

$\log M_0(dyne\text{-}cm)=1.5\log S+27.5$

Where M is the earthquake magnitude, S fault area, D the mean dislocation and M_0 the seismic moment. These relations assume a constant strain drop (dynamic similarity), proportionality of seismic moment to seismic energy (constant apparent stress), and the relation $\log T_0=0.5M$ where T_0 the predominant period of particle velocity. He compared results of Utsu and Seki (1954), Berckhemer (1962), Bath and Duda (1964), Chinnery (1969), Kanamori and Anderson (1975), and Ohnaka (1978). He argued that the discrepancy in the coefficients in these relations could be due to the use of different data and uncertainities in the evaluation of source parameters and magnitudes.

Kanamori (1977), considering the saturation problem of earthquake magnitude for great earthquakes with fault lengths greater than 100 km, proposed a new magnitude scale as a function of the strain energy drop (difference in strain energy before and after an earthquake). This scale does not suffer saturation and gives a minimum estimate of the strain energy for a partial stress drop. The strain energy is calculated via the seismic moment, i. e. $E_0=(\Delta\sigma/2\mu)M_0$, and the magnitude is calculated using the Gutenberg and Richter energy relation given by $\log E_0=1.5M\omega+11.8$. Singh and Havskov (1980) calculated relationships between $M\omega$ and seismic moment, according to whether they are intraplate or interplate events. They suggest

$M\omega=(2/3)\log M_0-10.73$ for interplate events

$M\omega=(2/3)\log M_0-10.46$ for intraplate events

$M\omega=(2/3)\log M_0-10.57$ if all events are grouped together

These magnitudes are close to Ms for earthquakes with fault lengths less than 100 km.

In the next 3 chapters I examine digital data detected, mainly from one single station at distances of 515 km, 180 km, and above the source 6 km in the light of these proposed empirical/theoretical relations. Obviously data from a single station can give biased results, but studies from ideal networks are generally rare for economic reasons. In the next chapters I argue that it is possible to have good results from single station data, however, more stations are always desirable (see also for example Bakun et al 1976, and Pearson 1981 for other studies using a single station).

2. Spectra of some Oaxaca Earthquake Aftershocks from RESMAC

This chapter is based on a published paper (Rebollar and Nyland 1980).

The Oaxaca earthquake of November 29, 1978, (Ms=7.8, 16.07N, 96.48W) yielded an opportunity for detailed study of an earthquake in a subduction zone. This is the first earthquake in Mexico recorded with a great variety of instruments in the near and far field both before and after the main event. This event had been forecast in a gap (Ohtake et al 1977), and later trapped (Ponce et al 1978).

Although the network that trapped the event (Ponce et al 1980) consisted of smoked paper recorders, five telemetering stations a combination of RESMAC (Lomnnitz and Gil 1976) and SISMEX (Prince et al 1973) were recording digitally at a distance of about 500 km from the epicentral area. Since November 15, 1978, the recording system for this group of telemetering seismic stations in Mexico had been in a final testing stage.

RESMAC stands for "Red Sismologica Mexicana de Apertura Continental". The RESMAC system was planned to cover all of Mexico. All the events are sent by microwave signals to IIMAS at "Universidad Nacional Autonoma de Mexico (UNAM)". The main task of the system will be to provide quick access to data for earthquakes in Mexico to Mexican and other investigators. It will be functioning in event detection mode. The RESMAC system also acquires data from the SISMEX network operated by "Instituto de Ingenieria" (II). SISMEX

(Prince et al, 1973) supplied data from three of their stations, Santa Rita (IIC), Tonantzintla (IIT), and El Pino (IIP).

Two days after the occurrence of the Oaxaca earthquake seven portable digital stations were deployed by "Centro de Investigacion Cientifica y Educacion Superior de Ensenada" (CICESE) and the University of California at San Diego (UCSD). This was a joint project between CICESE and UCSD. This network was operated from December first of 1978 to late April of 1979 (Munguia et al 1979). Several hundred events were recorded. Those aftershocks are being analysed by L. Munguia at UCSD as part of his PhD thesis at UCSD (personal communication).

The data acquired for the Oaxaca Earthquake of 1978 illustrates quite well the difficulties inherent in the collection of seismological data. Clearly the data has deficiencies, but just as clearly it is the best available data, particularly for the first 3 days of the aftershock sequence when there was only a very small operation monitoring aftershocks in the aftershock zone. An understanding of the behaviour of the aftershocks of this very large earthquake (in fact the largest world wide of 1978) is crucial to untangling the physical properties of fault zones.

S-wave spectra of the main event and 21 aftershocks have been calculated. Due to the bandwidth of the RESMAC system, the corner frequency of the shear wave spectrum of the main event is not observed. I do see two slopes at high frequencies (-2.0 and -2.8) intersecting at a frequency of 1.4 Hz. Comparison of the spectra of aftershocks with those obtained from the nearby portable digital stations shows a shift of corner frequency to the lower frequencies, typically of the order of 0.3 hz and in general, a smaller value, typically 4.3 smaller, for the seismic moment. The corner frequencies of the P-wave spectra are outside the observed frequency band. A magnitude-moment relationship given by $\log M_0 = 1.3M_l + 16.6$ was found. This relationship is the same calculated in chapter 3 for events of the Rocky Mountain House earthquake swarm and illustrates a similarity between inter and intra plate earthquake generating processes.

2.1 Tectonic Background of the Oaxaca Earthquake

Mexico has one of the most active plate boundaries in the world, the Middle America Trench. This plate boundary is formed by the subduction of the Cocos Plate below the central Mexican part of the American Plate. Subduction of the Cocos plate causes shallow and deep (no more than 400 km) seismic events in central Mexico. Shallow events are mainly the result of relative movement between oceanic and continental crust or of internal deformation within the plates. Intermediate (between 100 and 300 km) and deep earthquakes (recorded elsewhere between 300 and 750 km) occur in the interior of plates immersed within the asthenosphere and deeper mantle. Abundant literature about the tectonics of the Middle America trench can be found elsewhere (see for example Cox 1973).

The state of Oaxaca lies in the morphotectonic province of Sierra Madre del Sur (figure 1). Most of this province consists of schists and gneisses of uncertain, but probably Precambrian or Paleozoic, age. However, the highest mountain ranges expose middle Tertiary volcanics, whereas the lowlands are underlain by granites (Guzman and Zoltan de Cserna 1963).

2.2 The Oaxaca Data Set

The spectra and source parameters of the main shock and 21 aftershocks were obtained from the data recorded at the Cerrillo station (CRX). The distance from Cerrillo to the epicentre of the main shock is approximately 515 km. For studies in Oaxaca , the Tonantzintla (IIT) SISMEX station is one of the best stations of the system. Unfortunately calibration information for the SISMEX stations for 1978 and 1979 is not available to us. Three stations of SISMEX (IIC, IIT, IIP) and two stations of RESMAC (CRX, MEX) recorded the main shock and all subsequent aftershocks (with local magnitudes greater than 3) of the Oaxaca event. The main shock saturated must of the stations, however, Mexico and Cerrillo were exceptions. Mexico was moderately saturated

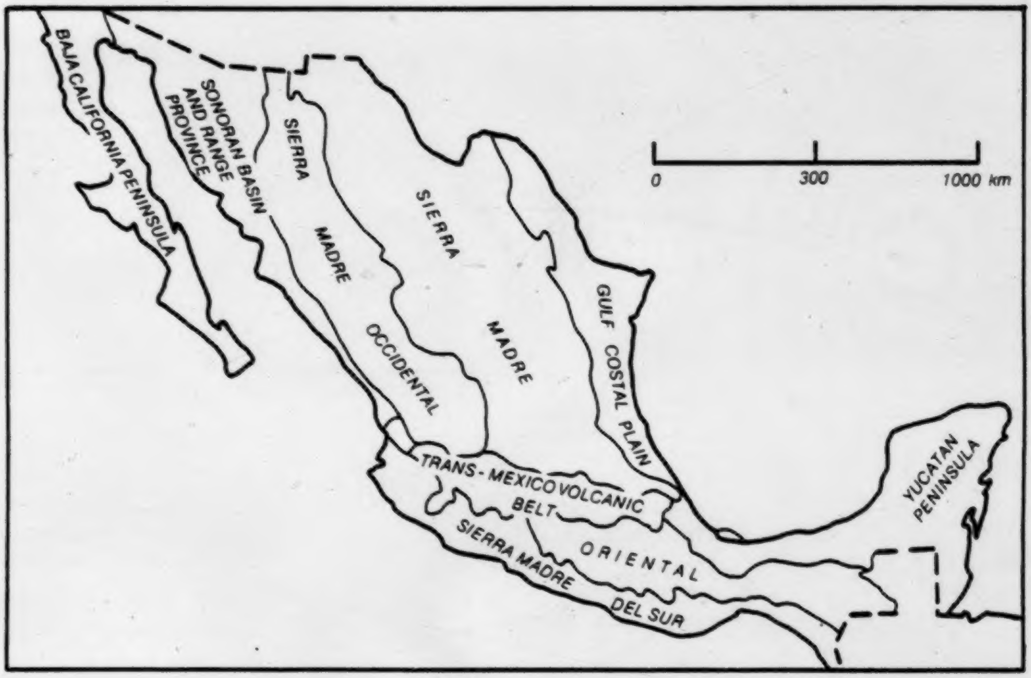
BAJA CALIFORNIA PENINSULA
SONORAN BASIN AND RANGE PROVINCE
SIERRA MADRE OCCIDENTAL
SIERRA MADRE ORIENTAL
GULF COSTAL PLAIN
TRANS-MEXICO VOLCANIC BELT
SIERRA MADRE DEL SUR
YUCATAN PENINSULA
0
300
1000 km

Figure 1.... Morphotectonic provinces of Mexico.

and is extremely noisy. Cerrillo is quiet and suffered no saturation. Acapulco station was installed 30 hours after the main shock.

Due to the instrument response of the RESMAC system (figure 2), source parameters for larger events are obscure. However, it was possible to get the slope at high frequencies and source parameters for events of magnitude between 3.6 and 5.0. The source parameters at the CRX station were compared with the spectra of some events from the nearby CICESE-UCSD portable stations (Munguia et al, 1979).

2.3 Instrumentation

The response curve of a typical RESMAC station is shown in figure 2 with the magnification curve for the CICESE-UCSD stations. A RESMAC station consists of a Mark seismometer (with period of one second and damping 0.7), an amplifier, two filters in cascade (period of 0.1 sec and damping 0.7), and an analog-to-digital converter (A-D). A PDP11 mini-computer used for data recording. The maximum output of the analog-to-digital comverter (A-D) is ±131072 "counts", which corresponds to an input of ±10 volts. The maximum velocity magnification is 162 counts/(micron/sec). The output of the A-D is recorded 36 times/sec giving a Nyquist frequency of 18 Hz.

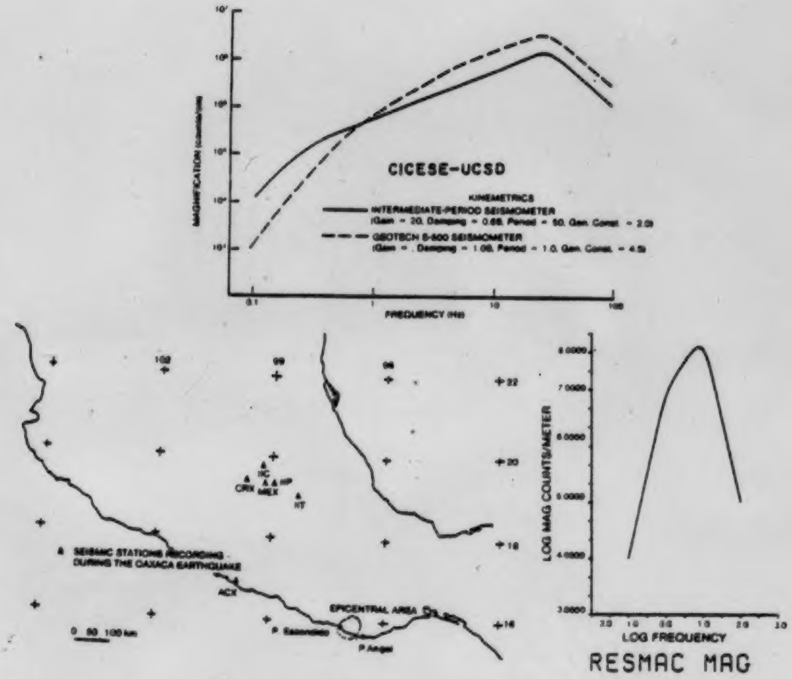

Figure 2.... The response curve for RESMAC and UCSD-CICESE stations and an index map of the area showing stations in 1978

The SISMEX system transmits data by radio link to Instituto de Ingenieria, where the recorded events can be digitized. While SISMEX records continuosly on analog magnetic tape, RESMAC does real time event detection on its input chanels.

The configuration of SISMEX and RESMAC stations in November 1978 made it difficult to get reliable epicentre locations in the Middle America trench. The seismograms (figure 3) are very complicated making it difficult to recognize different phases.

During fifty two hours after the main event the RESMAC system was triggered 151 times. During this interval of time fifty five events (appendix 1) were recorded but only nine (table 1) were clear enough at Cerrillo station for spectral analysis (table 2).

2.4 Data Analysis

From the travel time curves for a continental structure at normal depth (33 km), the phases that would appear in the seismogram at a distance of 510 km are: the refracted wave Pn, the direct wave Pg, the reflection PgPg (very close to Pg), the conversion SgPg, the refracted Sn wave, the direct Sg wave and finally the reflection SgSg. For this distance the surface waves do not appear very soon after the arrival of the S-wave. Consequently , it is unlikely that the energy spectrum is contaminated by surface waves. Instead the

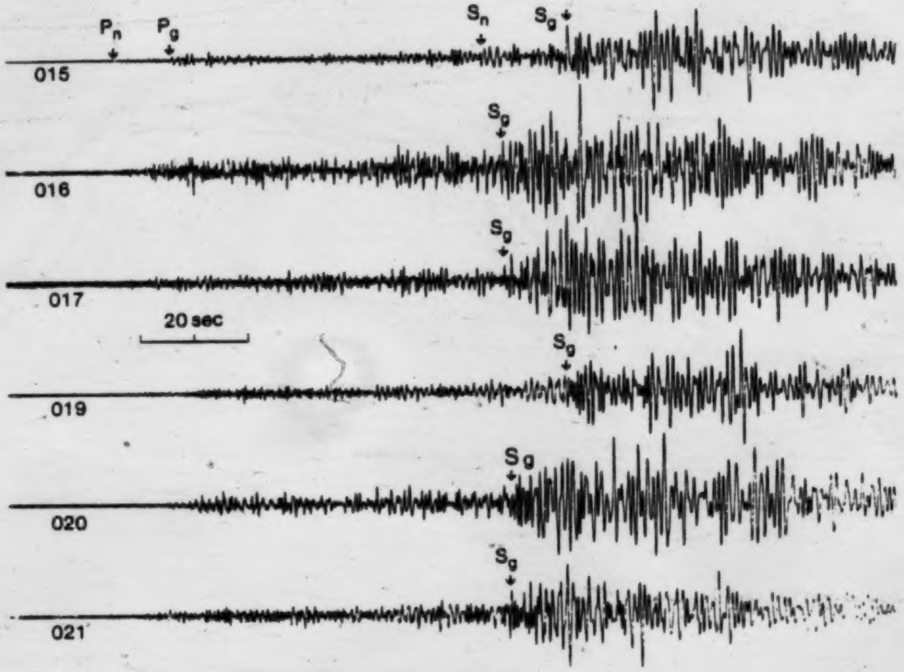

Figure 3.... Examples of Oaxaca seismograms.

[illegible]	logΩ_0	f_c	a	M_o	r	$\Delta\sigma$	MAGNITUDE	DATE
001	-2.54	0.72	-1.2	$3.37X10^{23}$	1.92	14.1	5.6	
002			-1.3				4.8	21:08:53 29-11-78
003	-4.56	1.0	-1.2	$3.22X10^{21}$	1.39	0.36	3.7	21:50:10 29-11-78
004	-4.11	0.93	-1.7	$9.08X10^{21}$	1.49	0.81	4.1	22:06:56 29-11-78
005	-4.86	.89	-1.5	$3.53X10^{21}$	1.56	0.28	4.3	22:31:25 29-11-78
006	-2.86	0.65	-2.3	$1.61X10^{23}$	2.15	4.79	5.0	23:08:50 29-11-78
007	-4.36	0.83	-2.4	$5.10X10^{21}$	1.67	0.32	3.6	23:39:39 29-11-78
008	-4.01	1.0	-1.9	$9.29X10^{21}$	1.39	1.02	4.2	00:01:53 30-11-78
009	-4.42	1.0	-2.4	$4.44X10^{21}$	1.39	0.49	3.8	01:32:16 30-11-78
010	-4.06	.74	-2.1	$1.01X10^{22}$	1.88	0.46	4.0	02:02:35 30-11-78
011	-4.62	1.12	-1.2	$2.8X10^{21}$	1.24	0.44		17:41:48 30-11-78
013	-4.44	0.91	-2.4	$4.24X10^{21}$	1.52	0.36	3.7	17:57:25 30-11-78
014	-4.8	0.89	-2.1	$3.45X10^{21}$	1.56	0.27	3.6	21:23:45 30-11-78
015	-3.36	0.87	-2.8	$5.1X10^{22}$	1.6	3.72	4.7	05:37:13 02-12-78
016	-4.06	0.83	-1.7	$1.01X10^{22}$	1.67	0.65	4.1	20:29:20 02-12-78
017	-4.4	1.0	-2.6	$4.65X10^{21}$	1.39	0.51	3.8	23:36:34 02-12-78
019	-3.92	0.91	-2.0	$1.41X10^{22}$	1.52	1.17	4.2	01:11:11 04-12-78
020	-3.48	0.51	-2.0	$3.87X10^{22}$	2.72	0.57	4.5	06:35:51 05-12-78
021	-3.9	0.71	-1.6	$1.47X10^{22}$	1.95	0.58	4.7	23:45:49 05-12-78
025	-4.26	1.07	-1.9	$6.21X10^{21}$	1.30	0.87	4.6	10:54:24 08-12-78
031	-4.31	0.91	-2.5	$5.73X10^{21}$	1.52	0.48	3.9	15:30:21 11-12-78
035	-3.74	0.66	-1.1	$2.13X10^{22}$	2.1	0.67	4.4*	21:50:40 18-12-78
039	-3.75	0.5	-1.7	$2.08X10^{22}$	2.77	0.29		08:53:50 28-12-78
040	-4.34	0.91	-1.9	$5.34X10^{21}$	1.52	0.45		18:40:07 28-12-78
041	-3.64	0.74	-1.5	$2.68X10^{22}$	1.88	1.2		19:19:47 28-12-78
042	-4.13	0.78	-1.7	$9.67X10^{21}$	1.75	0.48		19:46:09 28-12-78

Table 1.... Source parameters derived from RESMAC data recorded at Cerrillo.

Nov.29.78.21.08.53	IIT saturated
Nov.29.78.21.17.25	small event
Nov.29.78.21.35.19	not very clear signals
Nov.29.78.21.40.23	not very clear signals
Nov.29.78.21.50.10	spectrum analysed
Nov.29.78.21.54.01	not very clear signals
Nov.29.78.22.06.56	spectrum analysed
Nov.29.78.22.18.07	good signals at IIT,IIC and IIP

Nov.29.78.22.26.25	good signals at IIT,IIC and IIP
Nov.29.78.22.31.25	spectrum analysed
Nov.29.78.22.57.40	not very clear signals
Nov.29.78.23.08.50	spectral analysed
Nov.29.78.23.29.03	good signals at IIT,IIC and IIP
Nov.29.78.23.39.39	spectrum analysed
Nov.30.78.00.01.53	spectrum analysed
Nov.30.78.00.08.20	small event
Nov.30.78.00.28.32	small event
Nov.30.78.01.11.35	small event
Nov.30.78.01.32.16	good signals at IIT,IIC and IIP
Nov.30.78.01.58.33	small event
Nov.30.78.02.02.35	spectrum analysed
Nov.30.78.03.05.10	good event CRX down
Nov.30.78.05.11.37	small event crx down
Nov.30.78.05.52.28	good event CRX down
Nov.30.78.07.25.34	good event CRX down
Nov.30.78.07.49.59	small event
Nov.30.78.08.22.44	small event
Nov.30.78.10.20.32	good event CRX down
Nov.30.78.10.35.56	small event CRX down
Nov.30.78.10.43.54	IIT saturated CRX down
Nov.30.78.11.12.24	small event CRX down
Nov.30.78.11.42.51	small event CRX down
Nov.30.78.12.04.32	good event CRX down
Nov.30.78.12.24.37	small event CRX down
Nov.30.78.13.13.54	smal event CRX down
Nov.30.78.13.16.50	good event CRX down
Nov.30.78.13.49.51	goodevent CRX down
Nov.30.78.13.59.10	small event CRX down
Nov.30.78.14.41.13	small event CRX down
Nov.30.78.15.37.44	small event
Nov.30.78.16.08.44	good event CRX down
Nov.30.78.17.41.48	spectrum analysed
Nov.30.78.17.49.47	IIT saturated
Nov.30.78.17.57.25	good event clear at IIT,IIC and IIP
Nov.30.78.19.25.12	small event
Nov.30.78.21.23.45	small event
Nov.30.78.23.56.46	small event
Nov.01.78.03.03.59	small event
Nov.01.78.04.09.04	small event
Nov.01.78.04.38.58	small event
Nov.01.78.09.32.15	good signals at IIT, IIC and IIP
Nov.01.78.17.38.56	small event
Nov.02.78.02.01.04	small event
Nov.02.78.03.26.45	IIT and IIC saturated

Table 2.... Events recorded at RESMAC and SISMEX stations

fifty two hours after the Oaxaca event.

spectra will have energy from the phase SgSg and the scattering due to reflection near the station.

Spectra of P and S waves recorded at CRX were corrected for instrumental response and seismic attenuation. The epicentral distance was estimated from the average Sg-Pg times assuming a Vp velocity of 6.5 km/sec (based on unpublished refraction results at Pinotepa Nacional). This distance has an error of ±35 km. The uncertainty in the distance yields an error of one order of magnitude in the moment. Several values of Q were tested to gain more insight into the value of this parameter in the region. Since very little is known about Q in this area, anelastic attenuation was approximated with a Q of 500 for S-waves and a Q of 1242 for P-waves (as suggested by Anderson et al 1978). From the analysis of the spectra, the reliable bandwidth of frequencies was determined to be between 0.2 to 7.0 Hz. Consequently, the earthquake signal was band-pass filtered outside this range of frequencies.

The different time windows that were used in calculating the shear wave spectra (figure 4) show some increase in the spectral amplitude with an increase of the sample length. All spectral calculations were made with 2000 data points (55.6 seconds) of data. This implies the possible presence of scattered P and S energy. Reyes et al

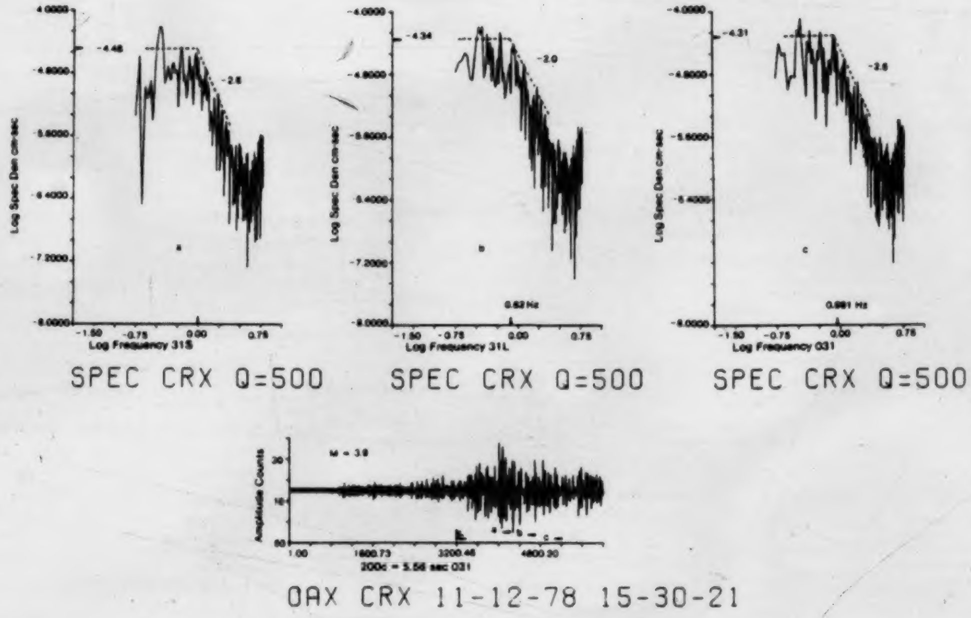

Figure 4.... Variation of the spectra with increasing sample length.

(1979) used hypocentral determinations of aftershocks to establish 2 trends in the distribution of aftershocks. One part of the aftershock zone dips at an angle of 20° while another part suggests a reverse fault zone dipping at 70° toward the trench. There are a large number of aftershocks on the first portion, on the second activity is scarce but is supported by a composite focal mechanism.

In order to compare RESMAC spectra with CICESE-UCSD data (figure 5), the spectra must be corrected for radiation pattern and free surface reflection of SV waves. Two of the events used in our comparison to CICESE-UCSD results are associated with the zone that dips at 20°. This admittedly weak result is the basis for assuming that all events analyzed here slipped on fault planes parallel the main thrust zone in a down dip direction. This corresponds to a dip of 20 degrees and an azimuth of 60 degrees. Nuttli, (1961), calculated the amplitude of S-waves at the free surface for different angles of incidence. Using Nuttli's formulas the ratio of the displacement amplitude at the free surface to the amplitude of the incident wave is 0.82. The previously mentioned unpublished refraction results (Singh, personal communication) were used to arrive at this number. An average depth of 35 km was assumed. At 60 degrees azimuth the average radiation pattern correction for Sv waves (assuming a rupture velocity of 0.9 Vs) is 0.84 (Madariaga 1977).

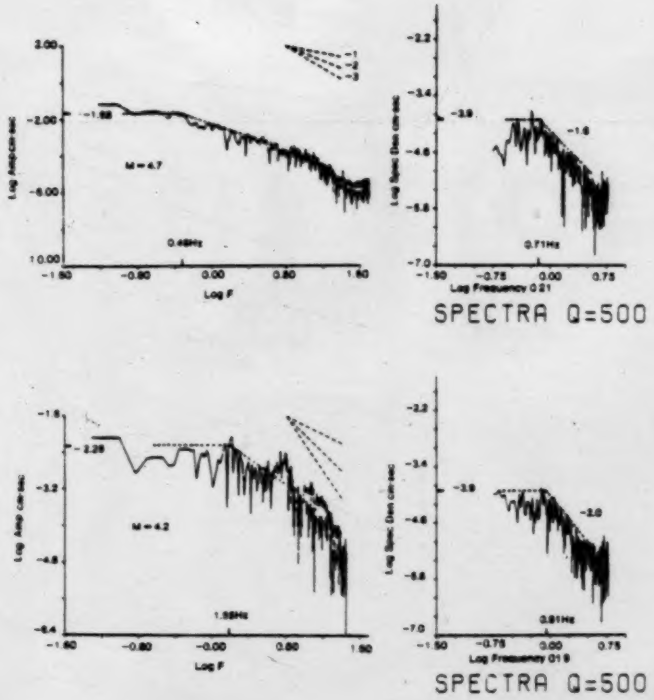

Figure 5.... Two examples of spectra for events recorded both by CICESE-UCSD and RESMAC stations.

Spectral amplitudes, corner frequency and slope at high frequencies (table 1) decrease for different values of Q (table 3). The corner frequency also tends to decrease but in an erratic way.

The response characteristics of the RESMAC system were such that it was only possible to get the slopes at high frequencies of the main shock, (-2.0 and -2.8 (figure 6)). The intersection for these slopes is at 1.4 Hz. The first aftershock of magnitude 5.6 was recorded nearly 13 minutes after the main event, a corner frequency at 0.7 Hz was found, although this means a small source dimension for a relatively large event. The second large aftershock of magnitude 4.8 was recorded approximately 74 minutes later, this spectrum does not show any corner frequency at all in contrast with the first aftershock, instead it is possible to see a slope of -1.3 at high frequencies (figure 7).

2.5 Source Parameters

The constants used in this analysis of source parameters (Brune 1970, 1971) are: S wave velocity=3.75 km/sec, density ρ=2.35 gr/cm^3. Table 2 shows the results of these calculations.

Two (figure 7) of the 21 aftershocks spectra show poorly defined corner frequencies. I compared (table 4) source parameters of the spectra of some events registered at both RESMAC and CICESE-UCSD stations. In general there is

CICESE-ULSD DATA

MAG	Q	$\log\Omega_m$	f_{cm}	∂
4.2	1000	-2.26	1.55	-1.50
4.7	1000	-1.68	0.49	-2.00
4.5	1000	-1.73	1.35	-2.50
4.4	1000	-2.00	0.68	-1.1

RESMAC DATA

Q	$\log\Omega_R$	f_{cR}	∂_R	Q	$\log\Omega_R$	f_{cR}	∂_R	Q	$\log\Omega_R$	f_{cR}	∂	AFTERSHOCK
												60
1000	-4.12	0.87	-2.40	300	-3.92	0.91	-2.0	350	-3.86	0.98	-1.4	[illegible]
1000	-4.00	0.69	-2.30	500	-3.90	0.71	-1.60	350	-3.89	0.81	-1.10	[illegible]
1000	-3.56	0.43	-2.20	500	-3.48	0.51	-2.00	350	-3.46	-0.47	-1.40	020
1000	-3.97	0.78	-1.80	500	-3.74	0.66	-1.10	350	-3.60	0.71	-1.00	035

Table 3.... RESMAC spectral parameters for diferent values of Q compared with the results from the CICESE-UCSD nearby stations.

RESMAC DATA

Q	$\log\Omega_R$	f_{cR}	∂	M_{oR}	T_o	$\Delta\sigma$	
500	-3.92	0.91	-2.0	1.41×10^{22}	1.52	1.17	019
500	-3.90	0.71	-1.6	1.47×10^{22}	1.95	0.58	021
500	-3.48	0.51	-2.0	3.87×10^{22}	2.72	0.57	020
500	-3.74	0.66	-1.1	2.13×10^{22}	2.1	0.67	035

CICESE-UCSD DATA

ΔM_o	Q	$\log\Omega_M$	f_{cM}	∂	M_{oM}	T_o	$\Delta\sigma$
4.87	1000	-2.26	1.55	-1.5	6.86×10^{22}	0.83	52.49
1.1	1000	-1.68	0.49	-2.0	1.63×10^{22}	2.61	0.40
4.32	1000	-1.73	1.35	-2.5	1.67×10^{23}	0.95	83.63
2.63	1000	-2.00	0.68	-1.2	5.65×10^{22}	1.88	3.71

NOTES

$\Delta M_o = \frac{M_{oM}}{M_{oR}}$; f_c = corner frequency HZ,

T_o = source dimension KM , $\Delta\sigma$ = Stress drop bars

M_o = Moment dynes - cm ∂ = slope at high frequencies

Ω = spectral density

Table 4.... RESMAC source parameters for Q=500 compared with CICESE-UCSD results.

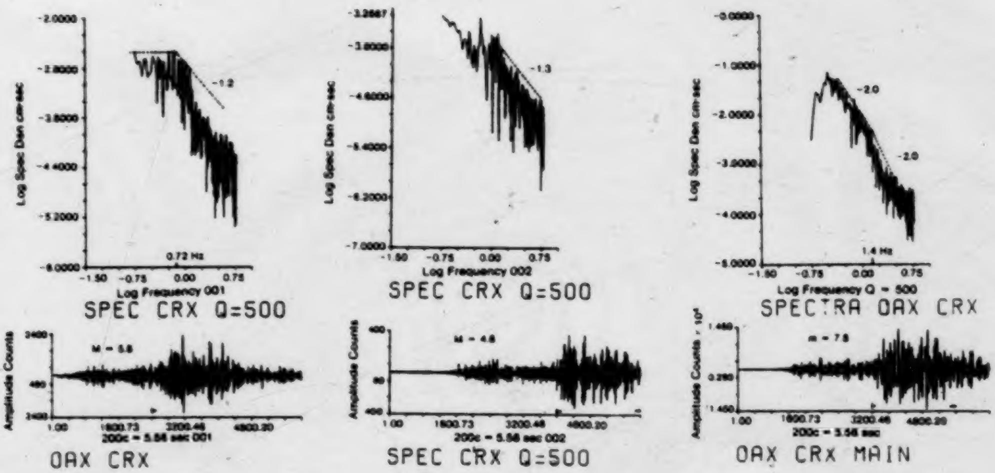

Figure 6.... Spectra of the main shock and the first two aftershocks recorded at RESMAC

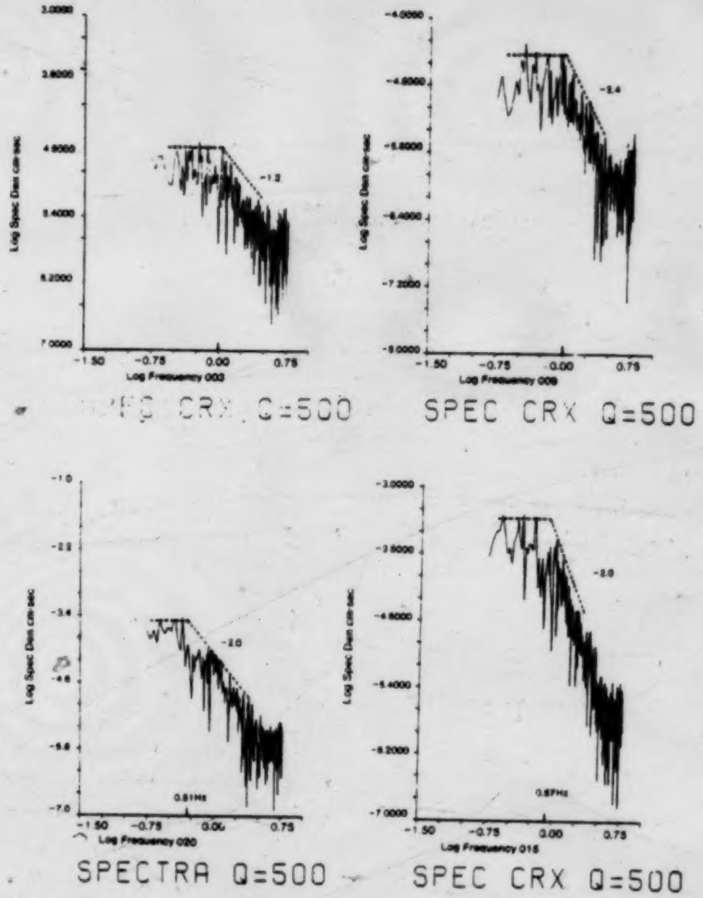

Figure 7.... The two upper spectra show well defined corner frequencies and the two lower spectra are not well defined.

not good agreement between corner frequencies (the largest difference is 0.8 Hz). CICESE-UCSD corner frequencies are larger than the RESMAC corner frequencies. This difference results in a discrepancy of 1.7 km in the source radius and a large discrepancy in the stress drop. This bias could be due to scattering in the crust (Dahlen, 1974), but it seems more likely to be evidence of variations in the focal mechanisms.

Unfortunately only CRX was sufficiently quiet for spectral analysis. It is evident from the seismograms and the time windows which have been used, that the RESMAC spectra contain scattered P and S waves. Consequently, scattering could increase the estimated fault size.

RESMAC moments are smaller, sometimes by a factor of close to 5, than CICESE-UCSD moments. The disagreement could be due to:

1) Differences in bandwidth between CRX and the CICESE-UCSD stations.

2) The bandwidth of CRX. The station was not originally planned to provide spectral information at teleseismic distances.

3) Uncertainties in the radiation pattern. I have only one station.

4) Energy losses due to conversion of the SV signal and due to scattering in the largely unknown structure between Oaxaca and Mexico.

Consequently calculations of the moment give a possible lower limit. The spectra of P-waves were calculated and do not show any corner frequency. This could be due to the lower amplitude of the P-waves.

2.6 Seismic Moment and Local Magnitude Relationship of the Oaxaca Aftershocks

Using twenty aftershocks of the Oaxaca event I calculated an empirical relationship between seismic moment (M_0) and local magnitude (M_L). This relationship was compared with a similar relationship for events from the Rocky Mountain House earthquake swarm (see chapter three). Even though these seismic sequences were generated in different tectonic enviroments (the Oaxaca aftershocks are interplate events, and the Rocky Mountain House earthquake swarm is an intraplate sequence). Both sets of data seems to fit the relationship given by $\log M_0 = 1.3 M_L + 16.6$ for magnitudes between 1.5 and 5.5 (figure 8). A more expanded discussion of this relationship is given in chapter three.

2.7 Conclusions

Source parameters of 21 aftershocks of a large earthquake on a subduction zone were obtained. Corner frequencies lie near one Hz, showing smaller values than those obtained with the nearby stations. This could be due to scattering along the path length and near the station.

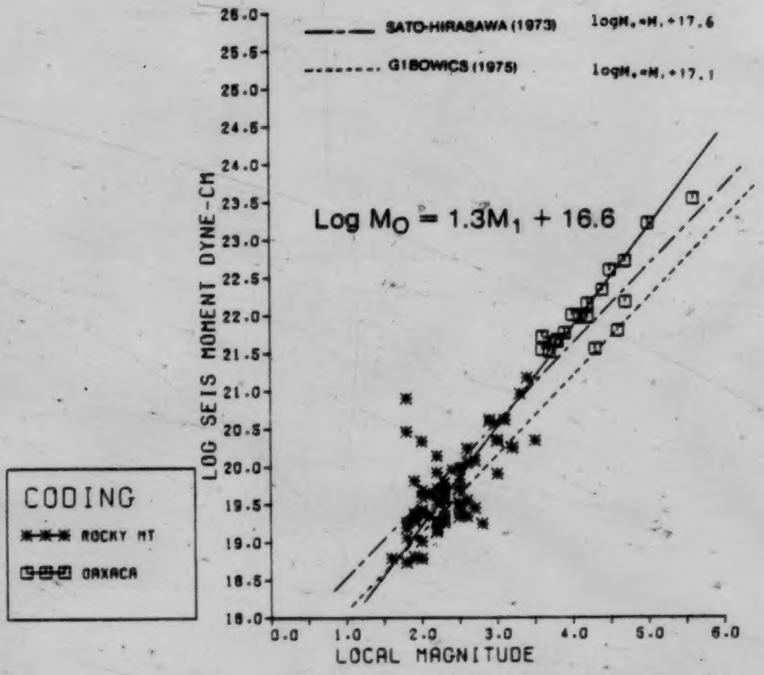

Figure 8.... Comparison of the Oaxaca seismic moments with the seismic moments of the Rocky Mountain House earthquake swarm

Seismic moments for the observed events with magnitudes from 3.6 to 5.6 range from 3.45×10^{22} dyne-cm to 3.3×10^{23} dyne-cm, with source dimensions from 1.2 to 2.7 km and a maximum stres drop of 4.7 bars. Consequently source dimension and stress drop are lower limits. P-wave spectra do not show any corner frequency, being very sensitive to scattering and noise level. Seismic moment is the more reliable parameter. The magnitude seismic moment relationship for the 21 events analysed fits the relationship given by $\log M_0 = 1.3M_L + 16.6$.

In this chapter I calculated the spectra of the Oaxaca earthquake aftershocks at about 515 km from the source. I can consider this a "large" epicentral distance. In the next chapter I analyse the refracted phase Sn and the spectra of the events from the Rocky Mountain House earthquake swarm detected at Edmonton, those events are approximately 180 km from Edmonton. Therefore, I can consider that spectral analysis at an "intermediate" distance from the earthquake source. The data in the next chapter will also permit comparison of processes on a subduction zone with the poorly understood processes that give rise to intraplate seismicity.

3. Focal Depths and source Parameters of the Rocky Mountain House Earthquake Swarm from the digital data at Edmonton

It is often assumed in earthquake seismology that similarity exists between large and small earthquakes (Aki 1967). This is the motivation for comparing a sequence of small earthquakes in an intraplate environment with the aftershocks of a large earthquake on a plate boundary, such as the Middle American Trench near Oaxaca.

In this chapter I make an analysis of the Rocky Mountain House earthquake swarm, such an intraplate sequence, from records taken at Edmonton (EDM) and Suffield (SES). From January 1976 to February 1980 one or both of these stations detected 220 events with magnitudes less than 4. Some of these events show well defined Sn, Sg and Pg phases and small variation in the difference of Sg-Sn and Sg-Pg at EDM. Analysis of the theoretical travel times using a structure determined for central Alberta yields an average focal depth of 20±5 km and an average epicentral distance of 175±5 km SW of Edmonton for 40 of these events. Since Sn was not clear on the remainder, it was not possible to get focal depths for all the events.

Seismic moments of 80 events with local magnitudes from 1.6 to 3.5 were found to be in the range of 6.0×10^{18} to 7.9×10^{20} dyne-cm. A relationship between local magnitude and seismic moment was $\log M_0=1.3M_L+16.6$; similar to one determined in California. A theoretical realtionship using Sato-Hirasawa (1973) model was calculated with different rupture velocities and source dimensions; It was found that it is strongly dependent on these parameters. Using a rupture velocity of .9 times the shear velocity and a source dimension of 1 km the model give $\log M_0 = M_L + 17.6$ The Sato-Hirasawa model fit well our data. The Gibowics (1975) theoretical relationship given by $\log M_0 = M_L + 17.1$ also fits our data. Source radii, where they could be determined, were between 500 to 60 meters and stress drops were from 0.01 to 1.5 bars.

The depth of focus, the low stress drops, and the statistical similarity to other natural earthquakes sequences suggest that at least part of this swarm is of natural origin.

This chapter is based on a paper submitted to Canadian Journal of Earth Sciences (Rebollar et al 1982)

3.1 Introduction

Destructive earthquakes are not common in Canada, although large events occur off the coast of British Columbia. Of all the seismic activity detected in Canada approximately two-thirds occurs in Western Canada (figure 9), mainly in British Columbia, Yukon, and the North West Territories (Whitham et al 1970).

The Rocky Mountains, one part of the North American Cordillera, and the Alberta plains show some seismic activity. Seismic events occurring on the Alberta plains are

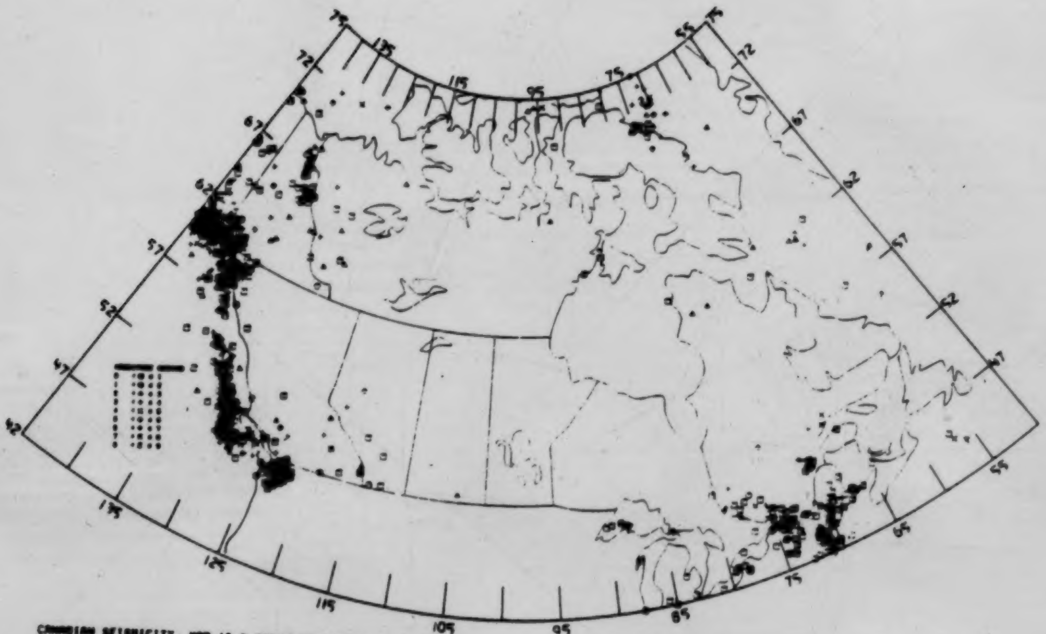
75
135
115
95
75
55
15
72
67
62
57
52
47
42
135
125
115
105
95
85
75
65
55
72
67
62
57
52
47

CANADIAN SEISMICITY. MAP IS A TRANSVERSE MERCATOR PROJECTION SHOWING ALL EARTHQUAKES RECORDED IN THE NOAA CATALOGUE WITH EPICENTERS IN OR NEAR CANADA UNTIL THE END OF 1977. SYMBOL TYPE DENOTES THE MAGNITUDE OF THE EVENT.

THIS MAP WAS PRODUCED BY THE TECTONOPHYSICS GROUP OF THE INSTITUTE OF EARTH AND PLANETARY PHYSICS. THE UNIVERSITY OF ALBERTA. EDMONTON. ALBERTA. CANADA.

Figure 9.... Seismicity of Western Canada.

usually small (Local magnitude $M_L \leq 4$) and thus are not often detected on more than a few seismic stations. Some may be triggered by secondary and tertiary recovery methods during hydrocarbon extraction. A somewhat higher seismicity level exists in the foothills of the Rocky mountains. This seismicity can be observed at Edmonton (EDM), Suffield (SES) and Penticton (PNT). The Rocky Mountain House earthquake swarm (figure 10) is a good example.

Since January 1976 EDM has been recording signals from a seismic swarm near Rocky Mountain House, appoximately 185 km SW of Edmonton. Due to the small magnitude of these events they have been seen mainly at EDM. Larger events (M_L near 3) have also been seen at Suffield station (SES) which is about 350 km from Rocky Mountain House. Therefore, this study is mainly concerned with the analysis of the Rocky Mountain House earthquake swarm detected at Edmonton and Suffield.

3.2 Analysis of the Data

The University of Alberta seismic observatory (EDM) records 3 components each of short and long period data in digital and analog form. The analog system is a part of a Canadian and Worldwide Network of Standard Seismograph stations. In the digital system the seismometer is coupled with an amplifier and a Butterworth filter. The data are recorded at 18 samples per second (short period) and 3

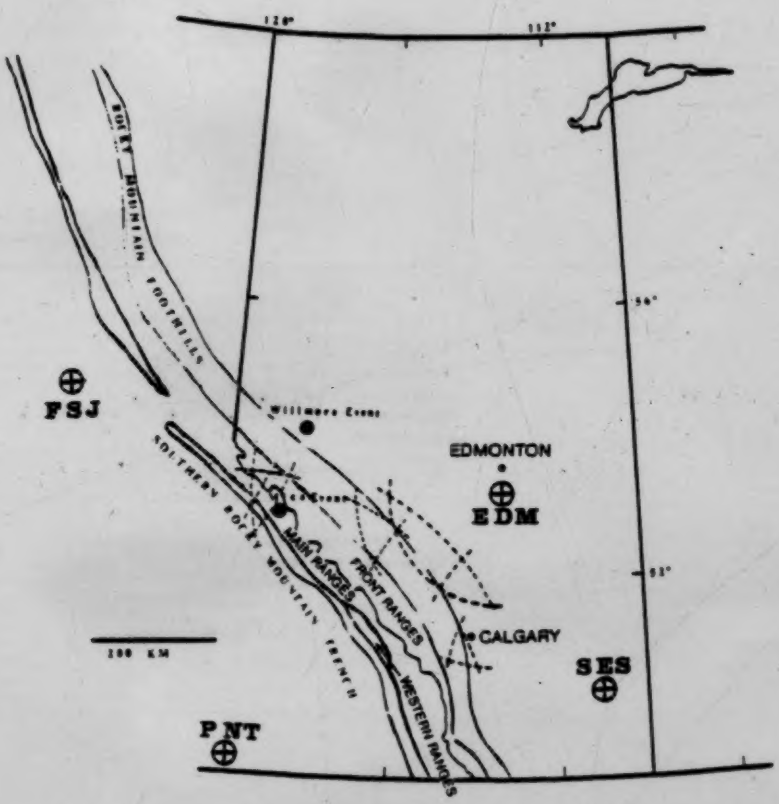
120°
112°
56°
ROCKY MOUNTAIN FOOTHILLS
FSJ
Willmore Event
EDMONTON
EDM
SOUTHERN ROCKY MOUNTAIN TRENCH
MAIN RANGES
FRONT RANGES
CALGARY
KM
SES
WESTERN RANGES
PNT

Figure 10.... Geologic provinces of the Southern Rocky Mountains and locations of some seismic events recorded at EDM, SES, and PNT.

samples per second (long period) and is written in a 2'S complement binary as a 14 bit bipolar word. The maximum signal is 13 bits plus sign (±8192 counts) and this is equivalent to ±10 volts level at the imput to the analog to digital converter. There is a WWVB bit inserted at bit position 15 (McCloughan and Kanasewich 1974). The response curve of the curve of the system (see Aki and Richards chapter 10 for details on magnifications curves) is given in (figure 11).

About 5 events per month apparently originating in South West Alberta have been detected on analog records at EDM (figure 12). There were apparently random bursts of up to 25 such events. This is unusually high activity compared to the local activity detected at EDM since 1970 (figure 13).

Some of the events of the swarm are simple, with well defined Pg, Sn, and Sg phases. However, some of the large events are complicated showing similar amplitudes of P and S waves. This could indicate variations in the source mechanism (figure 14). Pn is usually barely above the noise level. Neither the complex nor the simple events appear on the long period records. This suggests relatively deep foci.

From January 1976 to February 1980, it was possible to read Sg-Sn and Sg-Pg in 41 events out of 220 (table 5). Reading errors of Pg and Pn are of the order of 0.05 sec when the onset is clear, and 0.1 sec or greater for Sg and Sn, when a clear phase was recorded. The average time

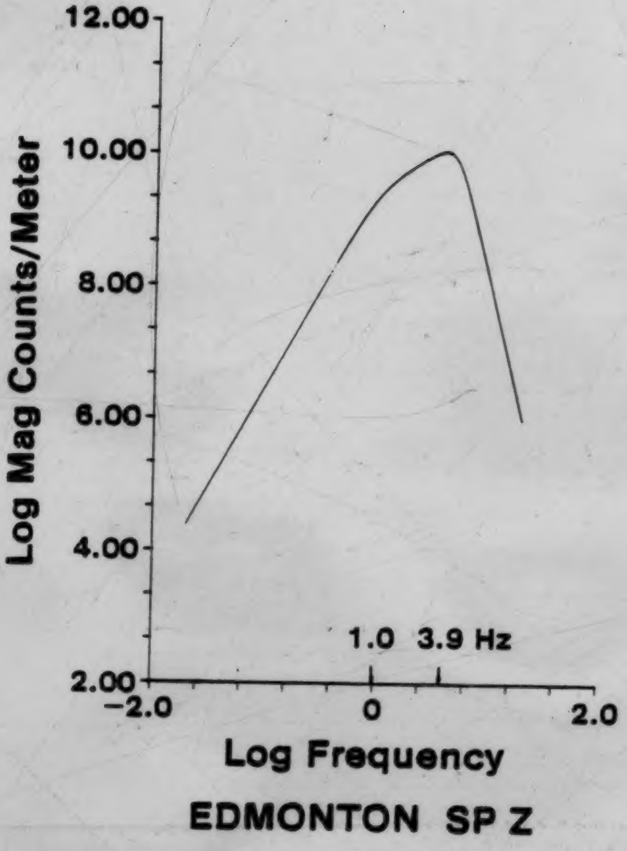

Figure 11.... Magnification curve of the short period seismic station, vertical component.

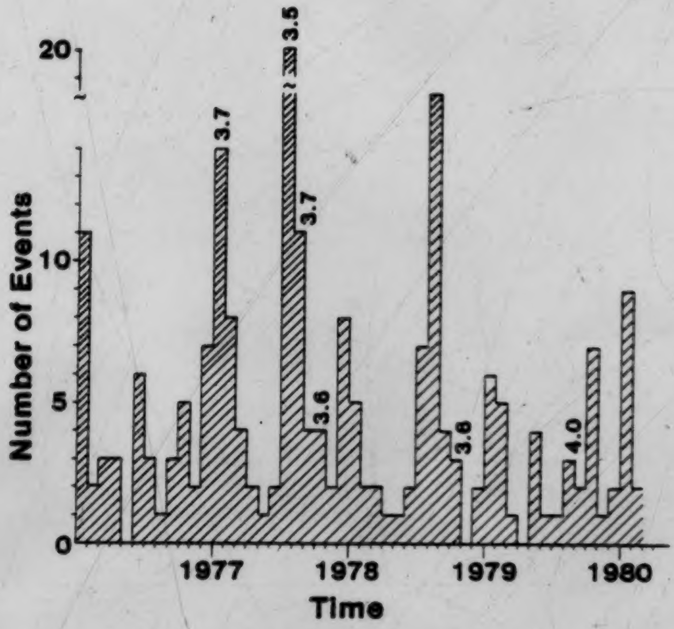

Figure 12.... Histogram of number of events from the Rocky Mountain House earthquake swarm recorded at EDM against time with no apparent frequency magnitude relation.

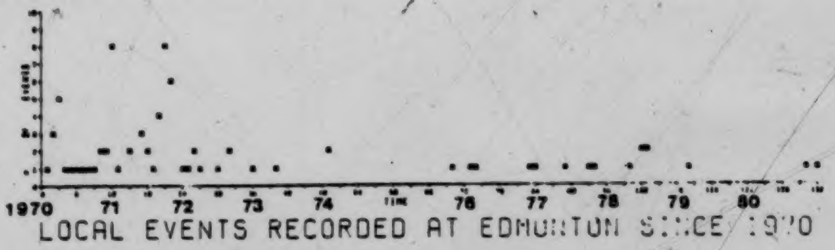

Figure 13.... Local events (S-P times of less than 60 sec) recorded at Edmonton station since 1970

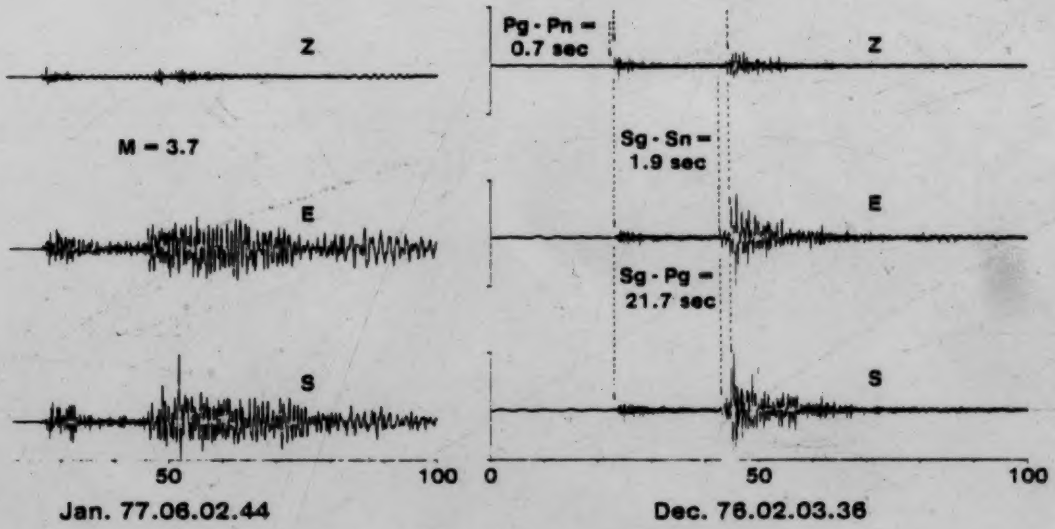

Figure 14.... Events recorded at Edmonton from the Rocky Mountain House earthquake swarm, left - complex event, right - simple event.

DATE	Pg-Pn	Sg-Sn		Sg-Pg	
		N	E	N	E
JAN.76.26.19.37	....	1.78	1.78	21.54	21.94
JAN.76.30.15.07	....	....	1.82	21.26	21.34
MAY.16.13.04.48	....	1.78	1.86	21.62	21.54
SEP.76.01.22.45	....	....	....	22.73	22.45
SEP.76.13.10.24	....	1.98	....	.....	.....
SEP.76.14.02.44	....	0.98	1.34	25.10	25.81
OCT.76.13.10.54	....	1.58	1.78	21.54	21.74
OCT.76.18.15.23	0.79	1.78	1.78	21.86	21.94
NOV.76.02.11.42	....	....	1.38	.....	21.50
DEC.76.09.07.28	....	1.78	1.78	21.74	21.98
DEC.76.23.22.18	....	2.17	2.10	21.74	21.94
JAN.77.05.23.28	0.59	....	....	.....	.....
JAN.77.08.02.44	0.51	....	....	.....	.....
MAR.77.01.07.49	....	1.78	1.98	.....	.....
APR.77.12.17.14	....	1.78	1.98	21.15	21.74
MAY.77.22.17.33	....	1.86	2.06	21.82	21.66
JUL.77.02.20.40	....	1.98	1.98	21.34	21.34
JUL.77.20.01.33	....	1.98	1.90	20.16	20.28
JUL.77.24.17.50	0.59	2.17	1.98	21.54	21.74
JUL.77.31.02.58	....	1.98	1.58	21.15	21.54
AUG.77.13.06.24	....	1.98	1.66	21.42	21.19
AUG.77.27.11.51	....	1.78	1.90	21.74	22.10
OCT.77.02.21.33	....	1.78	1.66	21.74	21.15
OCT.77.26.10.34	....	....	2.57	21.94	21.82
NOV.77.11.11.31	....	1.96	....	.....	.....
DEC.77.08.19.26	....	1.96	....	21.15	.....
DEC.77.23.70.52	....	1.98	1.78	21.42	21.15
DEC.77.30.21.25	....	1.98	2.13	21.24	.....
JAN.78.14.06.26	....	1.78	1.70	21.54	21.42
FEB.78.20.03.16	....	....	1.98	.....	22.00
JUN.78.28.08.07	....	1.66	....	.....	.....
JUL.78.18.22.16	....	1.98	1.98	21.86	21.94
AUG.78.15.01.12	....	1.78	1.78	21.70	21.34
AUG.78.16.08.42	....	2.06	1.66	21.58	21.34
AUG.78.29.01.03	....	1.86	1.90	21.30	21.54
JAN.79.05.02.14	....	....	1.78	.....	21.34
FEB.79.11.02.07	....	....	1.78	.....	.....
MAY.79.04.10.47	0.47	1.78	1.78	21.94	21.74
MAY.79.21.00.01	....	1.98	1.78	.....	.....
AUG.79.01.05.47	....	1.70	1.62	.....	.....
SEP.79.25.10.28	0.50	1.78	1.90	21.90	22.08

Table 5.... Pg-Pn, Sg-Sn and Sg-Pg phase differences recorded at Edmonton station (N North South and E East West Components)

difference for Sg-Sn was 1.9±0.2 sec and for Sg-Pg was 21.7±0.7 sec. The consistency of this difference suggests that the activity is confined to a small area. The average Pg-Pn difference of 0.6±0.1 sec was based on 6 of the 41 events. This group of events shows remarkably consistent differential travel times and as a consequence I feel justified in treating the data as a group. The average of the differential times should be representative of the group and it is this representative value I analyse.

3.3 Analysis of Refracted Phases

These average differential travel times have implications for the average depth of seismicity at Rocky Mountain House as observed at EDM. Obviously it would be better to have data from nearby stations to determine depths but equipment and technician limitations prevent this except for short intervals. In order to estimate source depth I assume a structure derived from seismic refraction profiles, calculate travel time curves for Pg, Sg, Pn, and Sn as a function of source depth and use the average Sg-Sn, Pg-Pn, and Sg-Pg times to constrain the depths. Since Sg-Sn and

Sg-Pg were tightly constrained we can place limits on the depths from which the seismicity originates if our structure is correct. I have tested the entire range of possible plains structures and conclude that no reasonable structure permits shallow source depths for the portion of the Rocky Mountain House seismicity which has observable Sn at Edmonton.

This conclusion is important. It seems highly unlikely that seismicity at depths exceeding 10 km is triggered by the relatively small changes associated with hydrocarbon recovery operations on the Strachan gas field which is near the swarm. The events studied at EDM are most likely not induced. This does not preclude the possibility that other activity exist and is related to hydrocarbon recovery. The possibility that the basement structures near the foothills are seismically active, albeit at a low level, also has interesting implications for the geodynamics of the North American plate.

Several observational constraints can be placed on the problem. The first, and most important, is the requirement that Sn must arrive before Sg. This must hold no matter what velocity model is used and no matter what source depth is used. The second derives from the spread in Sg-Sn. Although it was .2 seconds in my data I accepted solutions in which deviations of up to 0.35 seconds appeared. A third constraint, which is also crucial, is that Pn arrives before Pg. Here again I accept the pessimistic view that 0.35

second deviation from an observed average is acceptable.

Given these constraints I must solve an inverse problem which has no unique solution. I determine the range of velocity models, source depths and epicentral distances which fit our observations. In order to explore the problem I first derived what appeared to be a reasonable velocity model for the problem and then searched for a source depth and a distance to the activity that satisfied our average of Sg-Sn and Sg-Pg.

The crust is nearly 45 km thick in much of southern Alberta Clowes and Kanasewich (1970), Chandra and Cumming (1972), Cumming and Chandra (1975). Ganley and Cumming (1974) found a possible Moho from reflection record at 35 km near Edmonton. However, those profiles are too far from the Rocky Mountain House activity. The nearest reversed seismic refraction profile which gives reliable deep crust and mantle velocities is that determined by Richards and Walker (1959) from an approximately NS refraction profile near 113.5°W and between 50.8°N and 51.9°N (table 6). Obviously this profile serves only as a guide to structure but it can be used as a starting point for average velocity depth models on the wave path from Rocky Mountain House to Edmonton. The seismic work that was done closer to this area does not provide reliable lower crust or mantle velocities. In order to interpret the data I have at Edmonton such velocities are far more crucial than the shallow velocities.

Layer Thickness (km)	Vp (km/sec)	Vs (km/sec)
2.0	3.6	1.81
1.5	6.1	3.07
28.5	6.2	3.51
13.0	7.2	4.15
Half Space	8.2	4.73

Table 6.... The velocity structure (Richards and Walker 1959)

At a distance corresponding to that between Rocky Mountain House and Edmonton the Sg-Pg time does not depend on the depth of focus. It is thus possible to adjust this depth to satisfy observations of refracted S (Sn) which I obtained from digital data archived at Edmonton. It was however not always possible to match refracted P (Pn) as well. This is not surprising, for Pn is not well observed, even on the records I used. I found that the seismicity was associated with depths in excess of 10 km. Best estimates of the sedimentary section in this area suggest that the maximum depth of sediments in this area is approximately 16000 feet or 4.8 km (Bally et al 1966, keating 1966).

Obviously such depth calculations are model dependent. One way to explore the degree of this dependency is to determine the effect of small changes in the model. Another plausible structure (table 7) also yields the results that the average depth of the activity is greater than 10 km. The predicted values of the time differences for various phases (table 8) for this model are such that the average of the observed values indicates depths of the order of 20 km and epicentral distances on the range 170 to 180 km. Again Pg-Pn does not fit well. On the travel time plots for events at various depths with a dipping Moho and a flat Riel discontinuity we note that only once the source depth exceeds 15 km does Sn arrive before Sg. I cannot distinguish the effect of Moho dip on the travel times hence I compared my data (figure 15) with the travel times predicted for a flat Moho.

The data at EDM does not contradict the existence of shallow activity at Rocky Mountain House. Only 41 of the 220 observed events in the digital system showed positive Sn-Sg times. Small Sn-Sg or negative values of this phase difference would lead to masking of Sn in the Sg wave train. Those events for which Sn cannot be picked can be explained as occurring at depths of less than 10 km. The sharpness of an observed distribution of Sn-Sg suggests a concentration of activity at 20±5 km depth.

In this kind of calculation a compromise between computational effort and results is required. At this stage I have a strong suggestion, but certainly no proof, that the average depth of a significant fraction of the seismicity is in excess of 20 km. In order to explore this further I

Layer Thickness (km)	Vp (km/sec)	Vs (km/sec)
1.3	2.68	1.35
1.3	4.59	2.31
29.4	6.20	3.57
13.0	7.20	4.15
Half Space	8.20	4.75

Table 7.... A modified version of the Richards and Walker velocity structure

Depth	E. D.	Pg-Pn	Sg-Sn	Sg-Pg
5 km	170 km	-1.06	-1.71	20.90
5 km	185 km	-0.47	-0.68	22.68
10 km	170 km	-0.51	-0.75	20.92
10 km	185 km	0.07	0.27	22.70
15 km	170 km	0.06	0.23	20.95
15 km	185 km	0.64	1.25	22.73
20 km	170 km	0.65	1.27	21.00
20 km	185 km	1.23	2.28	22.78

Table 8.... A selection of predicted differential travel times for the modified Richard and Walker model

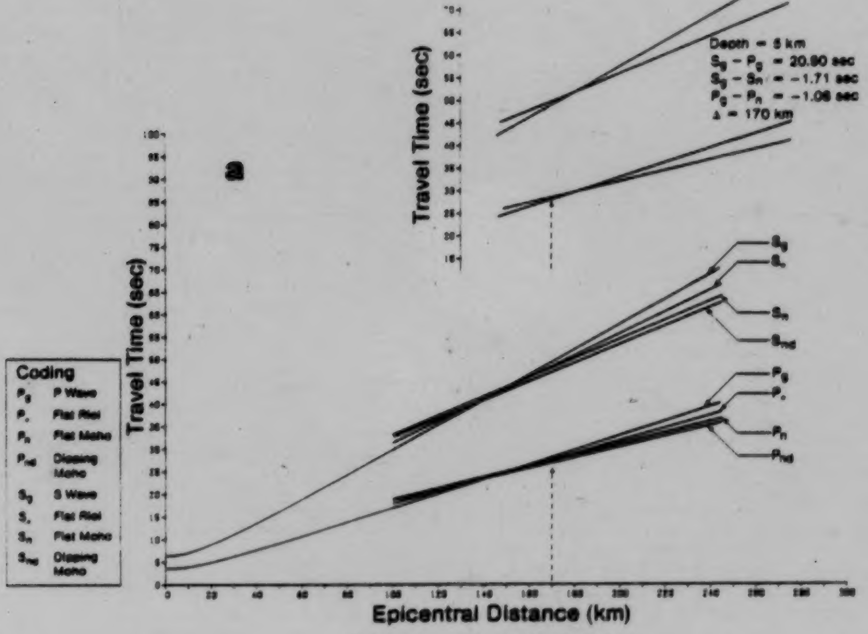

Source Depth 20 km

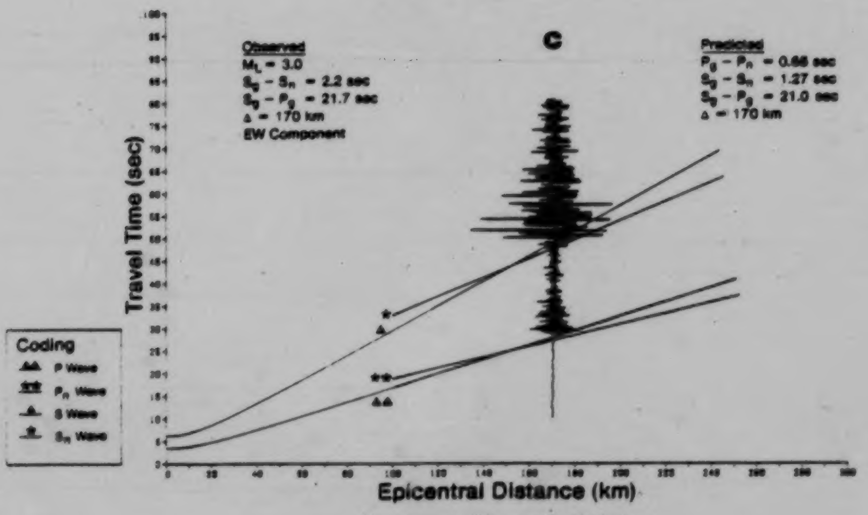

Source Depth 20 km

Figure 15.... Theoretical travel time curves for the Alberta model at different depths.The best match of Pg, Sn, and Sg with the theoretical travel time curves was for a source depth of 20 km.

simplified the characteristics of the velocity model and defined a priori reasonable bounds beyond which the solution of our inverse problem could not lie. I admit that 7 parameters are unknown to some degree. These are the average epicentral distance of the activity, the average depth of the activity, the P wave velocities of two layers and a half space and the layers thicknesses. I assumed that Poisson's ratio was 0.28 in order to relate S wave velocities to P wave velocities.

It is possible with a computer search algorithm (ZXSRCH from the IMSL library) to determine N possible heptads of numbers constrained within a 7 dimensional rectangle such that the N heptads are evenly distributed in the possible range (table 9) of the solutions. For no particularly good reason, other than the desire to limit computation, I set N to 1000 and let the computer find those heptads which define solutions to the inverse problem, Only two models fit (table 10). They both require focal depths in excess of 25 km.

Obviously a computer search of this type does not rigorously prove that dramatically different solutions do not exist between the points tested. I do however have now a reasonable basis for the statement that at least some of the seismicity at Rocky Mountain House originates at depths which suggest natural rather than induced causes. I also state that this depth can be determined if Sn-Sg can be observed.

165km	≤ Epicentral Distance	≤ 180km
.1km	≤ Focal Depth	≤ 40km
5.0km/sec	≤ Vp Velocity of the first layer	≤ 6.5km/sec
30.0km	≤ Thickness of the first layer	≤ 35.0km
7.0km/sec	≤ Vp Velocity of the second layer	≤ 7.6km/sec
10.0km	≤ Thickness of the second layer	≤ 20.0 Km
7.9km/sec	≤ Vp velocity of the half space	≤ 8.3km/sec

Table 9.... The bounds on the search for feasible models of the velocity structure

H	Vp	Vs	H	Vp	Vs
34.14	6.25	3.45	30.83	6.25	3.45
14.10	7.30	4.04	10.80	7.50	4.15
H. S.	8.10	4.48	H. S.	8.23	4.55

Table 10.... The only satisfactory models in a suite of 1000 reasonable ones

There is also shallow seismicity at Rocky Mountain House. One week of observations with Sprengnether DR100 recording system (Rebollar et al. 1981) found mainly shallow activity but one event with an S-P time of 2.1 seconds. Unfortunately this event cannot be located, for the Earth Physics Branch portable analog stations, and the Edmonton digital station were down. A program of recording at Rocky Mountain House is continuing in order to acquire data for several swarm events recorded both at Rocky Mountain House and EDM. This would provide final confirmation of deep seismicity at Rocky Mountain House and raise the very interesting problem of its cause.

Even with good observations of Sn the calculation of depth is problematical. A major change in the structure between EDM and Rocky Mountain House would destroy the conclusions. Then the identification of the phase I call Sn can be doubted. Proof will consist of simultaneous observation at EDM and at Rocky Mountain House of a deep event. I suggest this may be difficult. In 5 years there were 48 events on which Sn could be picked at EDM, so it may take some time to establish the case for seismic activity in the basement structures of the Rocky Mountain foothills.

3.4 Spectral Analysis

In order to extract good source information, high sampling rate high-dynamic range and a broadband system are desirable. However, there are some cases were digital data of lower quality will still produce some spectral information. Unfortunately the digital data for the Rocky

Mountain House Earthquake swarm is of the latter type. EDM was designed to detect teleseismic activity. It has a sampling rate of 18 samples per second and a reliable band of frequencies between 0.5 and 7 hz.

Our basic data are the 3 digitized components of the S phases of the signals identified as originating in the Rocky Mountain House area. These were always band pass filtered in this range of frequencies. By suitable rotations I isolated SH on the transverse component and combined the vertical and radial components of SV to isolate pure SV wave.

Clowes and Kanasewich (1970), studying the attenuation in Southern Alberta, found a Q of 300 in the sedimentary layers and a Q of 1500 for the basement. Therefore I approximate the attenuation with a Q of 1000 in order to take into consideration the sediments. The signal was corrected for attenuation, instrument response and distance. I use a sample length of 20 seconds in which is included Sn, Sg and scattered waves near the station. The seismic spectra was calculated and smoothed with a Daniel window of 0.2 Hz (figure 16). Corner frequencies were difficult to recognize in many cases due to the narrow bandwidth.

Source parameters can be derived from these spectra (Brune, 1970, 1971). Since only one station was used in this study, the radiation pattern was approximated as the rms average over the focal sphere for S waves (0.63). I calculate the correction for amplification at the free surface for SV waves using Nutlli's formulation (1961). The

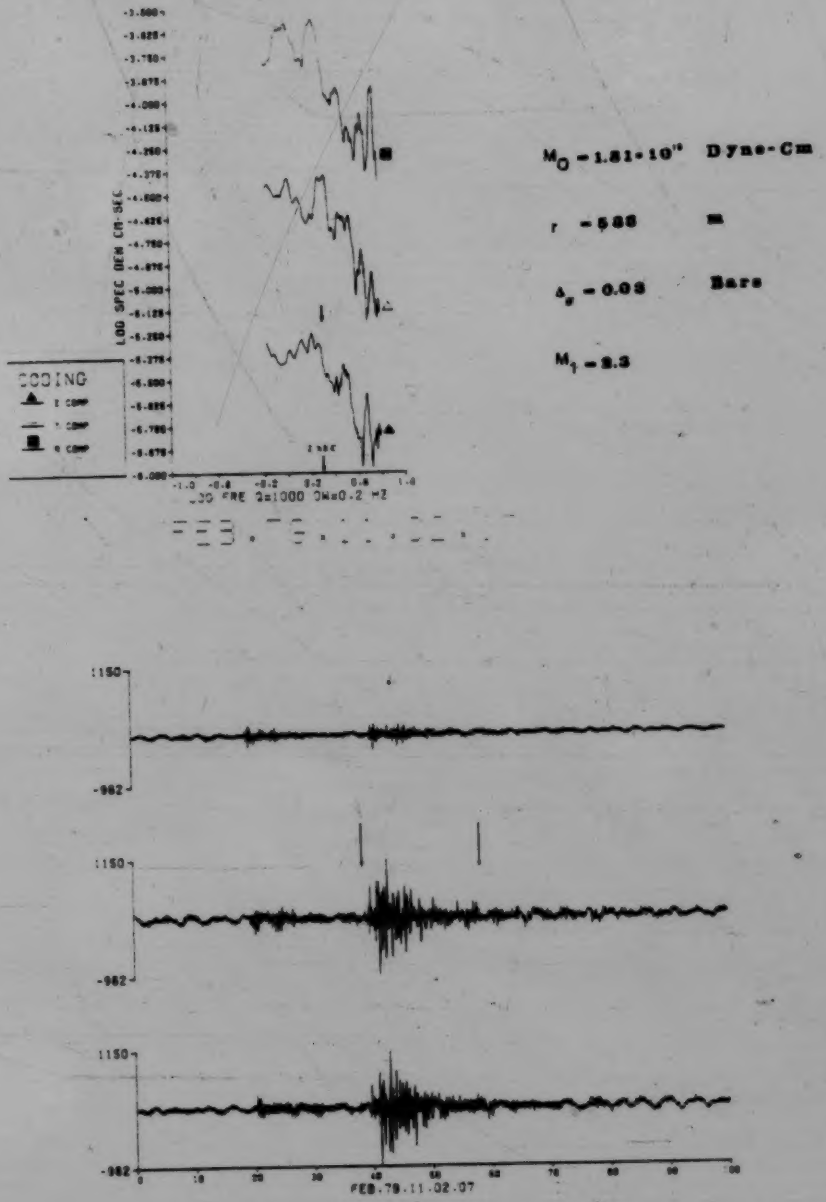

Figure 16.... Spectra of typical events. The amplitude of radial and tangential components has been increased in order to plot them together. The spectra were smoothed with a Daniel window -DW- of .2 Hz

correction for free surface amplification is 1.04 for SV vertical component and 1.75 for SV radial component considering an angle of incidence of 24.5 degrees.

The source parameters, seismic moment M_o, source radius r and stress drop are related (Brune 1970, 1971) to the spectral characteristics by

$$M = 4\pi\rho R\beta^3\Omega(0)/\mathcal{R}A \qquad \text{dyne-cm}$$

$$r = 0.37\ \beta/f_c \qquad \text{km}$$

$$\Delta\sigma = 106\rho R\Omega(0)f_c^3/10^6 \qquad \text{bars}$$

where β=3.37 km/sec is the S wave velocity, ρ=2.9 g/cc is the density, Ω = spectral amplitude at zero frequency, fc=corner frequency, R=epicentral distance, $\mathcal{R}$ = radiation pattern, A free surface amplification.

Computations were made on the spectra of 78 events. Usually the seismic moment calculated with the SH wave components was higher than that calculated with SV (table 11). This could be an effect of the fault orientation. The average seismic moment of each event was used. The corner frequencies was identified (between 1.8 and 2.9 sec) for 34 events. Those corner frequencies gave source radii from 500 to 600 meters and stress drops from 0.01 to 1.5 bars (figure 17). Obviously at this epicentral distance and with this

Occurrence Time (M.Y.D.H.M)	Seismic Moment M_0 dyne-cm	Source Dimension r	Stress Drop Δσ bars	M_L
JAN.76.25.19.27	3.87×10^{20}	557	0.16	1.8
JAN.76.26.19.37	4.13×10^{20}	569	0.78	2.5
JAN.76.27......	1.54×10^{19}	522	0.38	...
JAN.76.30.15.07	4.19×10^{19}	685	0.03	2.1
FEB.76.08.23.04	8.40×10^{19}	611	0.13	2.2
MAR.76.10.03.49	1.56×10^{19}	...	....	1.8
MAY.76.13.04.48	4.80×10^{19}	544	0.10	2.0
MAY.76.13.08.28	5.14×10^{19}	497	0.14	2.2
SEP.76.13.10.24	6.07×10^{19}	544	0.11	2.3
SEP.76.14.02.44	5.43×10^{19}	478	0.19	2.3
OCT.76.13.10.54	9.03×10^{19}	537	0.20	2.4
OCT.76.15.15.33	9.19×10^{20}	594	1.55	2.3
NOV.76.03.11.42	5.08×10^{19}	623	0.07	2.3
DEC.76.02.03.38	2.19×10^{20}	...	....	3.0
DEC.76.09.07.28	3.87×10^{20}	587	0.58	2.9
DEC.76.23.22.18	2.73×10^{20}	638	0.37	2.8
JAN.77.30.08.29	5.09×10^{19}	850	0.03	2.5
MAR.77.01.07.49	6.31×10^{19}	...	....	...
APR.77.12.17.14	1.69×10^{20}	499	0.38	2.0
MAY.77.22.17.33	2.22×10^{20}	...	....	3.0
JUL.77.02.20.46	1.73×10^{20}	497	0.40	2.6
JUL.77.20.01.23	3.52×10^{19}	520	0.07	2.2
JUL.77.25.01.38	2.61×10^{19}	555	0.02	1.5
JUL.77.25.08...	8.23×10^{19}	...	....	1.6
JUL.77.26.05.11	3.96×10^{19}	544	0.09	2.0
JUL.77.26.07.26	4.32×10^{19}	595	0.06	2.1
JUL.77.27.04.27	1.02×10^{19}	...	....	2.0
JUL.77.27.12.46	1.74×10^{19}	...	..	2.8
JUL.77.29.15.29	1.37×10^{20}	583	0.21	2.2
JUL.77.31.02.58	4.95×10^{19}	530	0.10	2.5
AUG.77.13.06.24	1.82×10^{19}	485	0.34	1.8
AUG.77.27.11.51	4.08×10^{20}	...	..	3.1
SEP.77.08.10.33	1.13×10^{20}	...	....	2.6
SEP.77.08.10.55	2.72×10^{19}	..	....	2.0
SEP.77.11.07.18	1.16×10^{19}	...	....	1.8
OCT.77.26.00.34	1.47×10^{21}	683	1.58	3.4
OCT.77.08.21.33	9.82×10^{19}	571	0.14	2.5
OCT.77.31.08.31	3.29×10^{19}	539	0.06	2.2
NOV.77.11.11.31	2.33×10^{19}	...	....	3.0
DEC.77.06.19.28	4.62×10^{19}	...	....	2.3
DEC.77.22.07.38	2.34×10^{19}	...	....	1.9
DEC.77.23.20.52	2.13×10^{20}	...	....	2.8
DEC.77.28.11.03	2.05×10^{19}	539	0.04	1.9
DEC.77.30.21.35	1.13×10^{20}	...	....	2.6
DEC.77.31.10.16	1.88×10^{19}	631	0.01	1.8
JAN.78.14.08.28	9.89×10^{19}	...	....	2.5
JAN.78.21.00.11	2.55×10^{19}	...	....	2.0
FEB.78.13.00.01	1.92×10^{19}	...	....	...
FEB.78.28.03.18	3.48×10^{20}	...	....	2.7
MAR.78.10.14.33	1.88×10^{19}	510	0.33	1.8
MAR.78.14.05.51	2.47×10^{19}	...	...	...
JUN.78.26.06.11	6.46×10^{19}	581	0.03	1.9
JUN.78.28.08.07	1.40×10^{19}	581	0.02	2.2
JUL.78.03.06.45	1.20×10^{19}	...	....	2.2
JUL.78.08.02.37	2.01×10^{19}	...	....	2.3
JUL.78.18.22.16	1.75×10^{20}	520	0.42	3.2
JUL.78.19.06.50	1.66×10^{19}	...	....	2.3
JUL.78.21.17.15	2.74×10^{19}	...	....	2.5
AUG.78.14.01.09	2.58×10^{19}	...	....	2.3
AUG.78.15.01.12	2.21×10^{20}	...	....	3.5
AUG.78.16.08.42	3.24×10^{19}	...	....	2.5
AUG.78.17.03.48	1.39×10^{19}	539	0.03	2.2
AUG.78.29.04.33	6.42×10^{19}	...	....	1.8
SEP.78.27.01.24	2.15×10^{19}	542	0.04	2.1
OCT.78.02.02.04	3.55×10^{19}	...	....	2.3
JAN.79.02.07.56	2.13×10^{19}	534	0.38	2.5
JAN.79.05.03.14	7.65×10^{19}	517	0.11	3.0
JAN.79.10.00.38	1.73×10^{19}	...	....	2.2
FEB.79.08.10.17	2.15×10^{19}	...	...	2.5
FEB.79.11.02.37	1.81×10^{19}	588	0.03	2.3
FEB.79.11.02.45	5.38×10^{19}	...	....	1.8
MAY.79.04.10.47	1.79×10^{20}	...	....	2.2
MAY.79.21.00.01	2.18×10^{19}	..	....	2.6
MAY.79.28.22.46	3.55×10^{19}	...	....	2.8
JUL.79.24.10.29	6.07×10^{19}	...	....	2.0
AUG.79.31.05.47	1.53×10^{19}	...	...	2.2
[illegible].79.[illegible].10.01	[illegible]			1.8
OCT.79.19.06.37	1.58×10^{21}			
OCT.79.21.05.13	2.89×10^{19}	...	....	2.7

Table 11.... Seismic moment, source dimension, stress drop, and local magnitude of some events of the Rocky Mountain House earthquake swarm

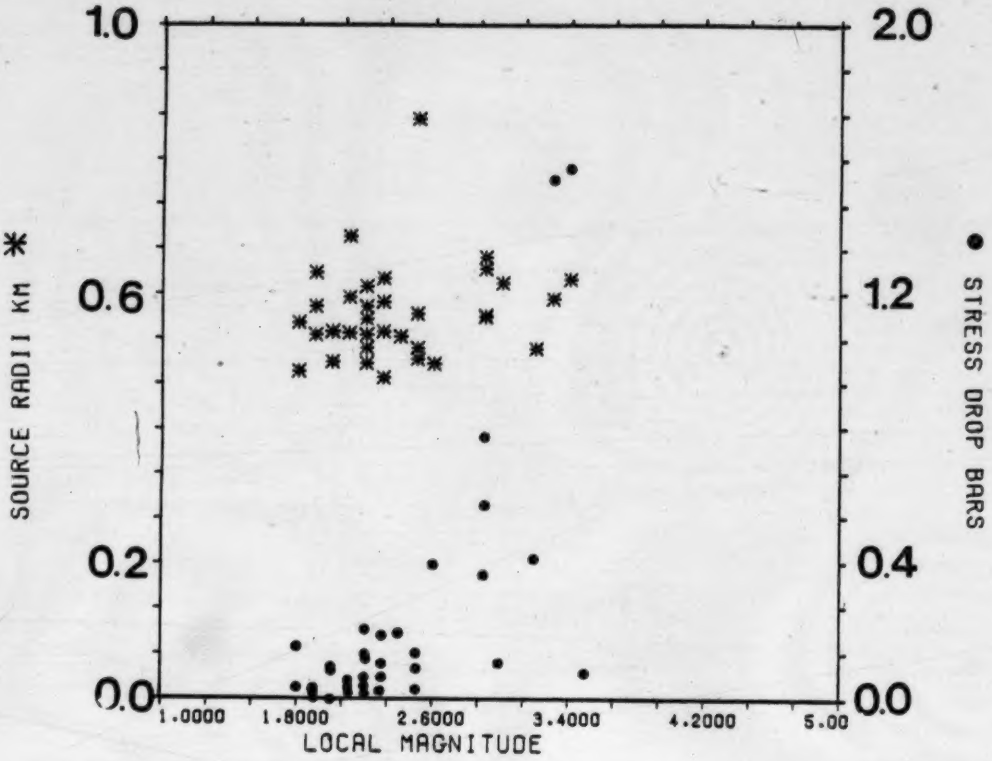

Figure 17.... Plot of local magnitude, source radii and stress drop.

narrow band system I sample only a restricted number of events.

3.5 Seismic Moment and Local Magnitude

Local magnitude is a useful measure of small earthquakes. Small earthquakes do not generate large surface wave amplitudes at periods of 20 seconds and at teleseismic distances the amplitude of P waves is small, so Mb and Ms are hard to determine.

Since I deal here with a relatively large collection of data which is individually rather uncertain, average behavior is probably the best representation of the spectral information. In addition to seismic moment local magnitude is relatively easy to determine and I have calculated local magnitudes for all events for which I have obtained seismic moments. Seismic moments range from 6.38×10^{18} ($M_l=1.6$) to 2.21×10^{20} ($M_l=3.5$) dyne-cm. A plot of M_0 against M_l shows more scatter (figure 18) than that on similar plots (Wyss and Brune 1968, and Thatcher and Hanks 1973). My linear trend is similar to theirs. The best fit to our data is

$$\log M_0 = 1.3M_l+16.6$$

This equation is a complicated function of source parameters, nevertheless, it can be interpreted in terms of a constant stress drop fault model (Kanamori and Anderson

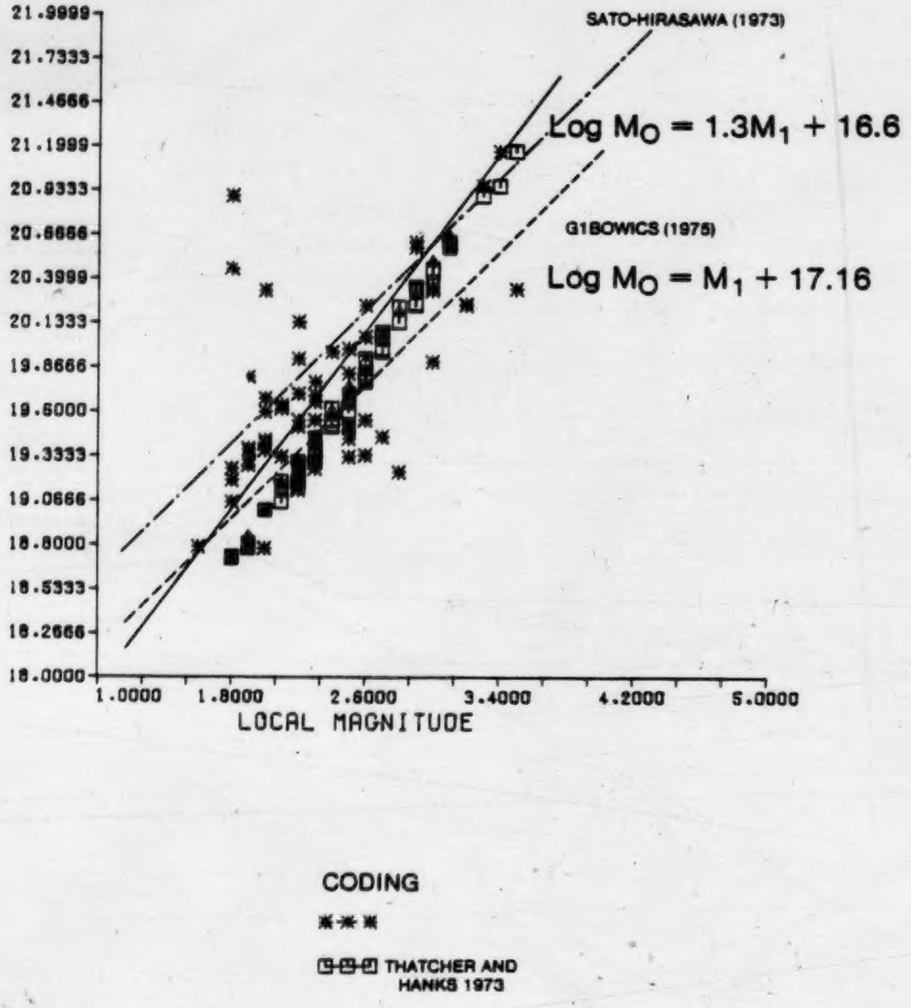

Figure 18.... Comparison of theoretical relationships between M_0 and M_1 for a circular fault with our experimental relationship, squares are the moments calculated using Thatcher and Hanks (1973) relation

1975, Sato 1979). I used the Sato and Hirasawa (1973) model for a circular fault in order to find a theoretical relationship between seismic moment and local magnitude. In general we can represent the spectral amplitude of the far-field displacement in the form

$$A(\omega) = M_o \mathcal{R} B(v, u, \tau, \phi, L, \text{or } r)/4\pi\rho R\beta^3$$

Where

ρ = density

R = epicentral distance

v = P or S wave velocity

u = rupture velocity

τ = rise time

r = source radius

L = fault length for a rectangular fault

$\mathcal{R}$ = radiation pattern

ϕ = azimuth

M_o = seismic moment

ω = angular frequency

B = source function

Local magnitude is defined as

$$M_L(0.8Hz)=\log A-\log A_0-1.35$$

where A is the recorded trace amplitude for a given earthquake at a given distance, and A_0 is that for a particular earthquake selected as standard (Richter 1958), and -1.35 is the correction for Edmonton station. Hence, substituting the spectral amplitude evaluated at a frequency of 0.8 Hz we have

$$M_L = \log M_o + \log\left[\frac{RB}{4\pi\rho R\beta^3}\right] + 2.05.$$

If we assume that all the events of the swarm have the same rupture velocity of 0.9 times the shear wave velocity, a shear velocity of 3.52 km/sec, a density of 2.9 gr/c^3, and rms average radiation pattern of 0.63 and a source dimension 2r of 1 km (this number comes from the spectral analysis) we get

$$\log M_0=M_L+17.6$$

for the Sato-Hirasawa model. This model seems to fit our data. The intercept (17.6) of the relationship, using Sato-Hirasawa model, was modeled for a wide variety of rupture velocities, shear wave velocities, densities, source dimensions, radiation patterns, and azimuths, using again the subroutine ZSRCH (IMSL, 1979). The best fit was found to be

$$\log M_0 = M_l + 17.1$$

assuming a shear and rupture velocity of the same magnitude (3.5 km/sec), a density of 2.8 gr/c^3, a source dimension of 100 meters a radiation pattern of 0.5 and a azimuth of 71°. Therefore, this search for a best fit tends to give smaller source dimensions, than those observed in our spectral analysis.

Gibowics (1975) calculated a similar theoretical relation using Randall (1973) graphical relations, assuming a circular fault and the asymptotic behaviour of the source function, given by

$$\log M_0 = M_l + 17.16$$

for source dimensions of less than 500 meters. This is essentialy the same relationship that I found.

It should be noted that the stress drops reported here are just that, fractions of an unknown absolute stress. The stress drops reported here are at best lower bounds on the actual values of the absolute stress.

3.6 Conclusions

Some of the events detected at Edmonton from the Rocky Mountain House Earthquake swarm appear to have a source depth of nearly 20 km. This conclusion is based on the match of refracted phases with theoretical travel time curves for a model of Central Alberta.

A portable digital seismic station, operated during August of 1980 at 52.26°N and 115.13°W, approximately 160 km SW of EDM, indicates mainly shallow activity (less than 6 Km). Nevertheless, there is one event with S-P time greater than 2 seconds, indicating a distant or deep event. Therefore, two kinds of activity, deep activity possibly associated with thrust faults of the basement of South West Alberta and shallow activity possibly induced by secondary and tertiary recovery methods in the Strachan gas field may exist.

Seismic moments calculated for events with local magnitude from 1.6 to 3.5 vary from 6.38×10^{18} to 2.21×10^{20} dyne-cm. A relation between seismic moment and local magnitude was found to be $\log M_0 = 1.3 M_L + 16.6$ for magnitudes from 1.6 to 3.5. This relationship is similar to that found in California by Wyss and Brune (1968) and Thatcher and Hanks (1972) for events with magnitudes in the range from 3.0 to 6.0. A theoretical relationship was calculated using Sato-Hirasawa (1973) model. A source dimension of one km and a rupture velocity of 0.9 the shear velocity was used. This relationship seems to fit our data best, and is essentialy the same calculated by Gibowics (1973). Source dimension and stress drop do not show any linear relation to local magnitude; this could be due to the poor resolution of our system.

In the next chapter I analyse the Rocky Mountain House earthquake swarm activity recorded at "short" epicentral distances (less than 6 km) by a Sprengnether DR-100 digital intrument. This provides further information on the reliability of source parameter estimates and a better insight into shallow activity.

4. Source parameters from shallow events in the Rocky Mountain House earthquake swarm

This chapter is based on a paper in press (Rebollar et al 1982). I report here source parameters of the Rocky Mountain earthquake swarm derived from three component digital data recorded on a nearby station. During 6 days in October 1980 21 events were recorded. Focal depths for these events are in the range of 2±2 km. Eleven events with local magnitudes from 2.1 to 2.8 yielded source parameters. Corner frequencies of the S-wave spectra were found in the range 6.2±0.5 Hz giving source dimensions of of 160±10 meters. The corresponding P-wave corner frequencies are in the range 8.6±3 Hz. The ratio of P to S corner frequencies varies from 0.9 to 2.1. There is a path effect between 13 and 16 Hz, that could have affected these ratios. The average fall-off over 3 components at high frequencies varies from -1.8 to -2.3. High stress drops, ranging from 47 to 263 bars and apparent stresses from 2.5 to 23 bars, were calculated. Five events have remarkably similar characteristics in the frequency and time domain. For these events the ratio of minimum strain energy W_0, according to Kanamori (1977), and the energy calculated using the integration scheme of Hanks and Thatcher (1972) was 3.7±0.5. A theoretical value gives 3.1. The seismic efficiency ranges from 0.2±0.04 to 0.17±0.8. Large seismic moments for a relatively small magnitudes were found. Some of these spectral characteristics are best explained as the result of displacement along a smooth fault.

During late September and early October of 1980, a local array of five analog vertical portable seismic stations was operated by R. J. Wetmiller of the Division Seismology and Geothermal Studies of Earth Physics Branch, Dept. of Energy Mines and Resources. One University of Alberta digital 3 component portable station was deployed near Rocky Mountain House Alberta in order to study the seismicity of the area. This area is the most active zone of seismicity in the South West Alberta. Some of this activity has been detected at Edmonton (Rebollar et al 1981). This is the first time that this kind of analysis has been done in South West Alberta at short epicentral distances (less than 5 km).

Events recorded by the analog and digital instruments were confined to an area of approximately 8 square km near 52° 12 N and 115° 14 W at a depth of 4±2 km (figure 19) (Wetmiller 1981). Those events may be confined in a hydrocarbon bearing sedimentary layer from the upper Paleozoic.

This study is mainly concerned with the evaluation of focal depths, and source parameters with a generally accepted source model (Brune 1970,1971). These source parameters are compared with already published data, theoretical models and results from laboratory experiments of shear crack displacements in an effort to explain their particular features.

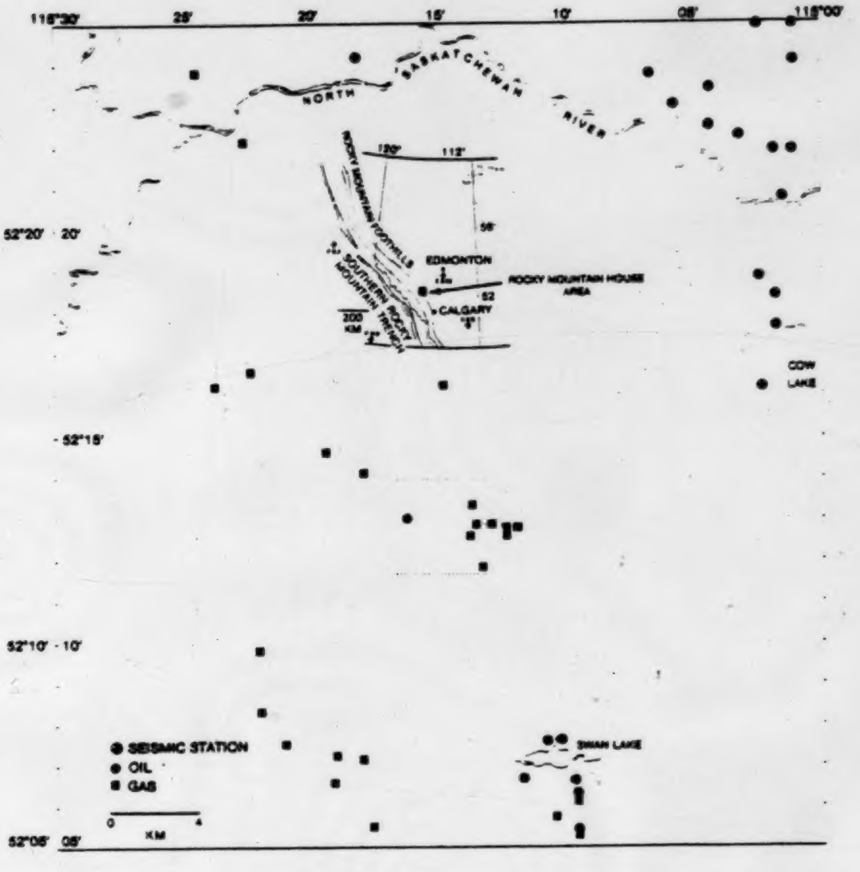
115°30'
25'
20'
15'
10'
05'
115°00'
NORTH SASKATCHEWAN RIVER
120°
112°
56°
ROCKY MOUNTAIN FOOTHILLS
SOUTHERN ROCKY MOUNTAIN TRENCH
EDMONTON
ROCKY MOUNTAIN HOUSE AREA
52
CALGARY
200 KM
52°20' 20'
COW LAKE
52°15'
52°10' 10'
SWAN LAKE
SEISMIC STATION
OIL
GAS
0
4
KM
52°05' 05'

Figure 19.... The location of the Rocky Mountain earthquake swarm. The dash square indicates the seismic locations reported by Wetmiller 1981 an the locations of the digital station. Almost all the locations were near the gas wells

4.1 Digital Recorder

A three channel Sprengnether digital recording system model DR-100 was used in this experiment. This recording system was connected to a five-pole antialiasing Butterworth filters and to Mark product L-4C-1.0 Hz seismometers, to provide a single 3 component portable station. The sampling rate used in this experiment was 100 samples per second. Absolute time was synchronized with the WWVB signal. A response curve for the combined recorder-seismometer for maximum gain of 120 and 60 db is given in (figure 20) The station was located at 52.23°N and 115.27°W, and operated from October 3 to October 9 1980 figure 19. The station was set up in sediments from the Cretaceous, and operated with a gain of 66 db due to local background noise (mainly wind generated and gas field activity).

4.2 Event Locations

In order to analyse the events we need a structural model. Richards and Walker (1959), from an approximately NS refraction profile near 113.5°W and between 50.8°N and 51.9°N, reported two sedimentary layers above the basement. The uppper one is of Mesozoic age with a thickness of 2 km and a P velocity of 3.6 km/sec. The lower one is from the Paleozoic with a thickness of 1.5 km and a P velocity of 6.1 km/sec (figure 21).

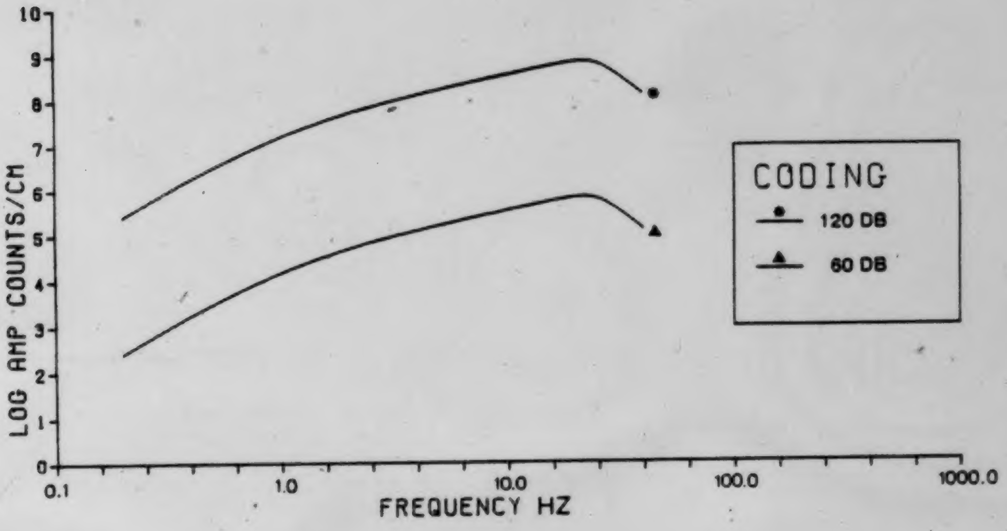

Figure 20.... Magnification curves of the digital station at 60 and 120 db. The station was operated at 66 db.

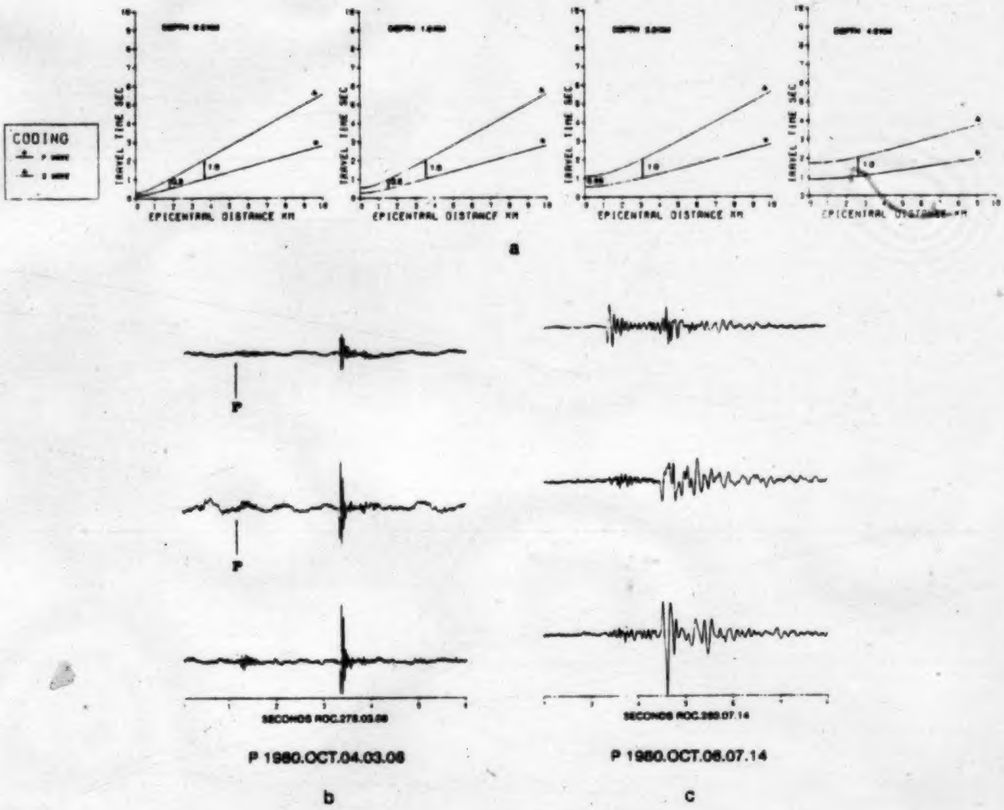

Figure 21.... Travel time curves for different depths using Richards and Walker model 1959. Arrows show S-P times of approximately .5 and 1 seconds of typical events. b) Possible deep event c) typical event

One of the events shows no discernible P or S waves. Five events are remarkable similar in all three components bottom of (figure 22) and (figure 23). This is not the first time that this kind of earthquakes has been observed. Geller and Mueller (1980), reported four similar earthquakes in central California at epicentral distances from 20 to 51 km. This also has been observed in the Victoria earthquake swarm of 1978 in the Valley of Mexicali, Mexico, and in the aftershocks of the Oaxaca eartquake of November 28 of 1978 (L. Munguia personal comunication). This similarity implies that they are clustered in space so that they sample the same path to the recording station. The maximum amplitude was recorded in the EW component, where there is a dominant signal with a period of about 0.2 sec, that correspond to a wave length of 0.6 km assuming a S phase velocity of 3.0 km/sec.

The S-P times of these events are in the range 1.0±0.4 seconds. The P arrival was read in the vertical component and the S arrival in the horizontal component. I calculated theoretical travel time curves using the Richards & Walker model (1959). A travel time curve for a source depth of two km gives an epicentral distance of 3 km, for a source depth of 4 km this correspond to an epicentral distance of 2.65 km. Deeper source depths do not predict the observed S-P time, for example a travel time curve for a source depth of 6 km predict a minimum S-P time of 1.2 seconds above the epicenter. Therefore these events have a source depth of

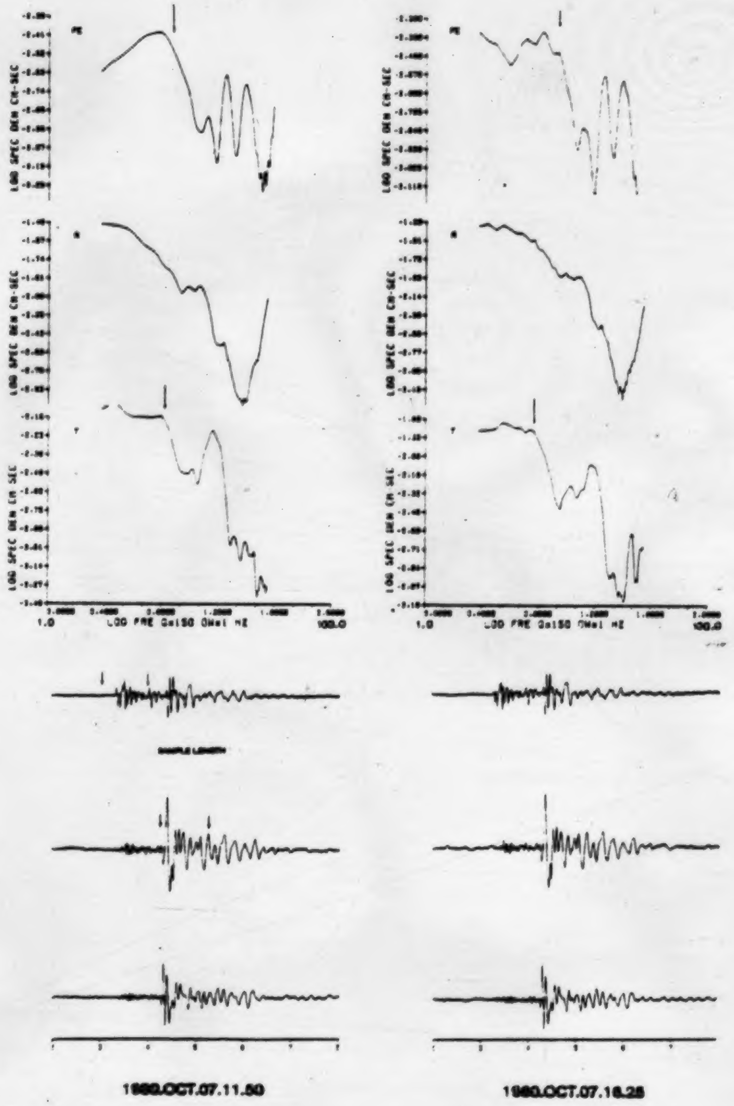

Figure 22.... Similar events and the spectra of the transverse T and radial component R of the S wave. PZ is the P-wave spectrum calculated from the vertical component, arrows show corner frequencies.

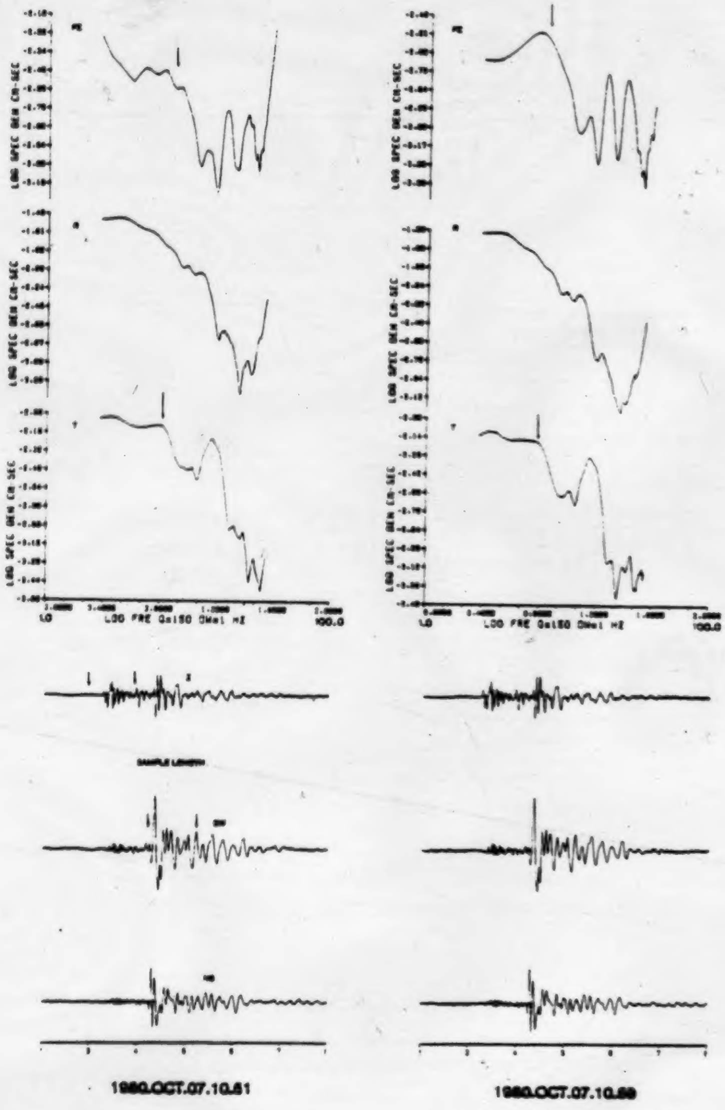

Figure 23.... Similar events and the spectra of the transverse T and radial component R of the S wave. PZ is the P-wave spectrum calculated from the vertical component, arrows show corner frequencies.

approximately 2±2 km figure 21.

These events do not have a large content of high frequencies, even though the station was very near the epicenter. It is well known that irregular rupture dislocations with variable slip and complex strength on the fault enhance high-frequency waves (Miyatake 1980a, 1980b). Perhaps these events correspond to a process in which a barrier is being repeatedly broken and healed. In this case the events share the same dynamic and kinematic characteristics. Another possibility is a collinear shear crack (Rudnicki and Kanamori 1981). Geller and Mueller suggest that the clustering and similarity indicates that these earthquakes can represent stress release at the same asperity.

One event with a relatively large S-P (2.1 sec) time was recorded, therefore is not possible to determine the approximate depth or epicentral distance. I filtered the signal for this event with different bandwidths and still observed clear P and S waves. Perhaps it is one of the deep events analysed using Sn phases at Edmonton. Unfortunately this event was not recorded at Edmonton (figure 21-b).

4.3 Calculation of the Spectra

Source parameters were calculated using Brune's (1970, 1971) model. This theory has been found to be valid in general both at short epicentral distances of a few kilometers and at teleseismic distances. See, for example, Hanks and Thatcher (1972), Hanks and Wyss (1972), and Hanks (1981) among others in an extensive literature.

Corrections applied before the calculation of seismic moment are: free surface reflection of SH or SV waves, radiation pattern, seismic attenuation, geometrical spreading, and instrument response. In this study eleven reliable events were used in order to get source parameters. Epicentral locations, azimuths and angle of incidence calculated by Wetmiller (personal comunication) were used. These events were rotated in order to have a "pure" SH wave in the transverse component, and the horizontal component of the SV wave in in the radial term. Corrections for free surface reflection of the radial and vertical component of SV waves were calculated using Nuttli's (1961) formulas. Taking into consideration short epicentral distances and the sedimentary layers of the South West Alberta, a Q of 150 was used to correct for attenuation in both S and P spectra. However, errors in the choice of Q are not critical because of short epicentral distances.

The sedimentary layers of the South West Alberta consist of shales, siltstones, sandstones, and carbonates with accumulations of hydrocarbons ranging in age from the Paleocene Period to the Cambrian period in the Paleozoic Era (Bokman 1963). Therefore, I assumed a P wave velocity of 5 km/sec, a density of 2.5 gr/cc and a Poisson ratio of 0.33 , in order to take into consideration the low velocity body waves of sediments reported by Richards and Walker (1959). Sample lengths of 1.0 and 1.5 seconds were used for S wave spectra and 0.5 seconds for P wave spectra. All the spectra were filtered between 1 and 45 Hz and smoothed with a Daniel window of 1 Hz.

4.4 Source Parameters and Discussion of the Spectra

Eighteen events with S-P times of the order of one second were analysed; of those eleven yielded source parameters. The spectra of these events show a significant path effect between 13 and 16 Hz in the transverse or North-South component and vertical component of the spectra. This effect is less prominent in the radial or East-West component. This path effect makes it difficult to recognize corner frequencies, and sometimes it suggests a spurious corner frequency at high frequencies, see figures 25 and 26. In the spectra of P waves this effect is even more noticeable, moving the corner frequency of four events up to 11 Hertz (figure 24). Spectra of some of the events are shown in (figure 25) and (figure 26). Similar events show a great resemblance in the spectra (figure 22 and 23).

Laboratory experiments have shown, that the spectra of waves radiated from the displacement of a homogeneous fault have a simple spectrum i.e. a low level amplitude an the fall-off at high frequencies with a few peaks decreasing in amplitude. However, displacement spectra from an

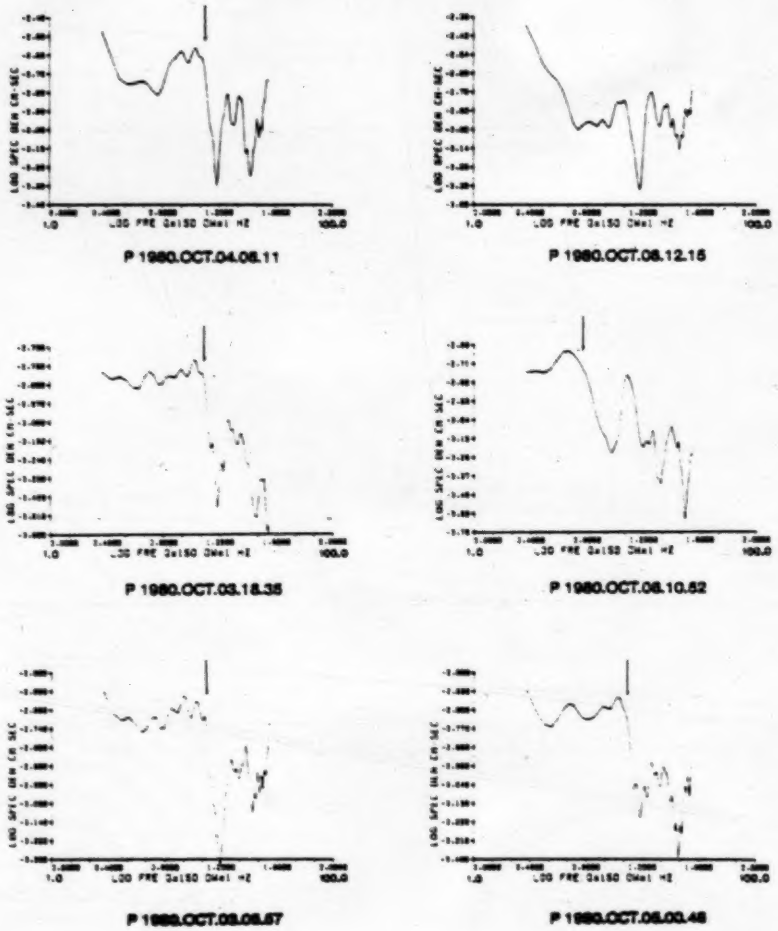

P 1980.OCT.04.06.11

P 1980.OCT.08.12.15

P 1980.OCT.03.18.35

P 1980.OCT.08.10.52

P 1980.OCT.03.06.57

P 1980.OCT.06.00.48

Figure 24.... P-wave spectra of the events of figures 25 and 26. These events show a possible path effect in the corner frequencies; P-wave corner frequencies were usually higher than S-wave corner frequencies

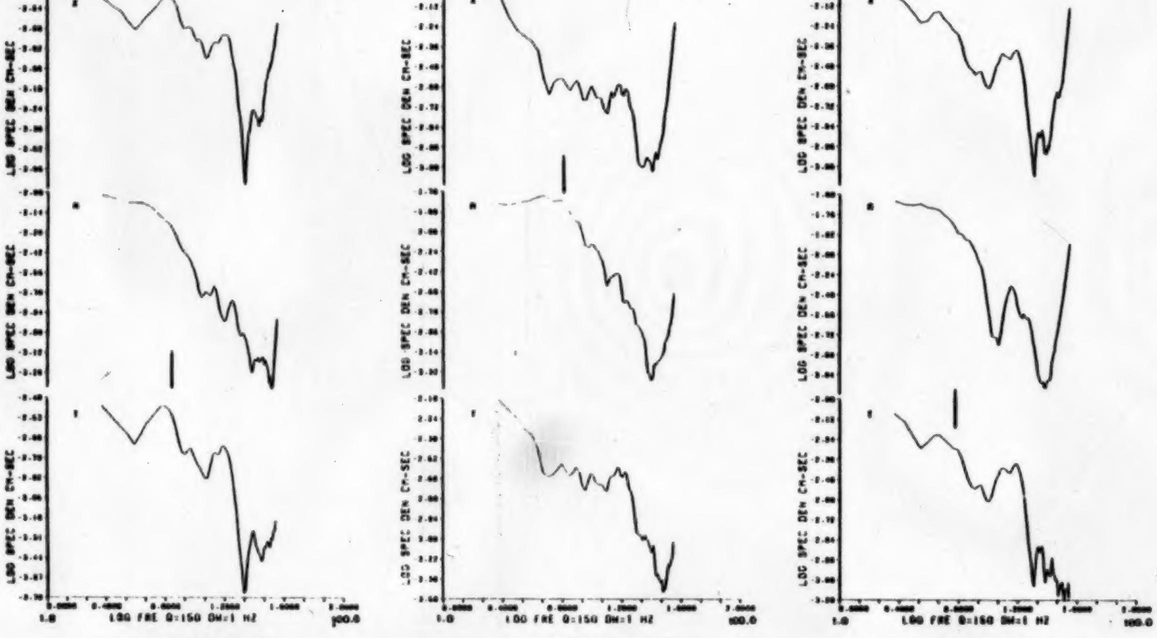

1980.OCT.03.05.57

1980.OCT.04.08.11

1980.OCT.08.10.52

Figure 25.... Spectra of the vertical Z, radial R, and transverse T component of the S-wave of the events used in this analysis. Arrows show corner frequencies. Some spectra show possible path inhomogeneities.

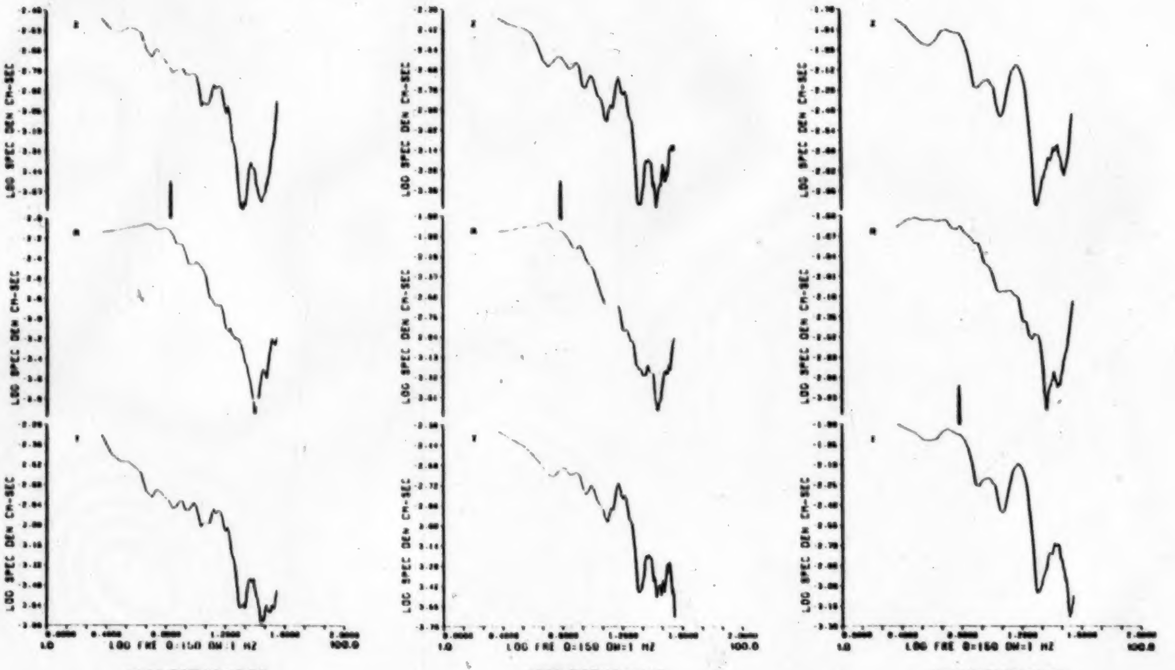

1980.OCT.03.18.35 1980.OCT.05.00.48 1980.OCT.08.12.15

Figure 26.... Spectra of the vertical Z, radial R, and transverse T component of the S-wave of the events used in this analysis. Arrows show corner frequencies. Some spectra show possible path inhomogeneities.

inhomogeneous fault (with asperities or obstacles) have a different form; the low level amplitude and the peaks in the fall-off at high frequencies are comparable in magnitude with the low level trend, suggesting two corner frequencies (Vinogradov 1978). Therefore, these results could explain high peaks at "high" frequencies in our spectra. However, the same experiments show that shear displacement along a homogeneous fault (without asperities) gives a high seismic moment for a relatively small magnitude. This is in agreement with our results. Since seismic moment is a more reliable parameter we conclude that those effects present in the observed spectra are more likely due to local inhomogeneities.

Corner frequencies were found in the range of 5.8 to 6.3 Hertz. This is equivalent to source dimensions from 161 to 148 meters. Some corner frequencies in the P wave spectra are strongly affected by path effects as can be seen in the spectra of figure 24. Hanks (1981) pointed out that source parameters calculated at a single station are more likely to be affected by path effects.

Stress drops for those 11 events were consistently high ranging from 47 to 263 bars. Previous work has found stress drops in the range of a few tenth of a bar to 100 bars for events with local magnitudes from -1.3 to 3.4, Wyss and Brune (1968), Douglas and Ryall (1972), Thatcher and Hanks (1972), Bakun et al (1976), Jonhson an McEvilly (1974), Fletcher (1980), Marion and Long (1980), and Rebollar et al

(1981).

Bakun et al (1976) reported stress drops of the order of 245 bars calculated from the spectra of P waves. Hartzell and Brune (1977) found stress drops in the range from 1 to 636 bars for 61 events of the Brawley earthquake swarm with magnitudes from 1 to 4.7.

Stress drops of possible deep events of the Rocky Mountain House earthquake swarm are of the order of a few tenths of a bar (Rebollar et al 1982). Since the shallow events have high stress drops this seems to contradict the observations that the stress drop increases with depth (Fletcher 1980, and Hartzell and Brune 1977). However, this observation could indicate that shallow events might be an indirect consequence of the extraction of oil and gas whereas deep events are more likely of tectonic origin. Figure 19 shows the epicenter area reported by Wetmiller (1981). Those epicenters tend to lie near the gas wells of the Strachan fields.

Source parameters of the five similar events are more homogeneous, reflecting almost the perfect match in the seismograms. A plot of local magnitude versus seismic moment (figure 27) shows consistently large seismic moments for this range of magnitudes. However, they follow the same slope as the relation $\log M_o=1.3M_l+16.6$ (Rebollar et al 1981). Large seismic moments for relatively small magnitudes have been observed in laboratory experiments of shear sliding along a smooth fault (Vinogradov 1978). This could

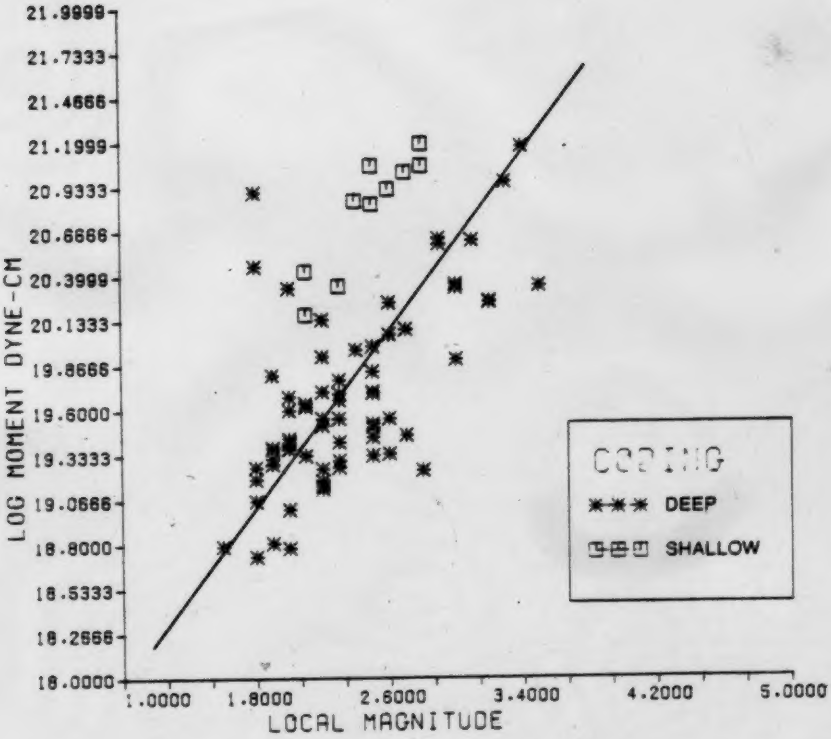

Figure 27.... A comparison of the relation of local magnitude versus seismic moment for deep events detected at EDM and shallow events recorded with the portable digital station. Heavy line is $\log M_0 = 1.3M_L + 16.6$.

explain those high moments, even though laboratory experiments are an over-simplification of a real earthquake.

The radiated energy E was calculated using Hanks and Thatcher (1972) integration scheme. They found an analytic expression by integrating the far-field shear displacement spectra proposed by Brune (1970), assuming a complete stress drop ($\epsilon=1$) and a fall-of at high frequencies of -2. Thatcher and Hanks (1972), however pointed out that uncertainities in the fall-of at high frequencies can give a misleading measure of the energy. In our case the average slope in the three components of the shear spectrum at high frequencies varies from 1.8 to 2.3 (table 12). Therefore, errors in the calculation of the radiated energy due to the slope at high frequencies are small. Most of the energy of small earthquakes is radiated in short period waves, hence, because of the small epicentral distances litle energy can be lost. Therefore, the integration scheme can give a better estimate of the radiated energy.

Energies range from 2.4×10^{15} ergs ($M_L=2.1$) to 2.1×10^{17} ergs ($M_L=2.8$). Radiated seismic energies calculated using Gutenberg and Richter, and Thatcher and Hanks empirical relations derived for California give smaller values, as we can see from (figure 28) This could mean that the integration scheme gives a better estimate of the radiated energy at short epicentral distances (less than 4 km).

Corner frequencies of P wave spectra were consistently larger than those of the S wave spectra. Only one corner

ID	RECORDING TIME	M_l	M_o	E_s	f_s	f_p	f_p/f_s	$\bar{\gamma}$	r	$\Delta\sigma$	η	$\eta\sigma$	$\Delta\sigma/\eta\bar{\sigma}$	Δ
1	1980.OCT.04.05.57	2.1	2.68×10^{20}	6.2×10^{15}	6.4	11.6	1.8	1.8	150	47.3	0.15	3.61	13.1	2.0
2	1980.OCT.04.18.35	2.1	1.47×10^{20}	2.41×10^{15}	6.7	11.6	2.1	2.0	169	62.1	0.08	2.56	24.2	1.0
3	1980.OCT.05.06.11	2.4	7.07×10^{20}	6.60×10^{16}	6.3	11.4	1.8	2.3	148	211.0	0.14	14.56	14.5	2.0
4	1980.OCT.06.00.48	2.3	2.21×10^{20}	8.28×10^{15}	6.3	11.3	1.8	2.2	148	74.7	0.16	5.84	12.8	1.0
5	1980.OCT.09.10.52	2.5	1.15×10^{21}	1.71×10^{17}	5.8	5.5	0.9	1.5	172	142.0	0.33	23.20	6.1	5.0
6	1980.OCT.09.12.15	2.8	1.56×10^{21}	2.18×10^{17}	6.3	-	-	1.9	150	263.3	0.17	21.80	12.08	3.0
				SIMILAR EVENTS										
7	1980.OCT.08.10.51	2.6	8.28×10^{20}	8.99×10^{16}	6.2	7.4	1.19	2.2	150	113.5	0.30	16.94	6.7	2.0
8	1980.OCT.08.10.59	2.5	6.70×10^{20}	5.30×10^{16}	6.0	7.1	1.18	2.1	155	92.1	0.27	12.34	7.4	2.0
9	1980.OCT.08.11.50	2.6	8.28×10^{20}	6.05×10^{16}	5.9	7.1	1.20	1.9	158	105.7	0.22	11.40	9.2	2.0
10	1980.OCT.08.16.25	2.8	1.15×10^{21}	1.39×10^{17}	5.8	7.3	1.26	2.2	161	146.0	0.26	18.86	7.7	2.0
11	1980.OCT.09.04.59	2.7	1.04×10^{21}	1.31×10^{17}	5.9	9.1	1.54	2.1	158	127.4	0.31	19.65	6.4	2.0

Notes

M_L = local magnitude, M_o = seismic moment (dynes-cm), E_s = radiated seismic energy (ergs), f_s, f_p = S-wave, P-wave corner frequency, γ = average fall-off of the spectra at high frequencies, r = source dimension (meters), $\Delta\sigma$ = stress drop (bars), η = seismic efficiency, $\eta\bar{\sigma}$ = apparent stress (bars), Δ = epicentral distance (km).

Table 12.... Spectral parameters for the events recorded in the portable digital station

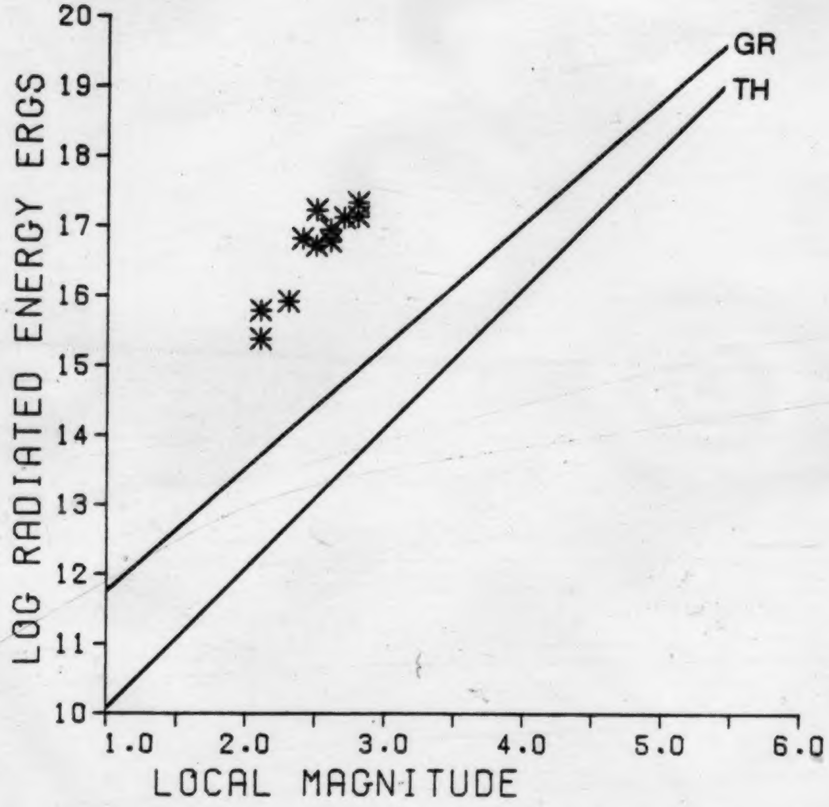

Figure 28.... Plot of local magnitude versus log of radiated seismic energy. GR is the Gutenber and Richter relationship and TH is the Thatcher and Hanks relationship.

frequency of P waves was found to be less than the corresponding corner frequency of the S wave spectra table 12. P wave frequencies seem to be more affected by local path effects. Those path effects are easily recognized because they appear in the same range of frequencies independent of the obvious variation in the radiation pattern that can be recognized by inspection of the seismograms. Ratios of the P and S frequencies (corner frequency shift) were found in the range of 0.9 to 2.1. However, the average ratio of fp to fs in the similar events is 1.2±0.2, more in agrement with the general observation that fp/fs is greater than one, and with theoretical models that treat earthquakes as equidimensional faults (Brune 1970, Madariaga 1976, Burridge 1975), or long and narrow faults with near-sonic or transonic rupture velocities (Savage 1974). Hanks (1981) suggests that the frequency shift is an intrinsic characteristic of the far-field spectra of body waves independent of source strength (seismic moment), hypocenter, epicentral distance or recording device.

The minimum strain energy drop W_0 (Kanamori 1977) is

$$W_o = \frac{\Delta\sigma}{2\mu} M_o$$

Which assumes a complete stress drop ($\sigma_2=0$) or if the Orowan (1960) condition is met ($\sigma_2=\sigma_f$). Substituting the moment and stress drop according to Brune (1970,1971), we get

$$W_o = \frac{212\pi}{1.26}\,\rho\beta R^2\Omega_o^2\ f_c^3$$

Where ρ is the density, β is the shear wave velocity, R is the epicentral distance, fc is the corner frequency, Ω_o is the low level amplitude of the SH spectra, and 1.26 is the product of the average radiation pattern and the free surface reflection of SH waves. The radiated seismic energy Es according to the integration scheme of Hanks and Thatcher (1972) is given by

$$E_s = \frac{128\ \pi^3}{15(1.26)^2}\,\rho\beta R^2\Omega_o^2\ f_c^3$$

Taking the ratio of W_o and Es we get $W_o = 3.1\ E_s$

If we assume that 1/3 of the seismic energy is contained in the P wave we have

$$W_o = 4.1\ E_s$$

This means that even though W_o is a minimum estimate of the energy, the integration scheme gives even lower values of the radiated energy. Values of W_o, Es, and the ratio of W_o/Es are given in (table 13). This ratio for the similar

M_L	MINIMUM STRAIN ENERGY DROP W_o (Kanamori, 1977)	RADIATED SEISMIC ENERGY E_s (Hanks and Thatcher 1972)	W_o/E_s
2.1	4.1×10^{16} ERGS	6.2×10^{15} ERGS	6.5
2.1	2.9×10^{16}	2.4×10^{15}	12.2
2.4	4.8×10^{17}	6.6×10^{16}	7.2
2.3	5.3×10^{16}	8.3×10^{15}	6.4
2.5	5.2×10^{17}	1.7×10^{17}	3.0
2.8	1.3×10^{18}	2.2×10^{17}	6.0
	SIMILAR EVENTS		
2.6	3.0×10^{17}	8.9×10^{16}	3.3
2.5	1.9×10^{17}	5.3×10^{16}	3.7
2.6	2.8×10^{17}	6.0×10^{16}	4.6
2.8	5.4×10^{17}	1.4×10^{17}	3.8
2.7	4.2×10^{17}	1.3×10^{17}	3.2

Table 13.... Comparison of minimum strain energy according to Kanamori 1977 and Radiated seismic energy by Hanks and Thatcher 1972

events is 3.7±0.5, in good agreement with the theoretical result ($W_o = 3.1 Es$) which does not include the contribution of the P-wave energy. However, events 1 to 6 give an average ratio of 6.8 with a large standard deviation of 3.

The apparent stress is defined (Wyss 1970) as

$$\eta\bar{\sigma} = \frac{\mu E_s}{M_o}$$

Where η is the seismic efficiency, $\bar{\sigma}$ is the average shear stress, μ is the shear modulus, E_s is the radiated seismic energy, and M_o is the seismic moment. Uncertainties in the evaluation of the apparent stress are a direct consequence of the uncertainties in the evaluation of the radiated energy. Therefore, the seismic efficiency is one of the most uncertain parameters in seismology. However, Wyss (1970) calculated a seismic efficiency of 0.1 for deep and intermediate earthquakes in South America. Apparent stress calculated by the Wyss formula range from 2.5 to 23.2 bars table 12. A plot of stress drop versus apparent stress can be compared with that calculated by Hartzell and Brune (1977). Even though there is some scatter it follow a similar trend (figure 29). Those differences indicate

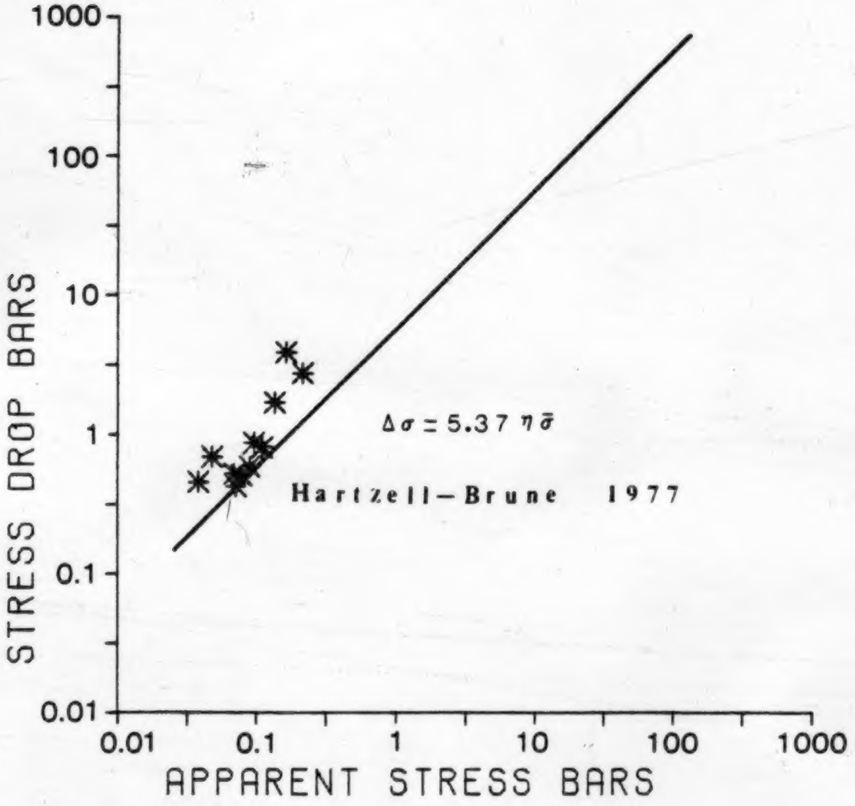

Figure 29.... Plot of apparent stress versus stress drop . The heavy line shows Hartzell and Brune 1977 relation for the Imperial Valley. Similar events have a relation of

regional variations in the apparent stress and consequently the state of stress in the crust of the Rocky Mountain House area.

The ratio of stress drop to apparent stress for similar events is almost constant at 7.4 with a standard deviation of 1.1. This ratio suggests a possible way to calculate absolute stress, however, in order to do this it is necessary to know the seismic energy and the frictional energy.

Following Wyss (1970), it is possible to calculate an approximate upper bound for the seismic efficiency given by:

$$\eta_{max} = \frac{2\eta\bar{\sigma}}{\Delta\sigma} \geq \eta$$

Seismic efficiency calculated in this way for the similar events gives a constant value of 0.2±0.04. This reflects the need to pick the correct corner frequencies in the spectra. Events 1 to 6 give 0.17±0.8 (table 12). These high values apparently suggest a high conversion of potential energy to elastic seismic energy for these shallow earthquakes.

4.4.1 Further Field Work

On September 19, 1981 I deployed, in the Strachan gas field, a Sprengnether DR-100 digital seismic station in order to detect deep seismic activity from the Rocky Mountain House earthquake swarm. This station is located at

52.23°N and 115.27°W, at the same place where it was located during the study of 1980. This station has been recording shallow activity (S-P times of less than one second), like that reported at the begining of this chapter, and possible deep activity.

During three months of observation two events were recorded both at the nearby station and at the analog and digital station of Edmonton. The first event occurred on September 23, 1981, and was recorded at 11 hours 37 minutes and 50.5 seconds at Edmonton. It has an S-P time of 20.5 seconds and does not show any refracted phase in the analog record. This could be due to its small magnitude (M_l=1.8). This event recorded in the Strachan gas field station shows a clear P and S wave. Due to drifting problems with the internal clock of the Sprengnether intrument in very cold weather, it is not possible to read with accuracy the arrival time of the signal. Even though the S wave saturated the instrument, it was possible to read an S-P time of 1.42 seconds, that is equivalent to a maximum epicentral distance of 11.5 km assuming a half space with a P wave velocity of 6 km per second. This also could be a possible deep event.

The second event was recorded at Edmonton on November 25, 1981, at 14 hours, 25 minutes, 12.5 seconds. This event with a local magnitude of M_l=2.8 show clear refracted phases in the analog system; it has a Sg-Pg of 20.8 seconds and a Sg-Sn of 1.2 seconds (A typical Sg-Sn in the digital records is 1.9 seconds). The Sprengnether station show clear S-P times of 1.54 seconds, that is equivalent to an epicentral distance of 12.6 km. Therefore, those events with S-P times of 1.5 seconds recorded in the portable digital station, if not definitely proving the existence of deep seismicity at least show the posibility of events with depths of more than 10 km, in agreement with our conclusion of chapter three. A definite solution of this problem requires the deployment of a network of three digital seismic stations for at least six months of continuous operation.

4.5 Conclusions

Events with S-P times of about one second, and source depths of 2±2 km, show different amplitudes of P and S waves, indicating dislocations with distinct fault orientations. Similar events have small variations in source parameters, perhaps indicating a process in which a barrier or asperity is being repeatedly broken and healed. Stress drops and apparent stress were consistently high for all the events. Hydrocarbon recovery operations can cause concentration of stresses in surrounding areas. This could result in brittle fracture in the sedimentary rocks or the granitic basement by activating ancient faults, joints, or by rupturing along pre-existing cracks. Laboratory experiments reveal a lesser accumulation of strain energy, and consequently stresses, in a closed fracture as compared with an open fracture (Shamina et al 1978). Therefore, high stresses could indicate a highly fracture zone, since stress drops represent minimum tectonic stresses related to the seismic events.

Radiated seismic energy calculated using $W_0=(\Delta\sigma/2\mu)M_0$ (Kanamori 1977) and Hanks and Thatcher (1972) give a ratio of 3.1; in good agreement with the observed ratio of 3.7±0.5 for the similar events. Larger energies were obtained for a given magnitude using Hanks and Thatcher (1972) method than those calculated using the empirical relationships of Gutenberg and Richter and Thatcher and Hanks for events in California. This could mean that the integration scheme gives a better estimate of the radiated energy at short epicentral distances (less than 4 km). Values of 0.2±0.04 and 0.17±.8 for the seismic efficiency were found, suggesting a high conversion of potential energy to elastic energy for these shallow earthquakes.

Corner frequencies of the S-wave spectra were found between 5.8 and 6.7 Hz, given source dimensions from 150 to 169 meters. The ratio of corner frequencies of P-wave and S-wave spectra give a value of 1.2±0.2 for the similar events, as is usually observed (Hanks 1981). However, corner frequencies for events 1 to 6 give ratios ranging from 0.9 to 2.1. These ratios could have been affected by local inhomogeneities. Evidence for such anomalies is found in our spectra between 13 and 16 Hz.

A plot of local magnitude versus seismic moment gives systematically large seismic moments for relatively small magnitudes. However, they follow the same trend as the relationship found for deep events by Rebollar et al (1981). Laboratory experiments show that displacement along a smooth fault is a possible mechanism of earthquakes with large seismic moments and a relatively small magnitude (Vinogradov 1978). This could explain those high moments.

5. Other seismicity of South West Alberta and Conclusions

Seismic records from the Edmonton seismological observatory since 1970 provide evidence for active seismic zones in the South West Alberta and in the Rocky Mountains. There is a seismic zone near Rocky Mountain House, and another near McNaughton Lake. An earthquake occurred in the Willmore Wilderness Provincial Park (The Willmore event) on October 9, 1977. The seismic moment of this event calculated at Edmonton from the SV spectrum was $6.7\pm2\times10^{22}$ dyne-cm. The seismic moment of the McNaughton lake earthquake of May 14, 1978 calculated from SV waves at Edmonton, was $7.6\pm2\times10^{23}$ dyne-cm. This compares reasonably with the value calculated from surface wave spectra (Rogers et al, 1980) at several stations.

During the last 10 years there has been a denser distribution of seismic stations in British Columbia than in Alberta. Alberta had only (table 14) two seismic stations in continuous operation (EDM and SES), making epicentral locations of micro-earthquake activity in South West Alberta difficult. Earth Physics Branch of Canada usually reports in its monthly bulletin, unlocated events detected in a single station. Those events recorded at Edmonton usually have local magnitudes between 1.7 and 2.5 and typically S-P times between 19 an 22 sec.

Seismic zoning maps of Canada, (Whitham and Milne 1972, Whitham et al 1970, Whitham 1975), suggest that the South West Alberta and the Alberta Plains lies in the zero zone.

Station	Start-up	Shut-down	Latitude	Longitude
EDM	?/04/63		53.2217N	113.3500W
SES	5/11/66		50.3958N	111.0417W
PHC	?/12/62		50.7070N	127.4370W
GDR	4/28/78		49.7817N	126.0550W
ALB	3/22/62	7/01/72	49.2720N	124.8300W
ALB	9/11/75		49.2720N	124.8300W
FSJ	5/12/65	4/17/79	54.4630N	124.2800W
HYC	9/01/75		49.2656N	122.5731W
PGC	?/08/78		48.6500N	125.4508W
PIB	11/01/75		48.8167N	123.3167W
PNT	1960		49.3167N	119.6167W
SKB	10/20/78		53.2478N	131.9963W
FSB	4/30/79		54.4767N	124.3283W
MCE	6/04/77		52.0030N	118.5620W
CUM	10/15/72		52.0869N	118.2117W
DAI	10/15/72		52.1986N	118.3844W
DWN	1/28/77		51.4656N	118.4681W
MCV	9/16/74		52.0081N	118.5608W
SPR	8/12/73		52.0153N	117.2564W
TAB	10/18/72		51.7511N	117.7617W
THO	10/15/72		52.6892N	119.1208W
VIC	1898	3/29/78	48.5200N	123.4200W
QCC	7/24/71	7/13/77	53.2550N	132.0883W
BLU	12/12/72	6/06/77	52.1533N	119.2764W

Table 14.... Active seismic stations in British Columbia and Alberta

In this zone the annual probability that accelerations of more than 0.01 g will occur is less than 1 %. This probably reflects the low level of seismicity in South West Alberta, but it could also reflect the detection threshold of the permanent stations (M, near 3.5).

5.1 Previous Studies

A seismicity map of Canada (figure 9) shows a great scatter of events along the Rocky Mountains. Historical and recent earthquakes have been located close to McNaughton lake in the Rocky Mountains (Rogers and Ellis 1979, Rogers et al 1980). This is the most active zone in the Rocky Mountain Trench. Some of this activity (events with magnitudes greater than 3.4) has been detected at Suffield (SES), Penticton (PNT), and Fort St. James (FSJ), and located by the Seismological Service of Canada, Department of Energy Mines and Resources, Ottawa.

Previous studies of seismicity in Western Canada have been concerned with the offshore seismicity of British Columbia, its tectonic relation with major plate boundaries and the detection threshold of the Canadian Network in Western Canada (Milne et al 1978). This study is mainly concerned with the description and interpretation of records of micro-earthquake activity in South West Alberta recorded at the Edmonton seismological observatory (EDM).

Of all the events recorded at Edmonton from the Rocky Mountain House earthquake swarm (table 15), fifteen events with clear Sn refracted phases were located by Ottawa.

A recent example of activity in this area, the Willmore earthquake (figure 30), occurred on October 9, 1977. It was located at 53.63°N and 118.29°W had a focal depth of 18 km, a reported magnitude of 3.3 (Ms) and 4.4 (mb). The McNaughton Lake earthquake of May 14, 1978, (Rogers et al

Date	Arrival Time	Epicentral	Location	Ml
M.D.Y.	H.M.S.	LATITUDE	LONGITUDE	MAGNITUDE
Jun2276	03.37.48	52.13°	115.24°	$M_1=2.7$
Sep1376	10.24.20	52.27°	115.42°	$M_1=2.2$
Oct1576	09.47.53	52.22°	115.39°	$M_1=2.1$
Oct2376	02.31.12	52.25°	115.46°	$M_1=2.3$
Dec0976	07.27.36	52.13°	115.22°	$M_1=2.8$
Dec2376	22.17.48	52.20°	115.29°	$M_1=2.8$
Dec3076	12.53.23	52.20°	115.34°	$M_1=2.5$
Dec3076	13.36.33	52.25°	115.46°	$M_1=1.5$
Jul0277	20.39.50	52.09°	115.18°	$M_1=2.7$
Jul0577	20.40.25	52.11°	115.14°	$M_1=2.4$
Jul2077	01.22.57	52.23°	115.24°	$M_1=2.0$
Jul2477	09.07.30	52.19°	115.23°	$M_1=3.5$
Jul2477	11.24.20	52.10°	115.13°	$M_1=2.3$
Jul2477	17.49.57	52.18°	115.22°	$M_1=3.4$
Jul2777	02.17.43	52.24°	115.30°	$M_1=3.2$
Jul2977	15.28.43	52.06°	115.15°	$M_1=2.1$
Jul3177	02.58.30	52.15°	115.20°	$M_1=2.7$
Aug1177	08.51.18	52.26°	115.34°	$M_1=2.8$
Aug1377	06.24.26	52.29°	115.32°	$M_1=2.2$
Aug1477	21.43.37	52.28°	115.21°	$M_1=3.7$
Aug1477	21.46.25	52.15°	115.15°	$M_1=2.5$
Aug1477	21.48.27	52.20°	115.19°	$M_1=2.8$
Aug2777	11.51.33	52.19°	115.24°	$M_1=3.1$
Sep0877	10.43.10	52.15°	115.19°	$M_1=2.4$
Oct2677	00.34.01	52.27°	115.26°	$M_1=3.5$
Jan1478	08.27.59	52.17°	115.23°	$M_1=2.3$
Jan2178	00.10.60	52.40°	115.36°	$M_1=1.8$
Feb2678	03.18.16	52.06°	115.24°	$M_1=2.8$
Sep2778	01.23.54	52.37°	115.41°	$M_1=2.1$
Oct0278	02.04.31	52.21°	115.46°	$M_1=2.2$
Jan0179	18.43.48	52.22°	115.35°	$M_1=2.5$
Jan0279	07.56.21	52.25°	115.39°	$M_1=2.4$
Jan0579	03.14.03	52.24°	115.38°	$M_1=2.8$
Feb0979	10.17.13	52.17°	115.31°	$M_1=2.2$
Feb1179	02.07.15	52.19°	115.31°	$M_1=2.3$
May2879	22.46.09	52.14°	115.14°	$M_1=2.7$
Jan0880	16.31.14	52.22°	115.22°	$M_1=2.3$
Jan0980	23.43.22	52.17°	115.07°	$M_1=2.2$
Jan2380	05.07.60	52.25°	115.12°	$M_1=2.0$
Sep0480	17.49.25	52.21°	115.32°	$M_1=2.7$
Sep0480	20.33.54	52.19°	115.35°	$M_1=2.7$
Sep0480	21.03.31	52.17°	115.33°	$M_1=2.6$
Sep1680	01.32.60	52.21°	115.25°	$M_1=3.0$
Sep1780	09.58.09	52.22°	115.24°	$M_1=3.4$
Oct2980	03.23.48	52.17°	115.19°	$M_1=2.1$

Table 15.... Events located by Earth Physics Branch of Canada from the Rocky Mountain House area since 1976.

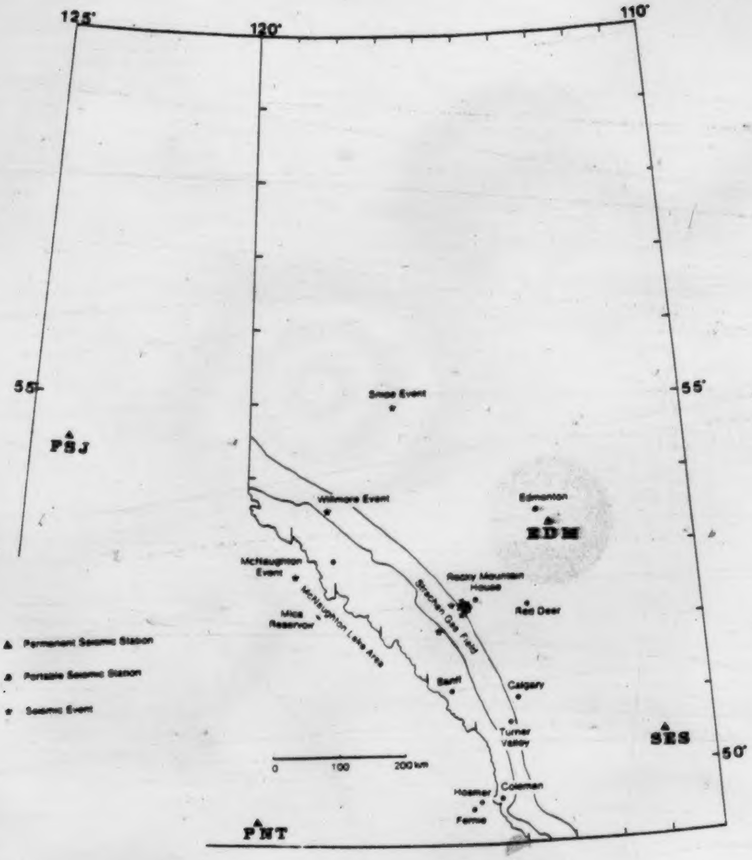
125°
120°
110°
55°
55°
50°
PSJ
PNT
SES
EDM
Snipe Event
Willmore Event
McNaughton Event
Mica Reservoir
McNaughton Lake Area
Strachan Gas Field
Rocky Mountain House
Edmonton
Red Deer
Banff
Calgary
Turner Valley
Coleman
Hosmer
Fernie
0
100
200 km
▲ Permanent Seismic Station
▲ Portable Seismic Station
★ Seismic Event

Figure 30.... Location of Snipe, Willmore and McNaughton events and some events located by EPB from the Rocky Mountain House earthquake swarm. Dash are depict maximum S-P time recorded ar EDM equivalent to 120 km

1980) showed .8 right-lateral strike slip faulting combined with .5 of thrust movement. The preferred fault orientation is N10°W. The maximum principal stress axis is nearly horizontal oriented in a northeast direction.

Earthquake swarms have been observed before and after the impounding of the McNaughton lake reservoir (Ellis et al 1976). Ellis and Chandra (1981) analysed the seismicity of the McNaugthon lake reservoir. They found an average of one earthquake with magnitude $M_l \geq 3$ every 2 years in the period of 1963 to 1972, and four earthquake swarms sequences in the period of 1973 to 1978. They suggest that the activity is mostly of tectonic origin. Earthquake swarms have also been observed near Bella Coola British Columbia and near Mould Bay (Milne et al 1969). Rogers (1981), based on the decreasing age of the Anahim volcanic belt from the coast to the Rocky mountains, the high level of seismic activity and the relocation of recent and historical earthquakes, suggests the possible existence of an active hot spot beneath the Rocky Mountains, near McNaughton lake.

In the Plains an earthquake occurred in 1909 in Southern Saskatchewan with a probable magnitude of 5.5 (Stevens 1977). More recently an event occurred in 1968, 50 km north-east of Bengough close to Amulet with a magnitude of mb=2.9 (Horner et al 1973). In 1972 the Bengough event occurred at approximately 49.35°N and 104.93°W. This event, in spite its small magnitude (mb=3.7), was throughly analysed by Horner et al (1973). They studied intensity isoseismals, magnitude, epicenter location, focal depth (approximately 10 km), and focal mechanism. In order to calculate the focal mechanism they used the radiation pattern of Love waves for a shallow event. The Bengough event was probably strike slip, striking approximately N 30° E.

No historical earthquakes have been reported in the South West Alberta or the Alberta Plains. However, the Snipe Lake earthquake, of magnitude mb=5.1, occurred on March 8, 1970. This event was felt over approximately 100,000 km^2 in west central Alberta. It was located near 55° N and 116.5° W with a probably focal depth of 9 km (Milne 1970). Even though the magnitude of this event was relatively high for this part of Canada it was not recorded clearly in many stations. Therefore, no fault plane solution is available, and the probably cause of this event is unknown. It occurred in an area where oil and gas is produced.

Milne and White (1958), using three seismic stations in the Crowsnest Pass area of Alberta and British Columbia during a period of three, years found a correlation between coal mining activity and seismic events. An average of five bumps per day was recorded in active mines. Using a small array (figure 30) at Fernie, Hasmer, and Anderson showed that the locations were confined near the coal mines. Local events detected at stations located at Fernie, Coleman, Turner Valley and Banff showed that there are micro-earthquakes (with magnitudes less than 3) extending from the International Border to Banff. The distribution seemed random in the South West Alberta and in the Rocky Mountain Range. However, this could be due to a poor time control. No relationship between mine tremors and local earthquakes was found.

5.1.1 Seismicity in South West Alberta as Seen by Edmonton

Seismograms recorded at the Edmonton seismological observatory have been read on a routine basis since 1963. Only first arrivals were read from 1963 to 1969 but S-P times have been available since 1970 (table 16).

A histogram of local events (S-P times less than 60 seconds) shows all possible events from the South West Alberta (figure 31). Care was taken to avoid mine blasts, which usually occur during working hours and at fixed intervals of time. The largest events were correlated with S-P times at SES, PNT, and FSJ; generally located by Ottawa table 15. A relatively high level of seismicity was observed from 1970 to 1972 (figure 31-a). Then the seismicity decreased to an average of 2.2 events per year. Figure 31-a only includes what I call the "Normal Seismicity of the South West Alberta". It does not include the Rocky Mountain House earthquake swarm (RMHES), that apparently started in 1976. Figure 31-b includes the Rocky Mountain house earthquake swarm. Events from the RMHES are easily recognised since they generally have an average S-P time of 21.7±0.7 seconds at Edmonton.

MONTH DAY YEAR	ARRIVAL TIME HOUR MINUTE SECOND	S-P TIME	LOCAL MAGNITUDE
JAN1676	20.21.09	21.0	
JAN2476	16.09.22	20.5	3.2
JAN2576	19.27.00	20.0	1.5
JAN2676	19.37.18	21.5	2.2
JAN2776	01.48.07	24.0	
JAN2776	04.13.00	20.5	
JAN2776	04.21.39	24.0	
JAN2776	05.33.27	22.0	
JAN2776	05.35.52	20.5	1.9
JAN2776	05.43.11	20.6	
JAN3076	15.07.26	20.0	2.2
FEB0876	18.49.02	21.0	1.7
FEB0876	23.04.14	20.0	2.4
MAR0676	09.35.36	20.0	
MAR0676	20.44.49	20.0	
MAR1076	03.49.54	22.0	1.9
MAY0176	06.44.09	21.0	2.0
MAY1376	04.48.04	20.9	1.9
MAY1376	06.26.43	21.0	2.2
JUN1876	11.26.17	20.2	2.1
JUN1876	14.28.04	20.5	3.4
JUN2176	21.59.29	18.0	2.3
JUN2276	03.38.14	21.0	2.7
JUN2776	13.28.03	20.2	2.2
JUN2976	00.40.43	23.0	2.1
JUL0876	05.24.08	20.6	2.6
JUL0876	05.26.00	20.7	2.1
JUL3076	11.57.15	21.0	2.2
AUG0876	18.16.02	20.0	2.3
SEP0176	22.45.31	20.5	3.2
SEP1376	10.24.48	19.2	2.2
SEP1476	02.44.43	22.5	2.4
OCT1376	10.54.05	20.7	2.5
OCT1576	09.48.21	20.7	2.1
OCT1576	15.33.56	21.5	3.2
OCT2376	02.31.40	21.1	2.3
OCT2776	06.20.53	20.0	1.7
NOV0376	11.42.54	20.8	2.4
NOV2976	02.28.47	20.5	2.2
DEC0176	15.52.46	20.6	1.8
DEC0276	03.36.16	19.3	3.0
DEC0976	07.28.03	20.1	2.8
DEC1876	19.51.06	22.0	1.6
DEC2376	22.18.17	20.3	2.8
DEC3076	12.53.51	20.5	2.5
DEC3076	13.37.01	21.0	1.5
JAN0577	03.10.44	20.5	2.6
JAN0577	03.41.24	20.5	1.7
JAN0577	10.48.35	21.0	3.0
JAN0577	23.28.11		3.9

JAN0677	02.44.30		3.7
JAN0877	04.40.13	21.0	2.0
JAN0877	07.05.33	19.1	2.3
JAN0877	12.32.22	21.0	2.6
JAN1477	16.27.52	20.3	3.0
JAN1977	11.18.32	20.3	2.8
JAN1977	14.21.38	20.5	2.0
JAN1977	21.12.15	19.5	2.9
JAN3077	08.39.25	20.8	2.7
JAN3177	18.40.00	20.3	2.5
FEB0377	17.30.48	18.5	2.4
FEB0477	14.34.25	21.0	2.5
FEB0477	16.26.07	20.0	2.3
FEB1077	20.25.50	20.5	2.8
FEB1177	05.20.33	21.7	2.1
FEB1577	03.52.06	20.0	2.7
FEB2477	18.42.28	20.5	2.2
FEB2577	04.00.19	21.0	2.6
MAR0177	07.49.39	20.8	
MAR0577	19.56.19	20.5	
MAR2377	13.15.58	20.6	2.2
MAR3077	19.58.02	20.0	2.0
APR1077	04.26.11	19.9	2.1
APR1277	17.14.05	19.6	2.1
MAY2277	17.33.17	20.6	3.1
JUN0477	06.59.37	20.9	2.1
JUN1877	04.06.46	19.1	3.4
JUL0277	20.40.15	19.7	2.7
JUL0377	10.44.37	20.0	2.3
JUL0577	20.40.52	20.1	2.4
JUL2477	09.07.56	20.7	3.5
JUL2477	10.03.06	20.8	1.2
JUL2477	11.24.48	19.9	2.3
JUL2477	11.33.41	21.0	1.2
JUL2477	11.52.30	21.0	1.2
JUL2477	16.06.13	20.0	1.7
JUL2477	17.50.23	19.5	3.4
JUL2477	21.59.54	20.0	
JUL2577	01.36.53	19.8	1.5
JUL2577	08.59.34	19.4	1.2
JUL2677	05.11.25	21.7	1.8
JUL2677	07.36.13	18.6	1.8
JUL2677	09.19.11	19.3	1.5
JUL2777	02.18.09	20.9	3.2
JUL2777	04.27.06	19.5	2.1
JUL2777	07.54.01	21.0	1.7
JUL2777	12.46.57	22.6	
JUL2977	15.29.11	20.7	2.1
JUL3077	15.06.08	20.0	1.7
JUL3177	02.58.56	19.0	2.7
AUG0277	06.54.54	21.3	
AUG0477	04.06.03	20.7	1.4
AUG1177	08.51.45	19.6	2.8

AUG1377	06.24.53	19.7	2.2
AUG1477	21.44.03	20.5	3.7
AUG1477	21.48.54	19.4	2.5
AUG1477	21.59.10	20.3	2.8
AUG1477	22.16.36	20.9	1.7
AUG1777	05.50.11	21.0	
AUG2377	06.36.12	19.9	1.4
AUG2777	11.51.59	21.0	3.1
SEP0877	10.33.37	19.8	2.8
SEP1177	07.18.16	21.0	1.9
SEP1277	09.46.13	18.8	2.1
OCT0277	21.33.52	19.6	2.6
OCT0277	21.47.16	21.0	2.3
OCT2677	00.34.27	22.5	3.5
OCT3177	09.31.58	20.0	2.3
NOV1177	11.31.48	20.5	2.1
NOV1977	03.01.03	22.5	2.1
DEC0877	19.28.30	19.5	2.4
DEC1077	01.03.08	21.0	1.7
DEC2277	07.38.53	20.4	2.0
DEC2377	20.52.40	19.5	3.1
DEC2477	12.12.18	20.2	2.2
DEC2877	11.53.40	20.1	2.0
DEC3077	21.25.25	20.2	2.7
DEC3177	10.16.58	20.6	2.0
JAN1378	14.27.54	21.0	
JAN1478	08.28.17	20.1	2.6
JAN1778	19.35.38	20.5	1.9
JAN1778	21.07.39	20.5	
JAN2178	00.11.24	20.7	2.1
FEB1378	00.01.11	20.0	
FEB2678	03.18.44	21.8	2.8
MAR1078	14.33.44	20.4	1.5
MAR1478	05.51.26	21.5	1.2
APR1478	10.07.14	21.6	1.7
MAY2078	14.14.08	20.7	3.0
JUN2678	06.11.06	20.1	2.0
JUN2878	08.07.29	20.6	2.4
JUL0378	08.45.05	20.7	2.3
JUL0678	02.37.11	21.0	2.3
JUL1878	22.16.45	20.7	3.3
JUL1978	06.50.37	20.0	2.4
JUL1978	08.49.42	21.1	1.7
JUL2778	10.09.45	21.3	1.7
JUL3178	17.15.16	19.7	2.6
AUG0378	10.13.51	21.8	3.0
AUG0878	18.51.50	21.3	2.1
AUG0978	03.34.16	20.4	2.2
AUG0978	13.09.50	20.2	2.7
AUG1278	09.52.25	21.4	1.9
AUG1478	01.09.10	20.3	2.5
AUG1578	01.12.23	21.0	3.6
AUG1578	06.59.19	20.8	3.4

AUG1678	08.42.56	20.5	2.6
AUG1778	03.46.55	21.3	2.3
AUG2478	15.20.07	19.7	2.7
AUG2778	20.55.05	20.5	1.9
AUG2878	21.24.21	20.8	3.1
AUG2978	01.03.20	19.1	2.0
AUG2978	09.27.21	21.0	1.7
AUG2978	12.30.33	22.0	1.8
SEP1278	13.21.28	22.0	1.9
SEP2078	16.00.47	20.7	2.3
SEP2678	01.35.51	21.0	2.0
SEP2778	01.24.20	20.0	2.1
OCT0278	02.04.59	20.7	2.2
OCT1178	05.09.30	20.3	2.0
OCT2578	03.33.07	20.8	2.1
DEC1178	13.32.00	20.8	2.1
DEC3178	00.27.16	21.1	2.1
JAN0179	18.44.17	20.8	2.5
JAN0279	01.01.06	20.5	1.7
JAN0279	07.56.50	21.4	2.4
JAN0579	03.14.31	21.2	2.8
JAN1079	00.39.34	21.4	2.3
JAN2879	20.02.53	20.5	2.1
FEB0179	13.13.51	20.3	
FEB0979	10.17.41	21.0	2.2
FEB0979	23.07.01	20.2	1.9
FEB1179	02.07.43	21.0	2.4
FEB1179	02.45.02	20.5	1.8
MAR2879	16.46.17	18.5	2.8
MAY0479	10.47.26	21.1	3.3
MAY2179	00.01.36	20.8	2.7
MAY2579	10.58.05	20.5	2.0
MAY2879	22.46.37	20.2	2.7
JUN0679	05.38.19	20.8	2.5
JUL2479	10.29.55	21.3	2.1
AUG0179	05.47.07	21.0	2.4
AUG0679	04.53.01	20.5	2.0
AUG1279	06.43.23	21.3	1.7
SEP0879	10.21.47	20.9	2.5
SEP2579	18.28.54	20.3	
OCT0679	10.01.11	21.6	1.9
OCT1779	04.49.01	20.9	2.0
OCT1779	04.49.01	20.9	2.0
OCT1979	08.37.30	21.0	
OCT2179	05.13.21	20.3	2.8
OCT2179	05.28.04	21.0	2.1
OCT2279	01.46.28	20.8	2.2
NOV1679	03.14.34	24.0	2.2
DEC1379	14.13.58	20.0	1.9
DEC2479	12.45.22	22.3	2.4
JAN0380	12.17.45	21.0	1.9
JAN0880	16.31.44	20.5	2.3
JAN0880	23.28.30	20.0	3.0

JAN0980	23.43.47	20.9	2.2
JAN1080	21.40.45	21.3	2.3
JAN1280	02.14.44	20.5	1.9
JAN1880	00.17.47	24.0	1.9
JAN2380	05.08.25	21.3	2.0
FEB1780	11.07.18	20.7	1.8
FEB1980	10.39.04	20.8	1.9
FEB1780	11.07.18	20.7	1.8
FEB1980	10.39.04	20.8	1.9
MAR0180	07.49.39	21.0	1.9
MAR0580	19.20.06	23.4	2.0
MAR0580	21.54.50	24.3	1.9
MAR0680	05.27.11	23.4	2.3
MAR1980	15.23.23	21.0	2.5
MAR2680	00.08.53	20.0	1.8
MAY0580	21.57.13	20.9	2.4
JUN0680	09.05.34	20.2	2.4
JUN1280	15.34.12	20.6	2.2
JUL2580	06.44.43	20.8	1.9
AUG0380	11.05.31	21.2	3.0
AUG0680	12.42.20	21.0	2.9
AUG2380	16.10.16	21.3	3.5
SEP0180	11.47.25	21.2	3.0
SEP0280	05.57.39	21.0	2.2
SEP0280	11.31.51	21.0	2.2
SEP0480	17.49.54	21.1	2.7
SEP0480	18.26.52	21.2	1.7
SEP0480	20.34.22	21.1	2.7
SEP0480	21.03.59	21.0	2.6
SEP0580	07.39.08	20.9	1.7
SEP0580	11.47.34	21.0	2.8
SEP0580	13.20.48	21.0	1.9
SEP0580	13.41.49	21.2	1.9
SEP0680	14.08.56	20.6	2.1
SEP0780	14.05.23	21.3	2.5
SEP0880	05.38.21	21.3	2.1
SEP0880	19.10.11	21.3	1.9
SEP0880	19.27.20	20.8	2.0
SEP0880	19.47.34	20.9	3.4
SEP0980	06.07.48	20.9	3.5
SEP0980	23.39.03	21.0	2.4
SEP1080	07.39.44	20.9	3.5
SEP1080	11.46.31	21.0	3.3
SEP1180	16.49.08	20.8	2.7
SEP1580	01.34.54	20.9	3.6
SEP1680	01.33.27	21.4	3.0
SEP1780	05.05.12	21.0	2.9
SEP1780	09.58.36	21.6	3.4
SEP1780	12.31.27	21.0	3.3
SEP1880	15.10.00	21.0	
OCT0280	09.28.59	21.0	3.6
OCT0980	12.40.30	21.6	3.3
OCT2980	03.24.15	20.9	2.1

OCT3180	00.40.37	21.0	2.4
OCT3180	00.50.23	21.0	2.5
OCT3180	05.16.31	20.5	2.4
OCT3180	18.23.45	20.5	2.6
DEC1380	09.31.48	21.0	2.4
JAN1981	12.59.10	20.7	2.7
MAR0981	12.00.39	20.5	2.3
APR1581	11.31.25	22.0	1.7
APR1681	12.08.24	19.5	2.1
JUN1681	05.03.23	21.0	2.7
JUN2481	17.40.20	21.0	2.4
JUL1481	07.09.00	20.3	1.8
JUL2781	13.14.59	20.1	2.3
JUL2881	21.32.50	21.8	2.8
JUL3081	15.16.35	20.9	3.0
JUL3081	20.01.17	20.8	2.6
AUG0181	08.31.10	21.0	2.1
AUG0381	00.27.54	20.8	2.0
AUG2081	14.26.54	20.8	3.8
AUG2781	12.00.14	20.7	2.1
AUG2981	10.01.29	19.4	1.9
SEP0181	04.43.11	20.0	2.0
SEP0481	07.54.23	24.0	2.1
SEP2381	11.37.50	20.5	1.8
OCT1581	01.45.24	21.0	2.2
OCT1981	00.10.11	21.3	2.3
OCT2081	10.38.15	20.7	2.6
OCT2181	09.19.56	20.9	2.7
OCT2281	13.41.53	19.9	2.2
NOV0581	11.27.58	21.1	1.9
NOV1281	04.47.15	21.3	2.8
NOV1381	14.14.36	21.3	3.4
NOV1481	07.22.34	20.3	1.9
NOV1481	07.26.50	20.8	3.0
NOV1481	10.00.10	20.9	2.1
NOV1781	12.10.18	19.8	2.1
NOV2581	14.25.12	20.8	2.8

Table 16.... Table of all the events recorded at Edmonton from the Rocky Mt. House earthquake swarm

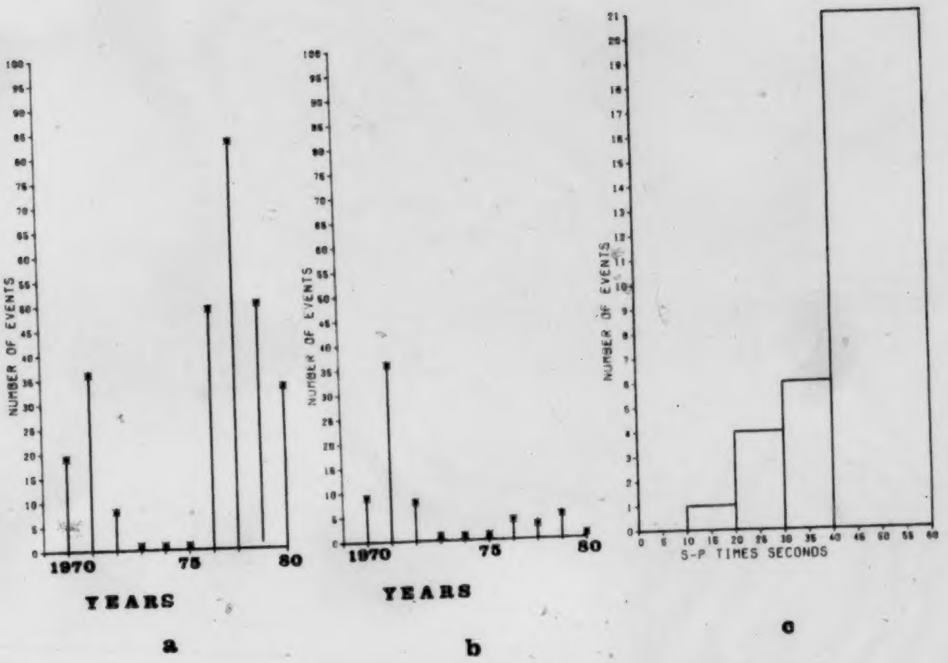

Figure 31.... a)Histogram of local seismicity recorded at EDM including RMH earthquake swarm. b) Without RMH earthquake swarm. c) Histogram of some well defined S-P times ar EDM

5.1.1.1 Relation to the Mica Array

Aside from the station at Edmonton the nearest seismic facility to the Rocky Mountain House Earthquake swarm is the Mica Array. I have examined an extensive sample of the records from this analog array of vertical seismometers and conclude that the S phase is too emergent as a rule to aid materially in refining locations by means of S-P time. In any case, exact locations are of secondary importance to this study. Its thrust is towards source mechanisms. The data at Mica are all recorded on analog magnetic tape, spectral studies such as I report here would require uncertain corrections for non-linearity in this recording medium and after the fact digitization. I have examined analog records very carefully; convincing evidence of the presence of the Moho refracted phases cannot be found from analog records alone. Finally, and most important, the ray path from Rocky Mountain House to Mica passes through considerably more complex geology than that to Edmonton. Even if the data could be reliably reduced its interpretation would be substantially more uncertain. Nevertheless I report here those results I have from Mica data.

Some events recorded at CUM station from the RMHES have an average S-P time of 24.5±0.8 seconds (table 17).

MONTH DAY YEAR	ARRIVAL TIME AT EDM	S-P AT EDM	ARRIVAL TIME AT CUM	S-P AT CUM
SEP1376	10.24.48	19.2	10.24.53	
OCT1376	10.54.05	20.7	10.54.11	23.6
OCT1576	09.48.21	20.7	09.48.27	26.3
OCT1576	13.33.56	21.5	15.34.03	
OCT2376	02.31.40	21.1	02.31.46	25.3
DEC0276	03.36.16	19.3	03.36.21	24.3
DEC0976	07.28.03	20.1	07.28.10	
DEC1876	19.51.06	22.0	19.51.11	26.0
DEC2376	22.18.17	20.3	22.18.23	26.0
DEC3076	12.53.51	20.5	12.53.59	24.4
DEC3076	13.37.01	21.0	13.37.06	24.9
JUL0277	20.40.15	19.7	20.40.15	23.8
JUL0577	20.40.52	20.1	20.40.59	24.6
JUL2477	09.07.56	20.7	09.08.03	23.1
JUL2477	10.03.06	20.8	10.03.06	24.0
JUL2477	11.24.48	19.9	11.24.54	24.0
JUL2477	11.33.41	21.0	11.33.48	23.6
JUL2477	11.52.30	21.0	11.52.36	24.0
JUL2477	16.06.13	20.0	16.06.19	25.0
JUL2777	02.18.09	20.9	02.18.15	25.0
JUL2777	04.27.06	19.5	04.27.11	25.0
JUL2777	12.46.57	22.6	12.46.55	20.0
JUL3077	15.06.08	20.0	15.06.08	23.6
AUG1177	08.51.45	19.6	08.51.51	24.3
AUG1377	06.24.53	19.7	06.24.53	24.6
AUG1477	21.44.03	20.5	21.44.10	24.0
AUG1477	21.48.54	19.4	21.49.00	24.0
AUG2777	11.51.59	21.0	11.52.06	24.0
SEP0877	10.33.37	19.8	10.33.43	25.5
OCT2677	00.34.27	22.5	00.34.33	

Table 17.... Events from the Rocky Mountain earthquake swarm detected at CUM

5.1.2 Summary

From the histogram of number of events against S-P times from the figure 31-c, and associated locations (Table 15) we can suggest.

1) Events with relatively small S-P times must lie in the Alberta plains (figure 32). Whether these events are of

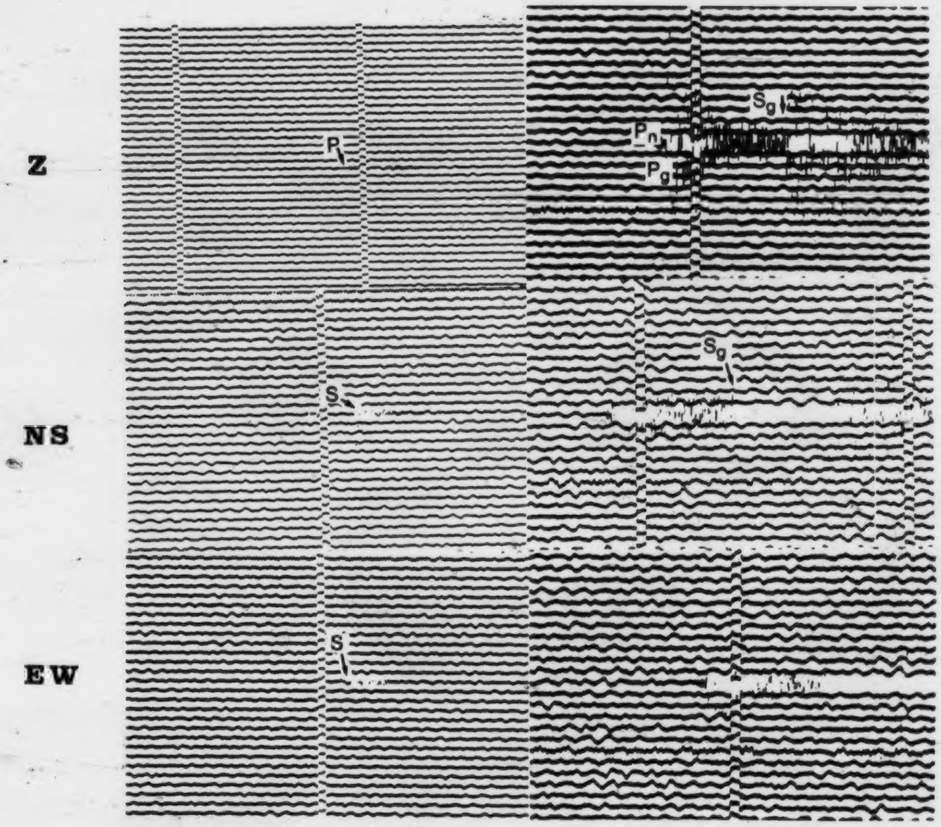

Figure 32.... Local events recorded at EDM. Right, an event with S-P=12 sec. Left, an event with Sg-Pg=27.3 and Pg-Pn=2.4 and was located by EPB at 51.95N and 115.76W.

tectonic origin or due to the oil or mining operations in the Alberta plains cannot be answered by this general discussion of the seismicity.

2) Events with S-P times between 20 and 30 seconds are probably close to Rocky Mountain House, approximately 180 km SW of Edmonton (figure 33). This is the most active zone in South West Alberta. I showed in chapter 3 that some of those events were mainly deep (nearly 20 km). However, most events detected with a temporary array of analog and digital seismic stations were not deeper than 4 km (Wetmiller 1981, Rebollar et al 1981 b).

There may be two kinds of activity associated with the Rocky Mountain House earthquake swarm. Deep seismicity (near 20 km) more likely of tectonic origin, and shallow seismicity (not deeper than 4 km) possibly associated with secondary recovery activity in the Strachan gas field.

3) Events with S-P times around 35 seconds (approximately 300 km from EDM), could come from any place between Calgary and the Willmore park area. Therefore, more evidence from a close network or other stations is needed (table 18).

4) S-P times between 40 and 60 seconds probably correspond to earthquakes that come from the area of McNaughton Lake (figure 34).

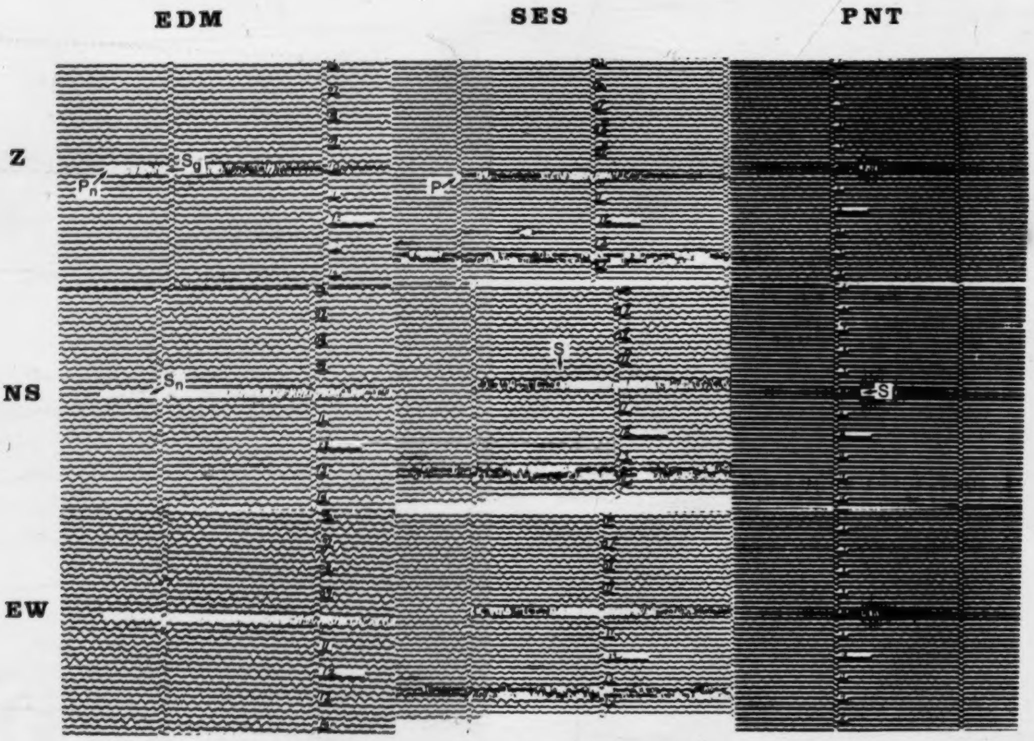

Figure 33.... Example of the Rocky Mountain House events detected in the analog stations at EDM, SES, and PNT. Some of those seismograms do not show clear phases.

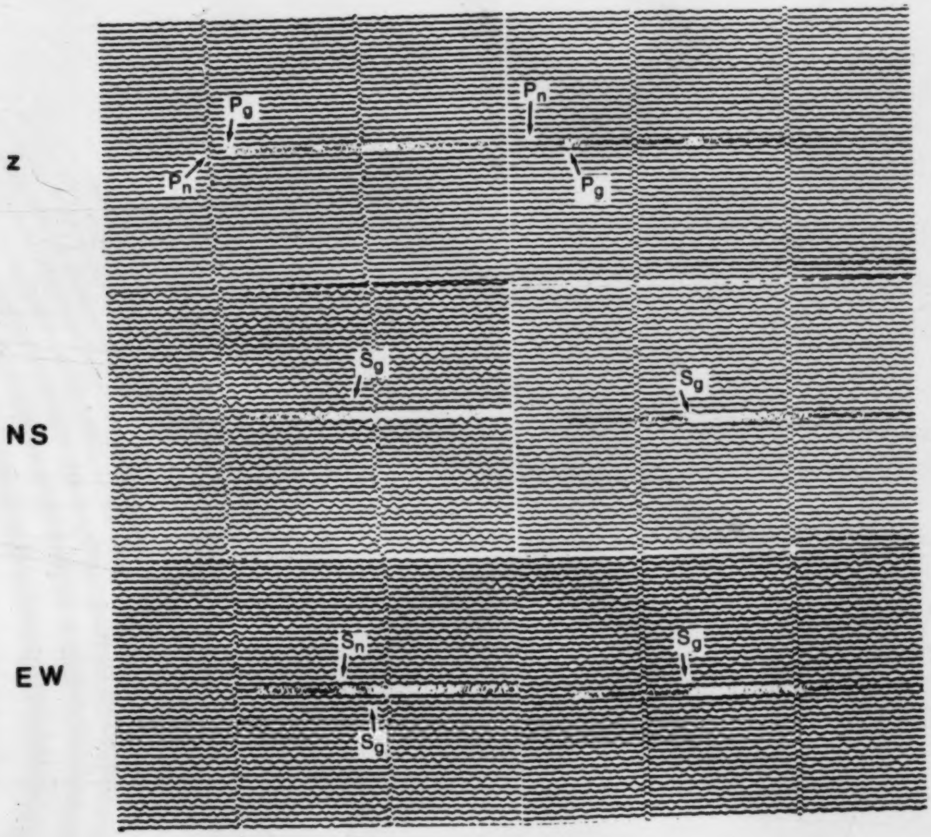

Figure 34.... Events with S-P times greater than 40 sec probably coming from the McNaughton lake area. Right event has Sg-Pg=44, Sg-Sn=11.5, and Pg-Pn=7.7 sec. Left event has Sg-Pg=46 and Pg-Pn=11 seconds.

M. D. Y.	H. M. S.	S-P SECONDS
APR2471	06.04.00	53
APR3071	22.32.09	58
MAY1171	19.30.47	57
MAY1571	23.22.35	53
MAY2471	19.17.19	53
JUN2671	19.14.35	57
JUN2871	22.31.43	48
JUN3071	22.33.22	52
JUL2571	01.57.17	29
JUL2771	22.13.29	44
AUG0471	23.15.39	42
AUG1771	23.24.44	42
AUG1871	05.18.45	35
AUG2071	18.07.30	38
FEB0172	20.25.33	18
AUG2072	13.20.09	32
AUG2172	02.36.44	37
APR2972	20.53.52	58
JAN0674	16.34.16	55
OCT2675	22.46.10	33
FEB2376	19.09.50	25
NOV2276	22.04.28	33
MAR1877	21.14.27	27
SEP1277	09.46.13	18
APR1378	05.11.03	29
JUN1478	07.15.54	21
JUL0878	07.26.51	50
FEB2479	15.50.19	52
JUL2980	12.57.28	28
NOV1880	12.03.46	12
DEC2280	11.36.51	27
MAR0681	20.31.41	27
MAR0681	23.01.22	39
MAR1081	10.02.22	47
APR2081	03.31.51	46

Table 18.... Events recorded at Edmonton with clear S-P times, that fall in the definition of local activity i. e. S-P times of less than 60 sec

5.1.3 Energy release and b value of the Rocky Mountain Earthquake swarm

Lacking an empirical relationship for the evaluation of radiated seismic energy of small earthquakes in Canada. I used Gutenberg and Richter's (1942, 1956) energy-magnitude empirical relationship in order to calculate the energy release of the Rocky Mountain House earthquake swarm.

Gutenberg and Richter considered the radiated energy contained in a spherical shell centered on the earthquake source. They assumed that this energy was radiated in a sinusoidal wave train and recorded on a standard strong motion instrument. Therefore, knowing epicentral distance, hypocenter, the physical constants of the standard intrument, acceleration, period and travel times of the signals, they found an empirical relationship given by $\log E = 11.3 + 1.8M_s$. Later, Gutenberg and Richter (1956), in a review of their original paper found the relationship given by $\log E = 9.4 + 2.14M_s - 0.024M_s^2$.

This empirical relationship depends on the theoretical study of seismic radiation at short epicentral distances, therefore it can give a reasonable estimate of the energy for small earthquakes from the Rocky Mountain House earthquake swarm.

An average of 10^{15} ergs per month was released during the 58 months since 1976. The contribution of small earthquakes to the total energy release is negligible (figure 35). The total energy released during this period was 5.6×10^{17} ergs equivalent to a single earthquake of magnitude (Ms) 3.9. The total energy release of possibly deep events, i.e. earthquakes that show clear Sn refracted phases, was 5.49×10^{17} ergs. This mean that 98 % of the total

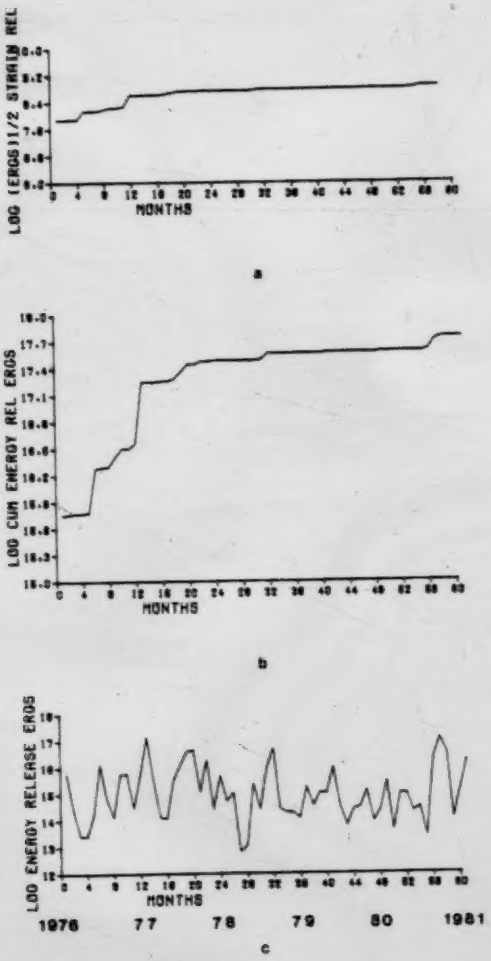

Figure 35.... Energy release, cumulative energy release, and strain release from the Rocky Mt. earthquake swarm calculated at EDM since 1976 to 1980

energy release was released by possibly deep events. This mean that largest earthquakes (with magnitudes between 2.8 and 3.5) are mainly deep. The cumulative seismic strain release (figure 36) yields a maximum strain release of $7.5x10^{8}$ ergs$^{0.5}$.

The strain release as a function of time (figure 35-a) shows a maximum release of strain energy during the first year of the swarm (1976). After that the strain is accumulated and represented by the flat part of the plot. However, whether the strain energy is released in small earthquakes or it is accumulated, cannot be answered from this short period of observation.

Using 242 events I calculated the cumulative number of events versus local magnitude (figure 36) or the Gutenberg and Richter frequency-magnitude relation given by $\mathbf{\log N=a-bM_l}$, where **N** is the number of earthquakes for unit time, **a** and **b** constants and M_l local magnitude. I used some of the magnitudes calculated by EPB and reported in their bulletin. For events not reported by EPB, I calculated the local magnitude according to Richter 1958 (see for example chapter 2).

There are three main factors that limit the accuracy of the evaluation of the **b** value. The magnitudes are uncertain, small events are undetected, and there are few events due to the short time of observation (Milne et al 1978). Uncertainties in the evaluation of magnitudes are difficult to estimate if the magnitudes are calculated at a single

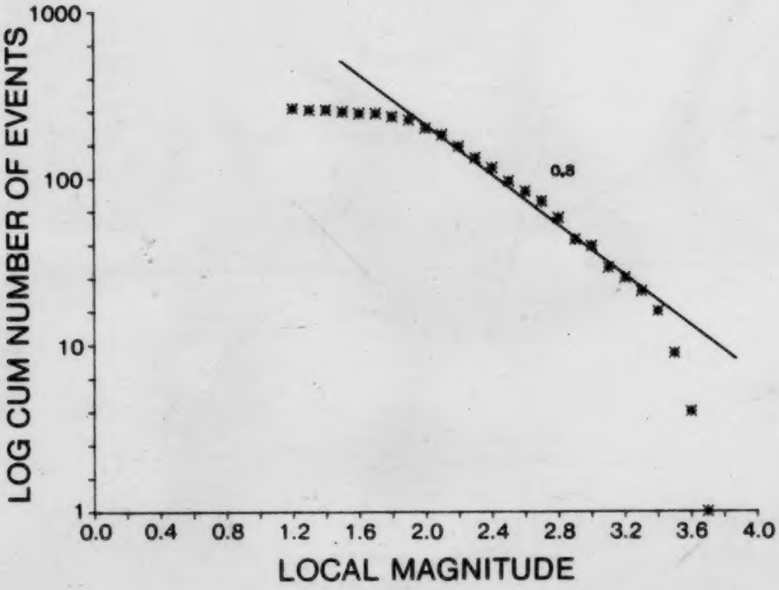

Figure 36.... Evaluation of the b value for the Rocky Mountain House earthquake swarm

station.

Edmonton station detects events from the Rocky Mountain House area, with magnitudes greater than 1.2, as can be seen from the frequency magnitude relationship, however, the system loses its sensitivity for magnitude 2 from this area. The b value for the Rocky Mountain House earthquake swarm is 0.8 and lies in the range of values (between 0.6 and 1.5) found by Everden (1970) using world wide seismic data, and is similar to the values found by Milne et al (1978) in Western Canada (those values range from 0.65 to 0.82).

The frequency-magnitude relationship has been found to vary in different tectonic regimes. Higher values of b have been found in spreading centers (Sykes 1970, Reichle 1975) and in volcanic areas (Suzuki 1959). Small values, near 1.0, are observed for intra-plate earthquakes, like this sequence, and in transform faults. This parameter usually is associated with the state of the stress (Mogi 1962, Scholz 1968, Berg 1968, Wyss 1973). However, Knopoff (personal communication) suggests that it is more likely to be associated with the roughness of the fault.

An analysis of the bulletin edited by the Earth Physics Branch of Ottawa, and the archives at Edmonton reveals that the Rocky Mountain House earthquake swarm is not a common geophysical event. The common pattern in the South West Alberta is scattered events without an aftershock pattern, much like the Willmore event (Ms=3.0), and the event (local magnitude 3.4) that occurred on December 22, 1981, with an onset at Edmonton at 11 hours 36 minutes and 51.2 seconds. This micro-earthquake was located by E.P.B. at 51.95°N and 115.76°W, approximately 220 km from EDM (see figure 32). However, this pattern of events without aftershocks could indicate that the aftershocks are too small to be recorded in the permanent stations. Therefore, the Rocky Mountain House earthquake swarm is an interesting phenomenon that needs to be studied more closely.

5.1.4 The Willmore Earthquake

Earth Physics Branch (EPB) located the Willmore event at 53.63°N and 118.29°W with a shallow depth and assigned an Ms=3 an mb=4.4 (see Nuttli, 1973). The U. S. National Earthquake Information Service (NEIS) located the event at 53.68°N and 118.03°W and assigned a mb=4.4 (figure 30).

This event (October 9, 1977) was not recorded clearly in many stations, nevertheless I plotted ten first motions (table 19), assuming a focal depth of 18 km for this event. Obviously there is no unique solution for the focal mechanism. Among those solutions it is possible to fit a strike slip fault, with either of two possible fault plane orientations, one of dip 80° and a dip direction of 120° and the other with a dip of 60° and dip direction of 24°. None of those agree with the strike of the Rocky Mountains. A normal fault with either a dip of 20° and dip direction of 94° or a dip 70° and dip direction of 274° is also possible. (figure 37)

Seismic Station	Latitude	Longitude
Mt. Dainard (DAI)	52.199°N	118.384°W
Mt. Thompson (THO)	52.689°N	119.120°W
Mt. Cummins (CUM)	52.087°N	118.212°W
Mica Creek Village (MCV)	52.008°N	118.561°W
Edmonton (EDM)	53.222°N	113.140°W
Penticton (PNT)	49.317°N	113.140°W
Victoria (VIC)	48.518°N	123.917°W
Yellowknife (YKC)	62.478°N	114.473°W
Inuvik (INK)	68.307°N	133.520°W
Mould Bay (MBC)	76.241°N	119.360°W
Albuquerque (ALQ)	34.942°N	106.457°W

Table 19.... Table of the seismic stations used in the plot of the equal-area projection of the Willmore earthquake

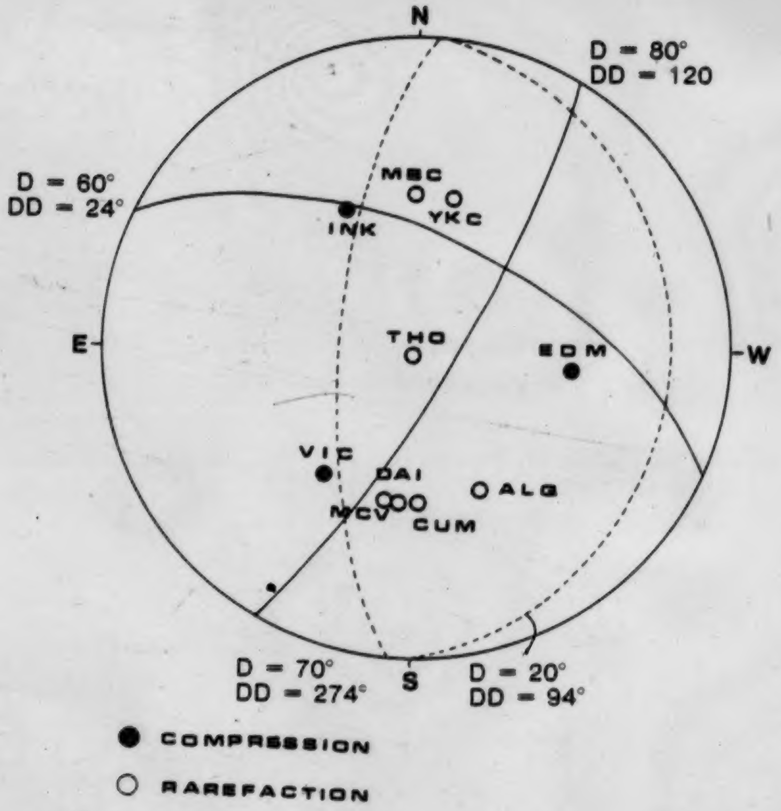
N
D = 80°
DD = 120
D = 60°
DD = 24°
MSC
YKC
INK
E
W
THO
EDM
VIC
DAI
ALG
MCV
CUM
D = 70°
DD = 274°
S
D = 20°
DD = 94°
● COMPRESSION
○ RAREFACTION

Figure 37.... A plot of ten first motions in an equal-area projection of the focal sphere showing probable fault orientations (D=Dip and DD=Dip Direction)

Edmonton station recorded this event in digital and analog format. I was able to calculate the seismic moment. Only the vertical component was not saturated at EDM (figure 38). Therefore, I used the spectrum of the vertical SV component of the shear waves in the analysis. The Sg-Pg time recorded at Edmonton was approximately 37 seconds. This gives an epicentral distance of 325 km assuming a half space with a P-wave velocity of 6.4 km/sec. The EPB location is 330±10 km from Edmonton. The spectrum was calculated assuming a Q of 1000, independent of frequency, a density of 2.9 gr/cm^3, an average radiation pattern of 0.63, a shear wave velocity of 3.7 km/sec, an epicentral distance of 325±10 km/sec, and an angle of incidence of 49°. Figure 38 shows the spectrum calculated at EDM. The logarithmic low level of the spectrum for the Willmore events is -3.1, and that gives a seismic moment of $6.7 \pm 2 \times 10^{22}$ dyne-cm.

In order to investigate the difference between the seismic moment calculated with body waves at a single station and the seismic moment calculated from surface waves at several stations, I used the McNaughton Lake earthquake of May 14, 1978. The moment calculated using the amplitude equalization method (see Aki and Richards 1980, chapter 7) was $4 \pm 2 \times 10^{23}$ dyne-cm (Rogers et al 1980). At Edmonton (figure 38) this event saturated both horizontal components. Hence, assuming the same physical constants as those used for the Willmore event, and the seismic moment calculated by Rogers et al (1980), I get a logarithmic low level amplitude

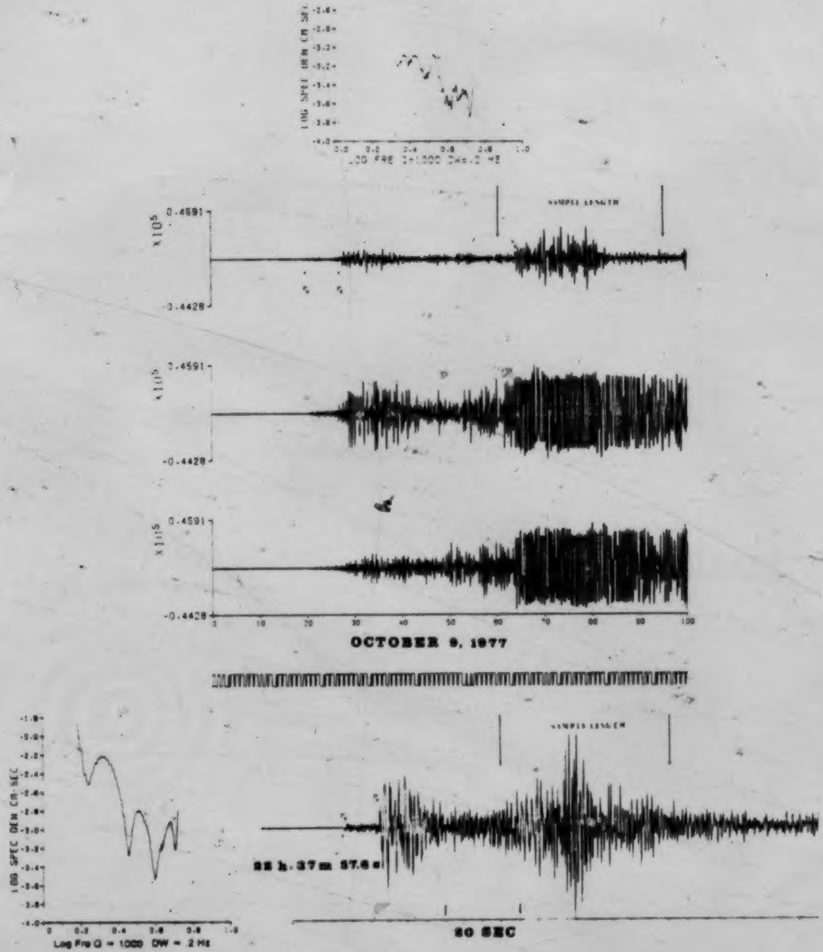

Figure 38.... Seismograms and spectra of Willmore (Ms=3) and McNaughton (M_L=4.8) events. Upper (Willmore) event show EW and NS saturated components. Bottom (McNaughton) shows the vertical component at EDM

of the spectrum of -2.4. The value observed at EDM is -2.2, which yields a seismic moment of 7.6x10^{23} dyne-cm (figure 38). However, the low level amplitude of the spectrum could have an error due to the bandwidth of the digital system of Edmonton.

If we consider the orientation of the fault (strike N 10 W, dip 38 SW, .8 strike slip, .5 thrust), the correction for the radiation pattern is 0.45 (see Aki and Richards 1980 page 115). Considering this correction I get a seismic moment of 10^{24} dyne-cm, if no correction is made for the radiation pattern we have 4.8x10^{23} dyne-cm, therefore, the seismic moment calculated at EDM gives 7.6±2x10^{23} dyne-cm, two times higher than that calculated by Rogers et al (1980). Kanamori and Anderson (1975) comment,

> "The seismic moment is one of the most reliably determined instrumental earthquake source parameters. For large earthquakes, in particular, the value of M_0 determined by different investigators seldom differ by a factor of more than two. For small earthquakes, the uncertainity is usually somewhat larger".

In view of this comment I consider the agreement satisfactory. However, probable errors in the evaluatiuon of these seismic moments are: errors in the epicentral distance, radiation pattern, attenuation, path inhomogeneities, and in our case a probably narrow bandwidth.

5.2 On the relation of Source Parameters to Tectonics

In this work I have derived a number of measures of earthquake behaviour in various areas. Their connection to geology, which was discussed above is not easy to establish unambiguously. The physical properties of the system are simply to complicated and the quality of the data is not high.

First an obvious question arises: How realistic are those source parameters? I cannot answer this question precisely, since there are many unknowns in the source region, and in the earth's crust in which the signals travel. Corrections for attenuation seem to be not critical, since Q has been observed experimentaly to be between 100 and 1000 for most earth materials, in a range of frequencies from 10^{-5} to 10^{3} seconds (Pilant 1979). A major problem in our observations is the loss of energy due to scattering and conversion of phases that could give rise to changes in the estimates of source parameters with a given model. Chapter two shows that source parameters calculated at distances greater than the fault length are usually smaller than those calculated at distances of the order of the fault length.

I studied two different earthquake sequences, at relatively large epicentral distances (180 and 500 km). Even though the amplitude response curves are different, for a typical RESMAC station and the Edmonton station, the useful information in both systems was between 0.2 and 7 Hz. Outside this range of frequencies the ratio of signal to noise was small. Therefore, in order to get more representative information about the earthquake source, it will be necessary to complement spectral analysis of body waves with spectral analysis of surface waves when the epicentral distance exceeds about 150 km. A typical example of this kind of study is that done by Hanks and Wyss (1972).

The seismic moment of the Willmore and McNaughton lake earthquakes were calculated from the spectral analysis of SV waves recorded at the Edmonton digital station. Those moments are $6.7\pm2\text{x}10^{22}$ dyne-cm for the Willmore event and $7.6\pm2\text{x}10^{23}$ dyne-cm for the McNaughton lake event. This last seismic moment compares moderately well with that calculated with surface waves (Rogers et al 1980).

5.2.1 Speculations on Tectonic Implications

Results from individual earthquakes or earthquake sequences, are important to an eventual understanding of the earthquake source and plate tectonics models. Orientation of principal stresses (calculated from fault plane solutions), magnitude of stresses (calculated from in-situ measurments), seismic moment and source dimension (calculated from spectral analysis), are important parameters of an earthquake source and the values of these parameters are in the final analysis controlled by the driving mechanism of plates. Seismic moments and source dimensions have been used to calculate the rate of slip of major plate boundaries (Brune 1968), and time recurrence of large earthquakes

(Singh et al 1981).

Intraplate earthquakes have been observed to lie along preexisting zones of weakess within areas of youngest orogenesis (Sykes 1978), or to be apparently due to effects of local topographic features in the plates (Stein 1978). By close analysis, Sykes (1978), found that seismic activity tends to be concentrated near ends of major oceanic transform faults, along preexisting zones of deformation, or along faults in old fold belts within the thicker lithosphere of the continents, hence, the study of earthquake sequences in intraplate enviroments may reflect varioations in strength within plates.

From spectral analysis of seismograms we can derive stress drops, seismic moment and source dimension. Earthquake stress drops of large intra- and inter-plate earthquakes are probably not greater than 100 bars. This is based on a large number of observations independent of source strength. McKenzie and Jarvis (1980) estimated a mean stress on plate boundaries of 150±50 bars with a probable upper bound of 500 bars, in agreement with seismically determined stress drops. Higher stress drops (630 bars) of micro-earthquakes in the sedimentary basin of the Imperial Valley of California have been observed (Hartzell and Brune 1977).

In this work I compared an interplate sequence of events (Oaxaca aftershocks) and an intraplate sequence (the Rocky Mountain earthquake swarm). They differ in some respects. The Oaxaca aftershocks have simple spectra with a well defined plateau at low frequencies, a recognizable corner frequency and a well defined asymptote at high frequencies. Therefore, stress drops calulated in the usual way can have meaning. A number of the events of the Rocky Mountain House earthquake swarm have more complicated spectra, even though the signals were recorded closer to the earthquake source than the records of the Oaxaca events and the structure between the Rocky Moountain House area and the Edmonton station is not complicated. This difference can be appreciated from the plot of local magnitude against seismic moment. The data from the Rocky Mountain House earthquake swarm have more scatter than the data from the aftershocks from the Oaxaca event.

This difference could result from differences in the state of stress in the crust and differences in the heterogeneity of the fault zones. The Oaxaca earthquake was a large simple event (Stewart et al 1981), and it has been found to be similar to past events in the Middle America Trench (Chael et al 1982). Apparently simple events can be associated with relatively homogeneous stress states and physical properties on the fault zone. Maybe the complicated spectra from the Rocky Mountain House earthquake swarm reflect an incipient fault or a possible reactivation of an ancient fault system which could be expected to have a more complex behaviour than a well established fault zone.

Although this study has not answered many of the problems of cause of the Rocky Mountain Earthquake swarm it appears a supportable hypothesis that 2 kinds of seismicity exist. There is small magnitude shallow seismicity and deeper seismicity probably associated with pre-Cambrian basement structures, which accounts for most of the energy release in the area. Many unknowns remain. For example, we do not know fault orientation, stress orientations, or a precise focal depth of these events. Nevertheless, whatever their values clues to the nature of the process exist in the forces acting on the lithosphere in this area and the stress strain relations obeyed by the lithosphere in this area.

5.2.1.1 Comments on Quantitative Aspects of Plate Dynamics

There are many poorly understood problems associated with the dynamics of the crust and upper mantle. The driving mechanism of plate tectonics, energies involved in the crustal faulting, magnitude of deviatoric stresses (total stress minus hydrostatic stress), and absolute stresses, are only a few.

Solomon et al (1980) summarized possible driving forces of plate tectonics. Among those they consider lithospheric cooling, latitudinal plate motion, crustal thickness inhomogeneities, lithospheric loading and unloading, plate boundary forces at ridges, trenches, transform faults, zones of continent-continent collision, and basal forces associated with viscous interaction between the lithosphere and asthenosphere.

Different magnitudes of deviatoric stresses in the crust can give rise to different phenomena, such as micro-earthquakes, large earthquakes, and topographic features in the crust. Hanks and Raleigh (1980) argue that away from plate boundaries the crust can support large deviatoric stresses, of the order of kilobars, in response to local or regional loads. For example, McGarr et al (1979) found evidence of high stress drops, greater than 700 bars, in deep mines in South Africa. Scholz (1980) argues that in some faults stresses of the order of a kilobar may exist.

Zoback et al (1980) found that shear stresses determined in wells near the San Andreas fault increase with depth. The depth of those wells ranges from 200 to 1000 meters. Apparently stresses increase linearly with depth at least up to 5 km. McGarr (1980) found that the maximum shear stress increases with depth from nearly 10-60 bars (1-6 MPa) in the first hundred meters, to 200 bars (20 MPa) to nearly 5 km. He calculated a theoretical relationship of the form A+Bz, where A and B are constants and z is the depth, for the increase of stresses with depth. There is great scatter of data in the first kilometer or so (see also for example Brace and Kohlsted 1980). The constants vary with tectonic environment.

McGarr (1980) comments

> "A vertical profile of measurements from the surface downward might show a monotonic change of the horizontal principal stress directions, with the implication that the stress trajectories measured at the surface may not be indicative of directions throughout much of the crustal section".

Bell and Gough (1979), and Gough and Bell (1980) found, from in situ measurements of oil-well fractures (breakouts) in Alberta, a remarkable aligment of the maximum principal stress in the northeast-southwest direction, i. e. perpendicular to the Rocky Mountains. However, those measurements were made in soft rock (siltstones, sandstones, and carbonate sediments) and at depths not greater than 2 km. Therefore, it could be possible that shallow earthquakes are triggered by those stresses in Alberta, these shallow events are those events with S-P times of less than 15 seconds and recorded at EDM, or the shallow events from the Rocky Mountain House swarm analysed in chapter 4.

5.2.2 A Speculation on the Cause of the Rocky Mountain House Earthquake Swarm

The suggestion that seismic activity originates in the pre-Cambrian formations is controversial. In order to explore its implications I consider, in a very superficial way, the tectonics of South West Alberta. Two structures could be relevant. They are the North American Cordillera and the Fond du Lac gravity trend (Walcott 1968)

The North American Cordillera runs from the Aleutian arc through the western third of North America into Mexico and Central America. The part of the North American

Cordillera that extends from the 49th parallel to the Tintina Trench, near the border with Alaska (The Canadian Rocky Mountains), is a relatively simple and well studied orogen. Its age has been determined as Paleozoic-Mesozoic (Thompson 1979) and its geology and tectonics have been extensively studied (Bally et al 1966, Thompson 1979, Martin 1963, Bokman 1963, Shaw 1963, Elliott 1976, Dahlstrom 1969,1970, Monger and Price 1979, Beaumont 1981). The Canadian Rocky Mountains are delimited on the east by the Interior Plains or Great Plains and to the west by the Western Omineca Crystaline Belt ,and they are usually divided into the Foothills, Front Ranges, Main Ranges (East and West) and the Western Ranges.

The Foothills consist of deformed Paleozoic Mesozoic clastic rocks. The deformation (shortening) is mainly thrust faulting in the southern part and folding in the north. Fold axes and fault strikes are parallel in most cases. Tear faults and normal faults are also common in the Foothills. The basement lies at approximately 3.0 km in the Interior Plains and dips gently to about 11 km below the Rocky Mountains (Bally et al 1966). The approximate depth below the Rocky mountain House area is 4.8 km based on reflection profiles (Bally et al 1966).

The Front Ranges are formed from a relatively few major thrust layers that are bounded by faults with several tens of kilometers of displacement. The Main Ranges consist of lower Paleozoic and Proterozoic rocks thrust eastward over the adjoining Front Ranges. The Rocky Mountain Trench is a narrow linear topographic depression extending over 1600 Km. In the south the trench is underlain by a westward dipping basement, and the location and strike of the trench is controlled apparently by a complex system of curved low-angle normal faults (Bally et al 1966).

Although conventional wisdom suggest that the Cordillera in this area is decoupled from the pre-Cambrian basement at the decollement zone (Bally et al 1966), significant stress concentrations in the basement can result from the load of the Rocky Mountains and the adjacent foreland basin. (They might also be present as possible residuals from the Laramide orogeny that gave origin to the Rocky Mountains). Beaumont (1981) considered a model of lithosphere flexure for the Alberta foreland basin under laterally migrating loads and predicted the bend of the basement, and consequently the deep root of the Rocky Mountains.

Monger and Price (1979) compiling the work of several authors suggest a Moho depth of 50 km below the Rocky Mountains adjacent to Rocky Mountain House. Therefore, this possible flexure of the crust could create enough stresses to generate micro-earthquake activity in the basement of the Rocky Mountains.

5.2.2.1 Is There a Relationship to the Athabasca Axis?

There is a gravity low extending northeast perdendicular to the Rocky Mountains (Douglas 1970). This anomaly extends from the area of Rocky Mountain House southwest of Edmonton Alberta to North Saskatchewan, and North West Territories. This feature is referred as the Athabasca axis in north Saskatchewan (Darnley 1981) or the Fond du Lac gravity low (Walcott 1968). This gravity low correlates with granitoids containing elevated levels of radioelements (Darnley 1981).

There exists geologic speculation (Darnley 1981) that this rock belt is the result of intrusion into a zone of tensional faulting that developed before the end of the lower Proterozoic. If this is in fact the case, it is reasonable to expect remnant zones of weakness in this portion of the lithosphere. Walcott (1968) studied a portion of this anomaly in Northeastern Alberta and Northern Saskatchewan. In order to explain the Fond du Lac gravity low, he proposed a crustal thinning, perhaps related to tensional stresses in the past, to 34km from 40km with a relatively low density below this anomaly. Such lateral density anomalies could lead to stresses related to isostatic compensation (McNutt 1980). In other regions such stresses may lead to seismicity, but analysis of the archives of the Edmonton seismic station (McGavin personal communication) shows no seismicity along this gravity anomaly.

The exception to this statement occurs where the Fond du Lac trend intersects the Canadian Cordillera. Here, in the region of Rocky Mountain House, the combination of loading stresses from the foreland and isostatic compensation stresses due to the crustal density gradients could conceivably activate zones of weakness in the pre-Cambrian crust. Such zones of weakness need not be large faults but they imply a degree of brittle yielding in the lithosphere at this point.

I do not suggest that major fault zones exist in the Pre-Cambrian basement, for SW NE reflection profiles in Southwest Alberta imply that the crystalline basement has not been involved in the shortening of the Canadian Rockies (Balley et al 1966). Structure contour maps of the top of the Devonian and of the top of the Sub-Cretaceous show NW-SE and NE-SW trends in central Alberta. Those trends could be faults (Robinson et al 1969).

I conclude therefore that deeper parts of the basement below the South West Alberta can undergo some deformation and consequently generate the deep seismicity I suggest is associated with the Rocky Mountain House Earthquake swarm.

5.3 Summary of Conclusions

Reasonably reliable source mechanism studies can be done with single digital stations at some distance from an earthquake. Source parameter estimates can be related systematically to those derived from close-in records. In general seismic moments derived from body waves at distant stations are smaller than those derived from near stations

The useful band of information on 2 vastly different systems, the RESMAC system, and the EDM station, turned out to be very much the same. This reflects a property of the seismic noise background and should be useful for other analyses of local networks.

Localized zones of seismic activity rather than a random distribution (Milne and White 1958) exist in South West Alberta. One such zone, the Rocky Mountain House area, is characterized by shallow events which might be related to hydrocarbon recovery operations and deeper events which may reflect yielding of the lithosphere under a combination of isostatic compensation stresses and the load of the Canadian Cordillera. More detailed research should be done with local networks in order to map this activity.

The shallow events at Rocky Mountain House are characterized by high stress drops, the deep events have low stress drops. This suggests distinctly different properties of the fault zones and supports the separation of this activity into 2 different types. The shallow events are probably related to secondary recovery processes in nearby gas fields, the deep activity may reflect reactivation of ancient zones of weakness in the pre-Cambrian basement.

6. References

Aki, K. Scaling law of seismic spectrum. **J. Geophys. Res.** 72, 1217-1231, 1967.

Aki, K. and Richards, P. G. Quantitative Seismology Theory and Methods. Volume I and II. **W. H. Freeman and Company San Francisco**, 1980.

Anderson, D.L., and Hart R.S., Q of the earth. **J. Geophys. Res.** , 83, 5869-5882 , 1978

Archambeau, C. B., General theory of elasto-dynamic source fields, Rev. Geophys. Space Phys. 6, 241-288, 1968.

Archambeau, C. B., Developments in seismic source theory. Rev. Geophys. Space Phys. 13, 304-306, 1975.

Bakun, W., and Bufe, C. G., Shear-wave attenuation along the San Andreas fault zone in central California. **Bull. Seism. Soc. Am.** 65, 439-459, 1975.

Bath, M. The energies of seismic body waves and surface waves. In: H. Benioff, M. Ewing, B. F. Howell, Jr., and Press (Editors), Contributions in Geophysics: In honor of Beno Gutenber. Pergamon, New York. pp. 1-16, 1958.

Bath, M. and Duda, S. J. Earthquake volume, fault plane area, seismic energy, strain, deformation and related quantities. **Ann. Geof.** 17, 353-368, 1964.

Ben-Menahem, A., Earthquake similarity laws. **Phys. Earth Planet.** Int., 15, P10-P18, 1977.

Ben-Menahem, A., The role of shear mach number in earthquake source dynamics., **Bull. Seism.** Soc. **Am.** 66, 1787-1799, 1976.

Ben-Menahem, A., and S. J. Singh., Computation of models of elastic dislocation in the earth, In:B. A. Bolt (Editor), Methods in computational physics, Academic press, New York, 12, 299-375, 1972.

Beaumont, C., Foreland Basins., **Geophys. J. R. Astro. Soc.** 65, 291-329, 1981.

Berckhemer, H. Die Ausdhnung der bruchflache im Erdbebenherd und ihr Einfluss auf das seismische Wellenspektrum, **Gerlands Beitr. z. Geophys.**, 71, 5-26, 1962.

Berg, E., Relation between earthquake foreshocks, stress and mainshocks. **Nature**, 219, 1141-1143, 1968.

Brace, W. F., and Kahlstedt, D. L., Limits on Lithospheric stress imposed by laboratory experiments. **J. Geophys. Res.** 85, 6248-6252, 1980.

Brune, J. N. Seismic moment, seismicity, and rate of slip along major fault zones. **J. Geophys. Res.** 73, 777-784, 1968.

Brune,J.N., Tectonic stress and the spectra of seismic shear waves from earthquakes, J. Geophys. Res., 75, 4997-5009 , 1970

Brune, J. N., (1971) Correction, **J. Geophys. Res.** 76, pp. 5002

Brune, J.N., Archuleta, R.J., and Hartzell, S., Far-field S-wave spectra, corner frequencies, and pulse shapes, J. Geophys. Res., 84, 2262-2272 , 1979

Bell J. S., and Gough D. I., Northeast-Southwest compressive stress in Alberta : evidence from oil wells **Earth**

Planet. Sci. Lett., 45, 475-482, 1979.

Bokman, J. Post-Mississippian unconformity in western Canada basin: In Childs, O. E., Editor, Backbone of the Americas, Tulsa, Am. Assoc. Petroleum Geologists Mem. 2, 231-242, 1963.

Burridge, R. The effect of sonic rupture velocity on the ratio of S to P corner frequencies. **Bull. Seism.** Soc. **Am.** 65, 667-675, 1975.

Burridge, R., and L. Knopoff. Body force equivalents for seismic dislocations. **Bull. Seism. Soc. Am.** 54, 1875-1888, 1964.

Bally A. W., Gordy P. L., and Stewart G. A. (1966) Structure, seismic data, and orogenic evolution of southern Canadian Rocky Mountains. **Bull. Canadian Petroleum Geology** Vol 14 pp. 337-381.

Bakun, W. H. Bufe, C. G., and Stewart, R. M. Body-wave spectra of central California earthquakes. **Bull. Seism. Soc. Am.** 66, 363-384, 1976.

Chinnery, M. A. Earthquake magnitude and source parameters, **Bull. Seism. Soc. Am.** 59, 1969-1982, 1969.

Clowes R. M. and Kanasewich E. R., Seismic attenuation and the nature of reflecting horizons within the crust.J. **Geophys. Res.**, 75, 6693-6705, 1970.

Chael, E. P., and Stewart, G. S., Recent large earthquakes along the Middle American Trench and Their implications for the subduction process. **J. Geophys. Res.** 87, 329-338, 1982.

Chandra N. N., and Cumming G. L., Seismic refraction studies in Western Canada. **Can. J. Earth Sci.**, 9, 1099-1109, 1972.

Cox, A. Plate tectonics and geomagnetics reversals. **W. H. Freeman and Company**, 1973.

Cumming G. L. and Chandra N. N. (1975) Further studies of reflections from the deep crust in Southern Alberta., **Can. J. Earth Sci.**, 12, 539-557.

Das, S., and Aki, K., Fault plane with barriers: A versatile earthquake model, J. **Geophys. Res.** 82, 5658-5670, 1970.

Dahlen, F.A., On the ratio of P-wave to S-wave corner frequencies for shallow earthquakes sources, Bull. Seism. Soc. Am., 64, 1159-1180 , 1974

Dahlstrom C. D. A., Structural geology in the eastern margin of the Canadian Rocky Mountains. **Bull. of Canadian Petroleum Geology** 18, 332-406, 1970.

Dahlstrom C. D. A., Balanced cross sections. **Can. J. Earth Sci.** 6, 743-757, 1969.

Douglas, B. M. and Ryall, A. Spectral characteristics and stress drop for microearthquakes near Fairview Peak, Nevada. J. **Geophys. Res.** 77,351-359, 1972.

Elliott D., The motion of thrust faults. **J. Geophys. Res.** 81, 949-963, 1976.

Engdahl, E. R., Flinn, E. A., and Romney C. F. Seismic waves reflected from the earth's inner core.

Ellis, R. M., Dragert, H., and Ozard, J. M., Seismic activity in the McNaughton lake area, Canada.,

Engineering Geology, 10, 227-238, 1976.

Ellis, R. M., and Chandra, B., Seismicity in the mica reservoir (McNaughton lake) area: 1973-1978. **Can. J. Earth Sci.** 18, 1708-1716, 1981.

Evernden, J. F., Study of regional seismicity and associated problems, **Bull. Seism. Soc. Am.** 60, 393-446, 1970.

Fletcher, J. B. Spectra from high-dynamic range digital recordings of Oroville, California aftershocks and their source parameters. **Bull. Seism. Soc. Am.** 70, 735-755, 1980.

Guzman, J. E., and Zoltan de Cserna. Tectonic History of Mexico **In Childs, O. E., Editors, Backbone of the Americas, Tulsa, Am. Assoc. Petroleum Geologist Mem.** 2. pp. 113-129, 1963.

Garza T., Gil J., Lomnitz C., Tubilla A., Estado de avance de la red sismologica Mexicana de apertura continental RESMAC. Ingenieria Vol XLVIII, Num 2 UNAM , Abril-Junio 1978 Mexico.

Geller, R. J. Scaling relations for earthquake source parameters and magnitudes. **Bull. Seism. Soc. Am.** 66, 1501,-1523, 1976.

Gibowicz, S. J. Variation of source properties: The Inangahua, New Zeland, aftershocks of 1968. **Bull. Seism. Soc. Am.** 65, 261-276, 1975.

Gutenber, B. and Richter. C. F. Earthquake magnitude, intensity, energy, and acceleration. **Bull. Seism. Soc. Am.** 32, 163-191, 1942.

Gutenberg, B. and Richter, C. F. Earthquake magnitude, intensity, energy, and acceleration (second paper). **Bull. Seism. Soc. Am.** 46, 105-145, 1956.

Gough D. I., and Bell J. S., Stress orientations from oil well fractures in Alberta and Texas. **Canadian Journal of Earth Sciences** 18, 638-645, 1981.

Ganley D. C. and Cumming G. L., A seismic reflection model of the crust near Edmonton, Alberta. **Can. J. Earth Sci.** 11, 101-109, 1974.

Geller, J. R. and Mueller, C. S. Four similar earthquakes in central California. **Geophysical Research Letters** 7, 821-824, 1980.

Garland, G. D., and Burwash, R. A., Geophysical and Petrological Study of Precambrian of Central Alberta, Canada. **Bull. Am. Association of Petroleum Geologists** 43, 790-806, 1959.

Haskell, N. A. Radiation pattern of surface waves from point sources in a multilayered medium. **Bull. Seism. Soc. Am.** 54, 377-394, 1964.

Hanks, T. C. and Thatcher, W. A graphical representation of seismic source parameters. **J. Geophys. Res.** 77, 4393-4405, 1972.

Hanks, T. C., and Wyss, M., The use of body-wave spectra in the determination of seismic-source parameters. **Bull. Seism. Soc. Ame.** 62, 561-590, 1972.

Hartzell, S. H. and Brune, J. Source parameters for the January 1975 Brawley-Imperial valley earthquake swarm.

Pure and Applied Geophysics. 115, 333-355, 1977.

Hanks, T. C. The corner frequency shift, earthquake source models, and Q. **Bull. Seism. Soc. Am.** 71, 597-612, 1981.

Hanks, T. C., and Raleigh, C. B., The conference on magnitude of deviatoric stresses in the earth's crust and uppermost mantle, **J. Geophys. Res.** 85, 6083-6085, 1980.

Horner, R. B., Stevens, A. E., and Hasegawa, H. S., The Bengough, Saskatchewan, earthquake of July 26, 1972. **Can. J. Earth Sci.** 10, 1805-1821, 1973.

Iida, K., and Aki, K., Seismic source time function of propagating longitudinal shear cracks, **J. Geophys. Res.** 27, 2034-2044, 1972.

IMSL 1979. International Mathematical and Statistical Libraries Inc., 6th floor, GNB Building, 7500 Bellaire Blvd., Houston, TX.77036 U.S.A.

Johnson, L. R., Seismic source theory. **Rev. Geophys. Space Phys.** 17, 328-336, 1979.

Johnson, L. R. and McEvilly, T. V. Near-field observations and source parameters of central California earthquakes. **Bull. Seism. Soc. Am.** 64, 1855-1886, 1974,

Kanamori, H., and Anderson, D. L., (1975). Theoretical basis of some empirical relations in seismology. **Bull. Seism. Soc. of America** 75. pp. 1073-1095

Kanamori, H. The energy release in great earthquakes. **J. Geophys. Res.** 82, 2981-2987, 1977.

Kanaswich, E. R., Clowes R. M., and McCloughan, C. H. A buried Precambrian rift in Western Canada. **Tectonophysics** 8, 513-527, 1969.

Keilis-Borok, V. I. An estimation of the displacement in an earthquake source and of source dimensions. **Ann. Geofis.** 12, 205-214, 1959.

Keating, L. F., Exploration in the Canadian Rockies and South West Alberta, **Canadian Journal of Earth Sciences** 3, 713-723, 1966.

Knopoff, L. Energy release in earthquakes. **J. Geophys. Res.** 1, 44-52, 1958.

Lomnitz, C., Gil, J., RESMAC, the new Mexican seismic array. **EOS** 57, 2, 68-69, 1976.

Maruyama, T. On the force equivalent of dynamic elastic dislocations with reference to the earthquake mechanism. **Bull. of the Earthquake Research Institute, Tokyo University** 48, 467-486, 1963.

Madariaga, R., Dynamics of an expanding circular fault, Bull. Seism. Soc. Am., 66, 639-666 , 1976

Madariaga, R., Implications of stress-drop models of earthquakes for the inversion of stress drop from seismic observations, **Pure Appl. Geopys.**, 115(112), 301-316 , 1977

Monger, J. W. H., and Price, R. A., Geodynamic evolution of the Canadian Cordillera- progress and problems, **Can. J. Earth Sci.** 16, 770-791, 1979.

Milne, W. G., and Rogers, R. P., Riddihough, McMechan, G. A., and Hyndman, R. D., Seismicity of western Canada.

Can J. Earth Sci. 15, 1170-1193, 1978.

Milne, W. G., The Snipe lake, Alberta earthquake of March 8, 1970. **Can. J. Earth Sci.** 7, 1564-1567, 1970.

Milne, W. G., and White, W. R. H., A seismic investigation of mine "bumps" in the Crowsnest Pass coal field. **The Canadian Mining and Metallurgical Bulletin**, 51, 678-685, 1958.

Molnar, P., Tucker, B.E., and Brune J.N., Corner frequencies of P and S waves and models of earthquake sources, Bull. seism. Soc. Am., 64, 1159-1180 , 1973

McGarr, A., Spottiswoode, S.M., Gay, N.C., and Ortlepp, W.D., Observations relevant to seismic driving stress, stress drop, and efficiency, J. Geophys Res., 84, 2251-2261 , 1979

Munguia,L., J. Brune, A. Reyes, J. Gonzalez, R. Simons, F. Vernon, 1979, Digital Seismic Event Recorder Records and Spectra for Aftershocks of the November 28, 1978, Oaxaca Earthquake, **Geofisica Internacional**, Vol 17, 3,1979

McCloughan C. H. and Kanasewich E. R. (1974). Geophysical data link manual. **University of Alberta.**

McGarr, A., Some constraints on levels of shear stress in the crust from observations and theory. **J. Geophys. Res.** 85, 6231-6238, 1980.

McKenzie, D., and Jarvis, G., The conversion of heat into mechanical work by mantle convection. **J. Geophys. Res.** 85, 6093-6096, 1980.

Martin L. J., Tectonics of Northern Cordillera in Canada: in

Childs, O. E., Editor, Backbone of the Americas, Tulsa, Am. Assoc. Petroleum Geologists Mem. 2, 243-251, 1963.

Mogi, K., Study of the elastic shocks caused by the fracture of heterogeneous materials and its relation to earthquake phenomena, Bull. Earth Res. Inst. 40, 125-173, 1962.

Miyatake, T., Numerical simulations of earthquake source process by a three-dimensional crack model. Part I. Rupture process. J. Phys. Earth 28, 565-598, 1980a.

Miyatake, T., Numerical simulations of earthquake source process by a three-dimensional crack model. Part II. Seismic waves and spectrum. J. Phys. Earth. 28, 599-616, 1980b.

Marion, G. E. and Long, L. T. Microearthquake spectra in the Southeastern United States. Bull. Seis. Soc. Am. 70, 1037-1054. 1980.

McNutt, M. Implications of Regional Gravity for State of Stress in the Eart's Crust and Upper Mantle. J. Geophys. Res. 83, 6377-6396, 1980.

Nuttli, O., The effect of the Earth's surface on the S wave particle motion, Bull. Seism. Soc. Am., 51, 237-246 , 1961

Nyland, E. (1981). Stress and strain in the North America Plate, Abstract G. A. C./ C. G. U. Meeting May 1981, Calgary.

Orowan, E. Mechanism of seismic faulting in rock deformation, A symposium. Geol. Soc. Amer. Mem. 79, 232-345, 1960.

Ohtake, M., Matumoto, T., and Latham, G.V., Seismicity gap near Oaxaca, southern Mexico, as a probable precursor to a large earthquake, **Pure. Appl. Geophys.**, 115, 375-385, 1977.

Ohnaka, M. Earthquake-source parameters related to magnitude. **Geophys. J. R. Astr. Soc.** 55, 45-66, 1978.

Pilant, W. L. Elastic waves in the earth. **Elsevier Scientific Company**, 1979.

Pearson, C., The relationship between microseismicity and high pore pressure during hydraulic stimulation experiments in low permeability granitic rocks. **J. Geophys. Res.** 86, 7855-7864, 1981.

Ponce, L.,McNally, K., Sumin de portilla, V., Gonzalez, J., Del Castillo, A., Gonzalez, L., Chael, E. French, M. Oaxaca, Mexico earthquake of 29 November 1978: A preliminary report on spatio-temporal pattern of preceding seismic activity in mainshock relocation. **Geofis. Inter.**, 17:2, 109-126, 1978.

Prince, J., H. Rodriguez, E. Z. Jawaski, G. Kilander, A strong Motion Radio Telemetry Network, Proceedings of the fifth World Conference on **Earthquake Engineering**, 1, 1095-1103, 1973.

Randall, M. J. The spectral theory of seismic sources. **Bull. Seism. Soc. Am.** 63, 1133-1144, 1973.

Randall, M. J., Stress drop and the ratio of seismic energy to moment. **Journal of Geophys Res.** 77, 969-970, 1972.

Reyes A., Gonzalez J., Munguia L., Nava A., Vernon F., Brune J. N., Locations of aftershocks of the Oaxaca earthquake using amoked paper and digital event recorders. **Technical report** Sept. 1979

Reichle, M. S., A seismological study of the Gulf of California: Sonobuoy and teleseismic observations, and tectonic implications, **PhD Tesis University of California San Diego**, 1975.

Richter, C. F., An instrumental earthquake scale, **Bull. Seism. Soc. Am.** 25, 1-32, 1935.

Richter, C. F. Elementary Seismology **W. H. Freeman and Company**. 1958.

Richards, T. C., and Walker, D. J., Measurements of the thickness of the earth's crust in the Albertan plains of Western Canada. **Geophysics** Vol. XXIV, 262-284, 1959.

Rudnicki, J. W. and Kanamori, H. Effects of fault interaction on moment, stress drop, and strain energy release. **J. Geophys. Res.** 86, 1785-1793, 1981.

Rebollar, C. J., and Nyland, E., Spectra of some Oaxaca earthquake aftershocks from RESMAC. **Geofisica Internacional** 19, 109-127, 1980.

Rebollar, C. J., Kanasewich, E. R., and Nyland, E. Focal depths and source parameters of the Rocky Mountain House earthquake swarm from digital data ar Edmonton. **Submitted for publication to the Canadian Journal of Earth Sciences.** 1982.

Rebollar, C. J., Kanasewich, E. R., and Nyland, E. Source parameters from shallow events in the Rocky Mountain House earthquake swarm. In Press **Canadian Journal of Earth Sciences**. 1982.

Rogers, G. C., Ellis, R. M., and Hasegawa, H. S., The McNaughton lake earthquake of May 14, 1978. **Bull. Seism. Soc. Am.** 70, 1771-1786, 1980.

Rogers, G. C. and Ellis, R. M., The eastern British Columbia earthquake of February 4, 1918., **Can. J. Earth Sci.** 16, 1484-1493, 1979.

Rogers, G. C., The McNaughton lake seismicity- more evidence for an Anahim hotspot?., **Can. J. Earth Sci.** 18, 826-828, 1981.

Savage, J.C., Relation between P-and S-wave corner frequencies in the seismic spectrum, Bull. Seim. Soc. Am., 64, 1621-1627 , 1972

Saito, T. and T. Hirasawa, Body wave spectra from propagating shear cracks. **Journal of Physics of the Earth** 21, 415-431, 1973.

Singh, S. K., Astiz, L., and Havskov, J., Seismic gaps and recurrence periods of large earthquakes along the Mexican subduction zone: A reexamination. **Bull Seism. Soc. Am.** 71, 827-843, 1981.

Scholz, C., The frequency-magnitude relation of microfracturing in rock and its relationto earthquakes, **Bull. Seis. Soc. Am.** 58, 399-415, 1968.

Stevens, A. E., Some twentieth-Century earthquakes., **Geoscience Canada**, 4, 41-45, 1977.

Stein, S., An earthquake swarm on the Chagos-Laccadive ridge and its tectonics implications, **R. Astron. Soc., Geophys. J.**, 55, 577-588, 1978.

Scholz, C., The frequency-magnitude relation of microfracturing in rock and its relation to earthquakes, **Bull. Seism. Soc. Am.** 58, 399-415, 1968.

Solomon, S. C., Richardson, R. M., and Bergman, E. A., Tectonic stress: Models and magnitudes. **J. Geophys. Res.** 85, 6086-6092, 1980.

Scholz, C. H., Shear heating and the state of state of stress on faults, **J. Geophys Res.** 85, 6174-6184, 1980.

Zoback, M. D., Tsukahara, H., and Hickman, S., Stress measurments at depth in the vicinity of the San Andreas fault: Implications for the magnitude of shear stress at depth. **J. Geophys. Res.** 85, 6157-6173, 1980.

Zoback, M. L., and Zoback, M., State of stress in the conterminous United States. **J. Geophys Res.** 85, 6113-6156, 1980.

Stewart, G.S., and Chael, E. Source mechanism of the November 29, 1978, Oaxaca, Mexico earthquake - A large simple event, Earthquakes Notes, 49, 47 , 1978

Singh, S. K., and Havskov, J. A Moment-Magnitude scale. **Bull. Seism. Soc. Am.** 70, 379-383, 1980.

Starr, A. T., Slip in a cystal and rupture in a solid due to shear. **Proc. Camb. Phil. Soc.** 24, 489-500, 1928.

Spottiswode, S. M. and McGarr. A. Source parameters of tremors in a deep-level gold mine. **Bull. Seism. Soc. Am.**

65, 93-112, 1975.

Shamina, O. G., Pavlov, A. A., and Strzhkov, S. A. Model studies of shear displacement along a pre-existing fault. **Pure and Applied Geophysics** 116, 900-912, 1978.

Savage, J. C. Relation between P- and S-wave corner frequencies in the spectrum. **Bull. Seism. Soc. Am.** 64, 1621-1627, 1974.

Savage, J. C. Relation of corner frequency to fault dimensions. **J. Geophys. Res.** 77, 3788-3795, 1972.

Sato, R. (1979). Theoretical basis on relationships between focal parameters and earthquake magnitude. **J. Phys. Earth**, 27, pp. 353-372.

Steketee, J. A. Some geophysical applications of the elastic theory of dislocations. **Canadian Journal of Physics** 36, 1168-1197, 1958.

Sahay, P. N., Seismic source theory. **Master of Science Thesis University of Alberta Canada.** 1980.

Shaw E. W., Canadian Rockies-Orientation in time and space: **in Childs, O. E., Editor, Backbone of the Americas, Tulsa, Am. Assoc. Petroleum Geologist Mem.** 2, 231-242, 1963.

Sykes, L. R., Earthquake swarms and sea-floor spreading. J. **Geophys. Res.**, 75, 6598-6611, 1970.

Suzuki, Z., A statistical study on the occurrence of small earthquakes (Fourth paper). **Tohoku Daigaku, Sendai Japan Science Reports Fifth Series Geophysics.** 11, 10-54, 1959.

Thatcher, W. and Hanks, T.C., Source parameters of Southern California earthquakes, J. Geophys. Res., 78, 8547-8576 , 1973

Tucker, E.B., Brune, J.N., Source mechanism and Mb-Ms analysis of aftershocks of the San Fernando earthquake, Geophys. J. Roy. Astr. Soc., 49, 371-426 , 1977

Tsuboi, C. Earthquake energy, earthquake volume, aftershock area, and strengh of the earth's crust. **Journal of Physics of the Earth** 4, 63-66, 1956.

Thompson R. I. (1979). A structural interpretation across part of the northern Rocky Mountains, British Columbia, Canada **Can. J. Earth Sci**. 16, pp. 1228-1241.

Utsu, T. and Seki, A. A relation between the area of the aftershock region and the energy of main shock, Zisin, 7, 233-240, (in Japanese).

Vargas, C. A., Minsoni, A., and Singh, K., Far-field displacement from a rectangular fault with two rupture velocities, **Pure. Appl. Geophys**. 118, 991-1006, 1980.

Vinogradov, S. D. Experimental observations of elastic wave radiation characteristics from tensile cracks and pre-existing shear faults. **Pure and Applied Geophysics** 116, 888-899, 1978.

Weertman, J. Continuum distributions of dislocations on faults with finite friction. **Bull. Seism. Soc. Am.** 54, 1035-1058, 1964.

Whitham K. Milne W. G. and Smith E. T. (1970). The new seimic zoning map for Canada 1970 edition. **The Canadian**

Underwriter, June 15th, 1970.

Whitham, K., The estimation of seismic risk in Canada. **Geoscience Canada**, 2, 133-140, 1975.

Whitham, K., Protection of the public from earthquake hazards in Canada. **Geophysics**. 12, 1-5, 1972.

Walcott, R. I., The gravity field of Northern Saskatchewan and Northeastern Alberta. **Department of Energy, Mines and Resources Observatories Branch, Canada** 1-21, 1968.

Wyss, M., Towards a physical understanding of the frequency distribution. **Geophys. J. R. Astro. Soc.** 31, 341-359, 1973.

Wyss, M., and Brune, J. N. Seismic moment, stress, and source dimensions for earthquakes in the California-Nevada region. **J. Geophys. Res.** 73, 4681-4694, 1968.

Wyss, M. Stress estimates for South American shallow and deep earthquakes **J. Geophys. Res.** 75, 1529-1544, 1970.

Wetmiller, R. J. Microseismicity in the Rocky Mountain House seismogenic zone, Western Canada. **Abstract G.A.C./C.G.U. Meeting May 1981, Calgary** Energy, Mines and Resources, Ottawa.

7. Appendix 1

Plots of the first 52 hours of aftershocks from the Oaxaca Earthquake.

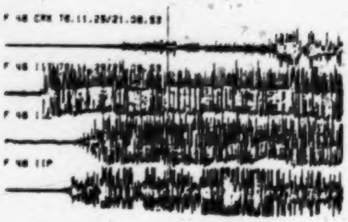
F 46 CRX 78.11.29/21.38.53
F 46 IIT
F 46 IIC
F 46 IIP

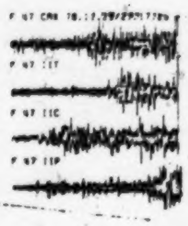
F 47 CRX
F 47 IIT
F 47 IIC
F 47 IIP

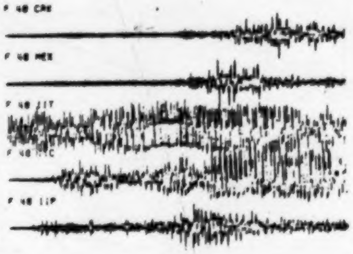
F 48 CRX
F 48 MEX
F 48 IIT
F 48 IIC
F 48 IIP

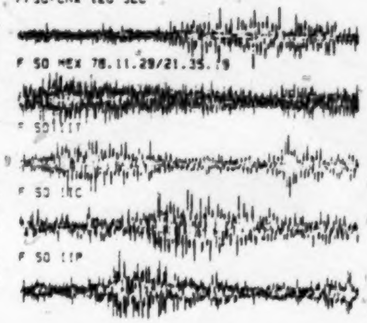
F 50 CRX 120 SEC
F 50 MEX 78.11.29/21.35.19
F 50 IIT
F 50 IIC
F 50 IIP

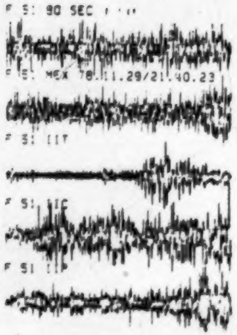
F 51 90 SEC
F 51 MEX 78.11.29/21.40.23
F 51 IIT
F 51 IIC
F 51 IIP

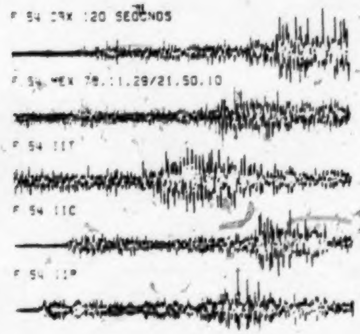
F 54 CRX 120 SECONDS
F 54 MEX 78.11.29/21.50.10
F 54 IIT
F 54 IIC
F 54 IIP

1 H

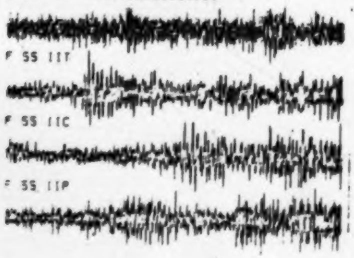
F 55 MEX 78.11.29/21.54.01
F 55 IIT
F 55 IIC
F 55 IIP

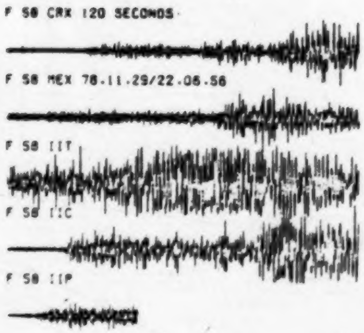
F 58 CRX 120 SECONDS
F 58 MEX 78.11.29/22.06.56
F 58 IIT
F 58 IIC
F 58 IIP

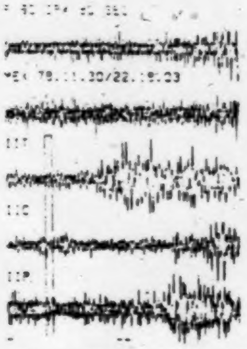
F 80 CRX 80 SEC
MEX 78.11.30/22.19.03
IIT
IIC
IIP

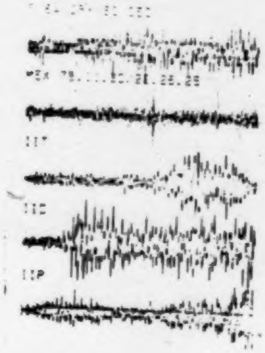
MEX 78.11.30/22.26.25
IIT
IIC
IIP

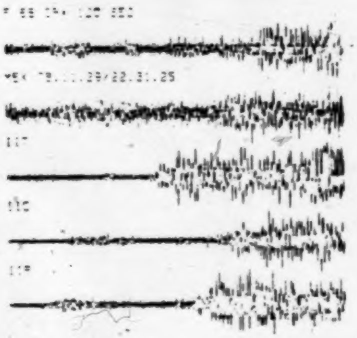
F 65 CRX 120 SEC
MEX 78.11.29/22.31.25
IIT
IIC
IIP

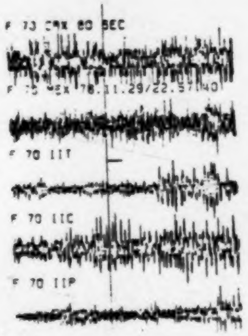
F 73 CRX 80 SEC
F 70 MEX 78.11.29/22.57.40
F 70 IIT
F 70 IIC
F 70 IIP

2 H

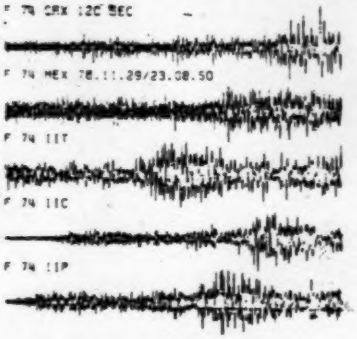
F 74 CRX 120 SEC
F 74 MEX 78.11.29/23.08.50
F 74 IIT
F 74 IIC
F 74 IIP

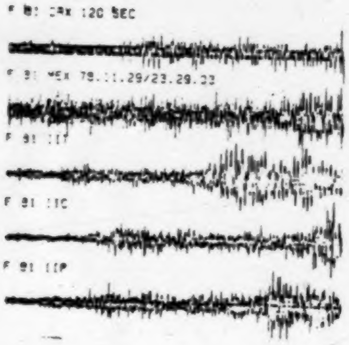
F 81 CRX 120 SEC
F 81 MEX 78.11.29/23.29.33
F 81 IIT
F 81 IIC
F 81 IIP

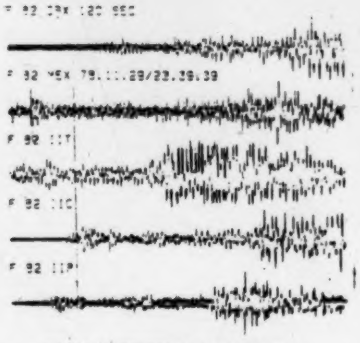
F 92 CRX 120 SEC
F 92 MEX 78.11.29/23.39.39
F 92 IIT
F 92 IIC
F 92 IIP

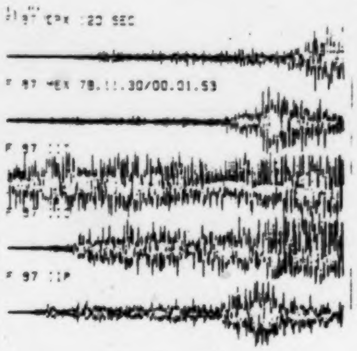
F 97 CRX 120 SEC
F 97 MEX 78.11.30/00.01.53
F 97 IIT
F 97 IIC
F 97 IIP

3 H

4 H

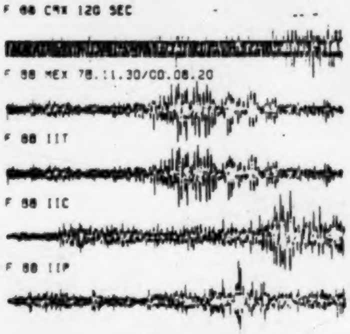
F 88 CRX 120 SEC
F 88 MEX 78.11.30/00.08.20
F 88 IIT
F 88 IIC
F 88 IIP

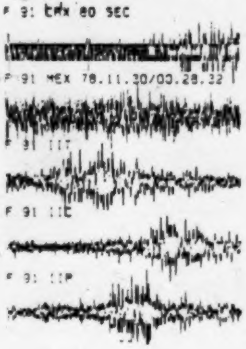
F 91 CRX 80 SEC
F 91 MEX 78.11.30/00.28.32
F 91 IIT
F 91 IIC
F 91 IIP

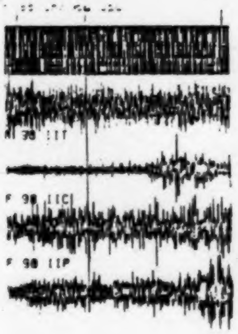
F 98 IIT
F 98 IIC
F 98 IIP

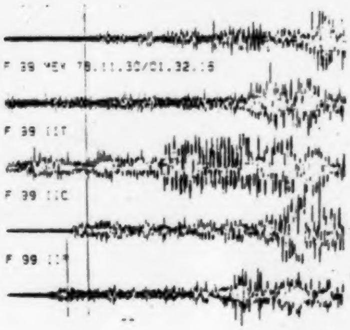
F 99 MEX 78.11.30/01.32.16
F 99 IIT
F 99 IIC
F 99 IIP

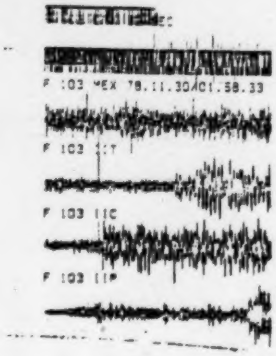
F 103 MEX 78.11.30/01.58.33
F 103 IIT
F 103 IIC
F 103 IIP

5H

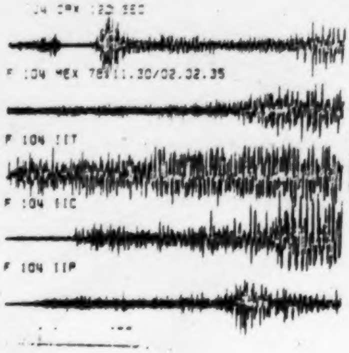
104 CRX 120 SEC
F 104 MEX 78.11.30/02.02.35
F 104 IIT
F 104 IIC
F 104 IIP

7H

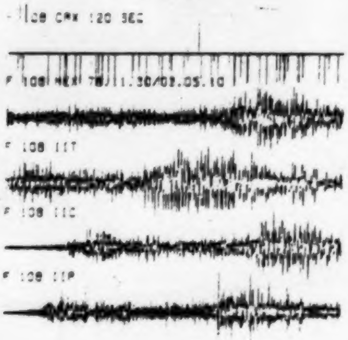
108 CRX 120 SEC
F 108 MEX 78.11.30/02.05.10
F 108 IIT
F 108 IIC
F 108 IIP

6H

8H

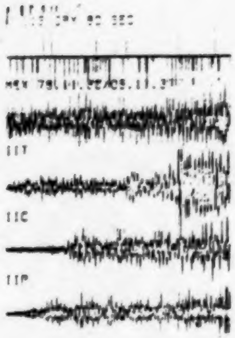
CRX 90 SEC
MEX 78.11.30/03.11.3
IIT
IIC
IIP

9 H

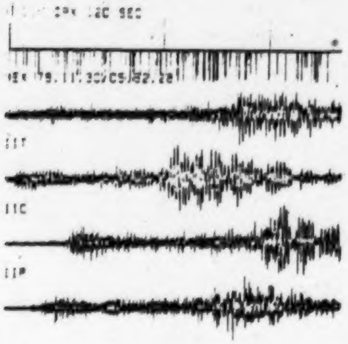

10 H

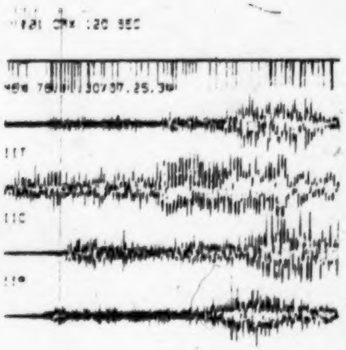

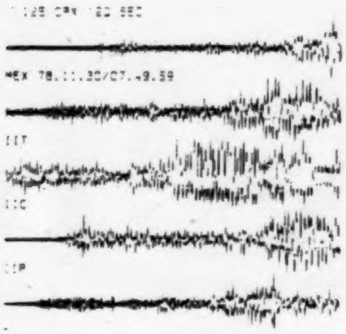

11 H

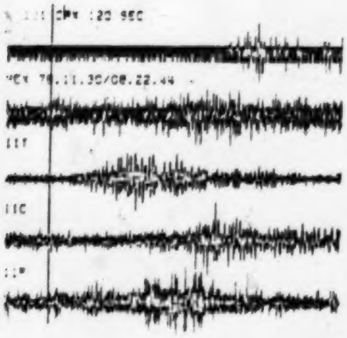

12 H

13 H

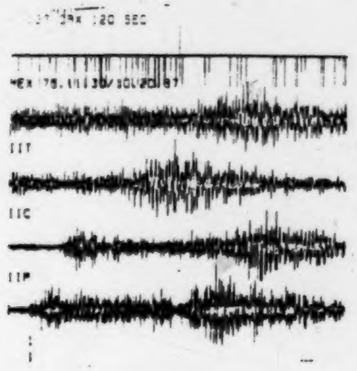
CRX 120 SEC
MEX
IIT
IIC
IIP

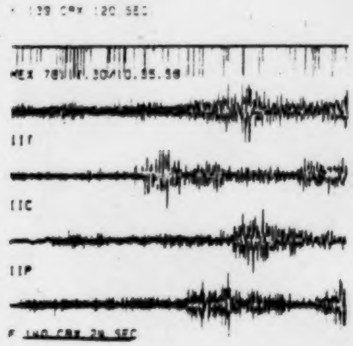
CRX 120 SEC
MEX 78.11.30/10.35.38
IIT
IIC
IIP
CRX SEC

14 H

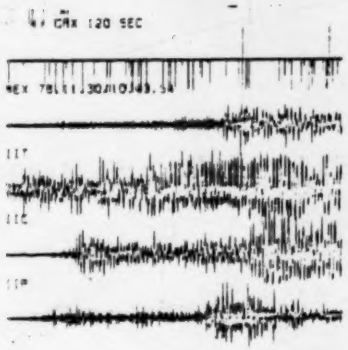
CRX 120 SEC
MEX
IIT
IIC
IIP

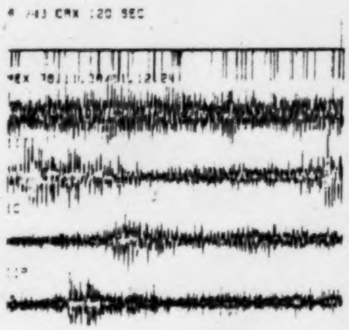
CRX 120 SEC
MEX
IC
IIP

15 H

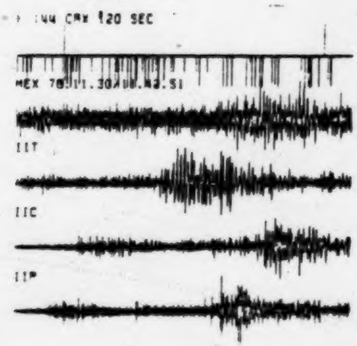
CRX 120 SEC
MEX 78.11.30
IIT
IIC
IIP

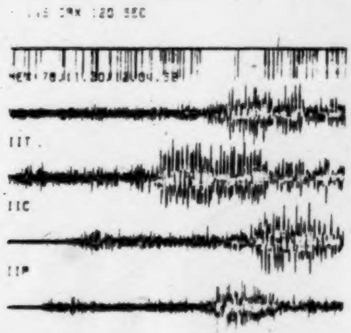
CRX 120 SEC
MEX 78.11.30
IIT
IIC
IIP

16 H

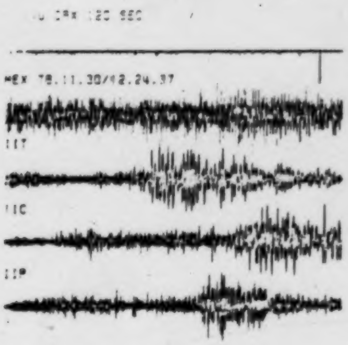
U CRX 120 SEC
MEX 78.11.30/12.24.37
IIT
IIC
IIP

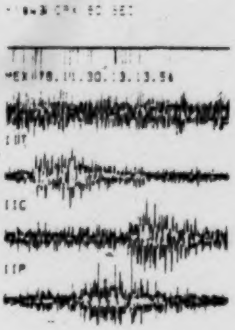
CRX 80 SEC
MEX 78.11.30.13.13.56
IIT
IIC
IIP

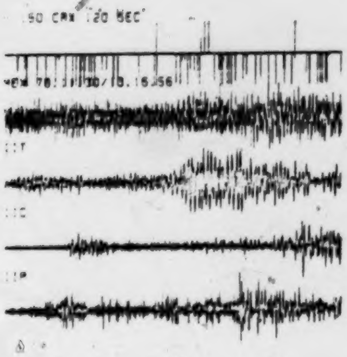
50 CRX 120 SEC
MEX 78.11.30/13.16.56
IIT
IIC
IIP

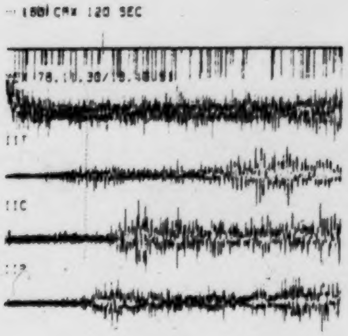
180 CRX 120 SEC
78.11.30/13.48
IIT
IIC
IIP

17 H

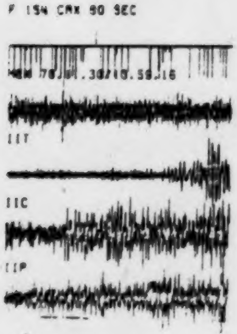
F 154 CRX 80 SEC
MEX 78.11.30/13.59.16
IIT
IIC
IIP

18 H

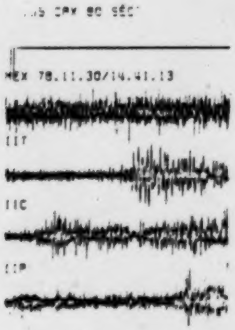
S CRX 80 SEC
MEX 78.11.30/14.41.13
IIT
IIC
IIP

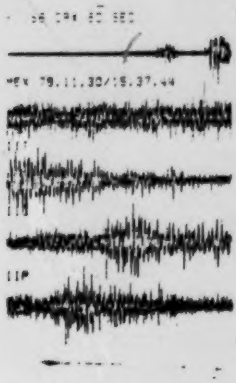
56 CRX 80 SEC
MEX 78.11.30/15.37.44
IIT
IIC
IIP

19 H

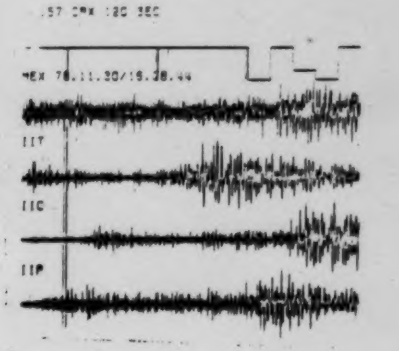
57 CRX 120 SEC
MEX 78.11.30/15.38.44
IIT
IIC
IIP

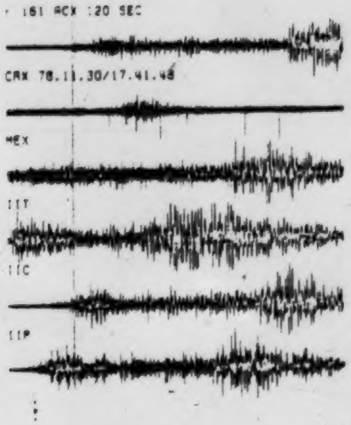
161 ACX 120 SEC
CRX 78.11.30/17.41.48
MEX
IIT
IIC
IIP

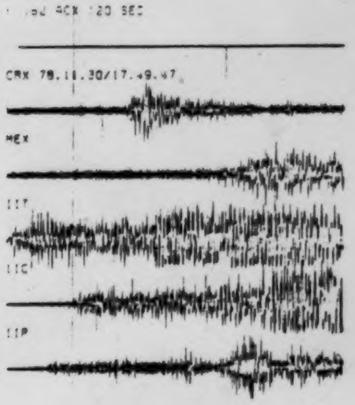
62 ACX 120 SEC
CRX 78.11.30/17.49.47
MEX
IIT
IIC
IIP

20 H

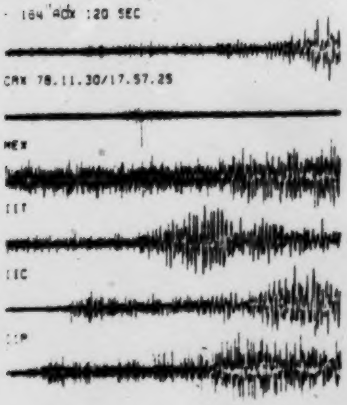
164 ACX 120 SEC
CRX 78.11.30/17.57.25
MEX
IIT
IIC
IIP

21 H

22 H

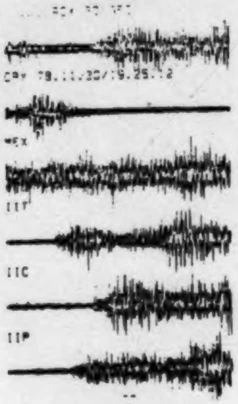

23 H

24 H

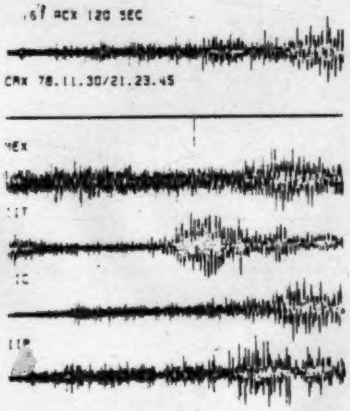

25 H

26 H

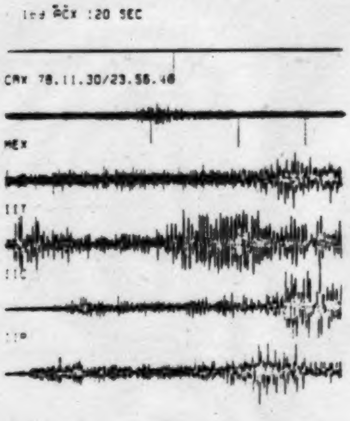

27 H

29 H

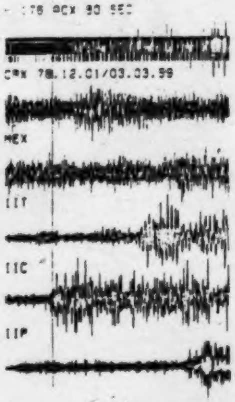

28 H

30 H

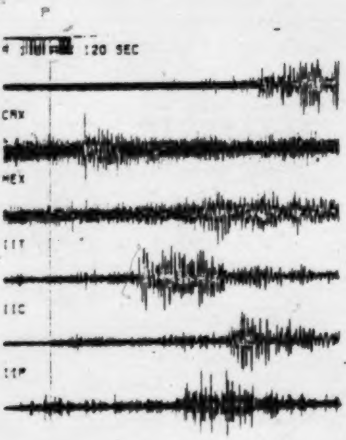

31 H

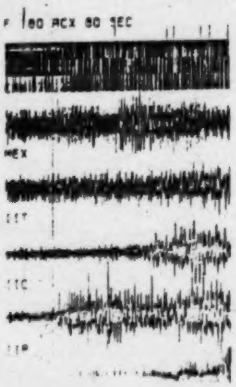

32 H

33 H

34 H

35 H

36 H

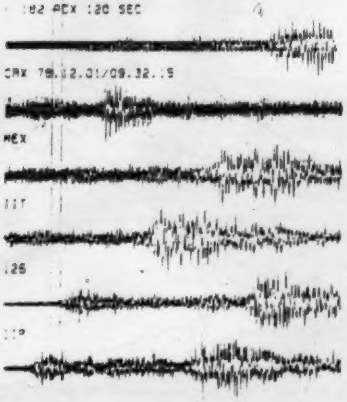

37 H

38 H

39 H

40 H

41 H

42 H

43 H

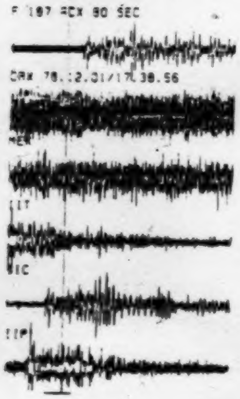

8. Appendix 2: Program listings

LEE program calculates the spectra of the aftershocks of the Oaxaca earthquake of November 29, 1978, recorded in the RESMAC system. The data is stored on tapes 001400, 001401, 001402, and 001403.

LEE2 program is an iterative program to read and plot the data recorded on the RESMAC system.

KADATA.S program calculate the spectra of S or P body waves of the events from the Rocky Mountain House earthquake swarm recorded in the DR-100 Sprengnether digital system.

RDANIEL program calculate the spectra of the body waves of the earthquakes detected at the digital permanent station of Edmonton, from the Rocky Mountain House earthquake Swarm.

```
                 $R *FORTG T=5
C
C ******************** LEE PROGRAM ************************
C
C        YOU NEED TO MOUNT THE TAPE LIKE THIS
C
C        $MOUNT 001401 9TP *T* SIZE=512 MODE=800
C
C     EVENTS 019,020,021,035 ARE IN THE FILES 28,36,62,217
C                 OF THE TAPE 001401
C
C  ALL THE DATA IS IN THE TAPES 001400 001401 001402 AND 001403
C
C
C                     OUTPUT FILES
C
C        7  = -SAM      SAMPLE LENGTH
C        8  = -SPEC     LOG OF THE SPECTRA CORRECTED FOR INSTRUMENT
C                       DISTANCE AND ATENUATION (Q).
C        10 = -Q        SEISMOGRAM
C        11 = -SPEC     SPECTRA CORRECTE BY ATENUATION AND DISTANCE
C                       BUT WITHOUT THE CORRECTION OF THE INTRUMENT.
C        12 = -SW       SPECTRA WITH CORRECTION OF INSTRUMENT DISTANCE
C                       AND ATTENUATION (Q).
C
          INTEGER ILFTL,ILFTR,ILSTL,ILSTR,IARR(60)
          DIMENSION D(8)
          INTEGER*2 IB(512),IB2(512),IE(40000)
          REAL ISAM(40000),AI(4000),AR(4000)
          INTEGER SHFTR,SHFTL,ALL,ALL1,ALL2,YES/'YES '/
          INTEGER ILF(100),ILS(100),IL,IR,IMA,IMAN,IEXP,LNUM
          INTEGER*2 LX,IS(512)
          REAL AMP(3000),FF(6000),DAT(7000),DATC(6000)
          REAL A(10000),FFLOG(6000),SAM(10000)
          DOUBLE PRECISION AMPLOG(6000),AMPOUT(6000)
          COMPLEX C(3000)
          INTEGER NN,MINI,NBS,NB
          LOGICAL*1 FREE(1)/'*'/
          DATA YES/'Y'/,ANO/'N'/
C
C   THIS IS THE CODE REQUIRED TO READ THE RESMAC TAPES
C
          REAL PI/3.141592654/
 1000     FORMAT(A1)
    9     WRITE(6,10)
   10     FORMAT(' WHICH FILE DO YOU WANT ?')
          READ(5,FREE,END=64) IWF
          CALL SKIP(IWF,0,6)
C
C       READ FIRST BLOCK, (DECODE THE EVENT INFORMATION)
C
          CALL READ(IB,LX,0,LNUM,6)
          DO 1 I=1,45
          ALL1=IB(I)
          ILFTL=SHFTL(ALL1,16)
          ILF(2*I-1)=SHFTR(ILFTL,24)
          ILFTR=SHFTL(ALL1,24)
          ILF(2*I)=SHFTR(ILFTR,24)
    1     CONTINUE
          WRITE(6,300)
  300     FORMAT(' YEAR MONTH DAY HOUR MIN SEC ')
          WRITE(6,200) (ILF(I),I=2,7)
          WRITE(6,400)
  400     FORMAT(' NUM OF STA THAT DETECTED THE EVENT')
          WRITE(6,499) ILF(39)
  499     FORMAT(15X,I4)
          WRITE(6,500)
  500     FORMAT(' STATIONS THAT DETECTED THE EVENT ')
          DO 2 I=40,45
    2     ILF(I)=ILF(I)/2
          WRITE(6,200) (ILF(I),I=40,45)
  200     FORMAT(1X,8I4)
C
C           READ SECOND BLOCK
C
          CALL READ(IB2,LX,0,LNUM,6)
          DO 3 I=1,7
          ALL2=IB2(I)
          ILSTL=SHFTL(ALL2,16)
          ILS(2*I-1)=SHFTR(ILSTL,24)
          ILSTR=SHFTL(ALL2,24)
          ILS(2*I)=SHFTR(ILSTR,24)
    3     CONTINUE
          WRITE(6,550)
C
C
C  DON'T TAKE IN CONSIDERATION THE 550 FORMAT  BECAUSE THIS WAS
C                        CHANGED
C
  550     FORMAT(' DIS OF STA IN THE SECOND BLOCK ')
          WRITE(6,200) (ILS(I),I=3,13,2)
          WRITE(6,600)
C
C
```

```
      C    THIS IS IMPORTANT BECAUSE IT TELL YOU HOW MANY BLOCKS IN EACH
      C    STATION WERE RECORDED. FOR EXAMPLE IF 6 STATIONS RECORDED AN
      C    EVENT YOU CAN GET
      C
      C       ARRAY IN BLOCKS OF THE STATIONS
      C         3  48  93  0  135  183 228
      C
      C                    THIS  MEAN
      C
      C     CHANEL                     BLOCKS                STATION
      C       0                      3   -  48                 CRX
      C       1                      49  -  93                 ACX
      C       2                      94  -  135                MEX
      C       4                      136 -  183                IIT
      C       5                      184 -  228                IIC
      C       6                      229 -  END OF FILE        IIP
      C
      C      THEREFORE IF YOU WANT STAION 4 (IIT) THEN YOU NEED
      C      TO SKIP 135 BLOCKS AND THEN YOU ARE AT THE BIGINING
      C                            OF IIT
      C
  800   FORMAT(' ARRAY IN BLOCKS OF THE STATIONS ')
        DO 4 I=34,40
        ALL2=IB2(I)
        ILSTL=SHFTL(ALL2,16)
        ILS(2*I-1)=SHFTR(ILSTL,24)
        ILSTR=SHFTL(ALL2,24)
        ILSTR=SHFTR(ILSTR,24)
        ILS(2*I)=SHFTL(ILSTR,8)
  4     IARR(I)=ILS(2*I-1)+ILS(2*I)
        WRITE(5,99) (IARR(I),I=34,40)
  99    FORMAT(1X,7I8)
        WRITE(5,702)
  702   FORMAT(' DO YOU WANT ANOTHER FILE?')
        READ(5,1000) DE
        IF(DE.EQ.YES) GO TO 5
      C
      C     AT THIS POINT, NOW, YOU KNOW IN WHICH BLOCKS ARE THE
      C     THE STATIONS. THEREFORE, YOU CAN CHOOSE THE STATION
      C                       THAT YOU WANT
      C
        WRITE(5,700)
  700   FORMAT(' HOW MANY BLOCKS DO YOU WANT TO SKIP ? ')
        READ(5,FREE,END=64) NBS
        CALL SKIP(0,NBS,3)
        WRITE(5,701)
  701   FORMAT(' HOW MANY BLOCKS DO YOU WANT TO READ ?')
        READ(5,FREE,END=64) NB
        N=256*NB
        CALL GETSAM(N,NB,ISAM,A)
        WRITE(5,804) N
  804   FORMAT('YOU HAVE',I5,' SAMPLES !')
        WRITE(5,800)
  800   FORMAT('HOW MANY SAMPLES DO YOU WANT TO PLOT ?')
        READ(5,FREE,END=64) NN
        WRITE(10,12) NN
        WRITE(5,805)
  805   FORMAT('FROM  WHICH SAMPLE DO YOU WANT TO PLOT?')
        READ(5,FREE,END=64) ISAIN
        NNN=ISAIN+NN-1
        WRITE(10,101) (A(I),ISAM(I),I=ISAIN,NNN)
        WRITE(5,803)
  803   FORMAT('DO YOU WANT TO GET A SPECTRUM ?.')
        READ(5,1000) DES
        IF(DES.EQ.ANO) GO TO 64
        WRITE(5,801)
  801   FORMAT('SAMPLING INTERVAL MINI & MFIN ')
        READ(5,FREE,END=64) MINI,MFIN
        NN=MFIN-MINI
        DO 13 I=1,NN
        J=MINI-1+I
  13    DAT(I)=ISAM(J)
      C
      C         THE SIGNAL IS FILTERED
      C
        CALL BNDPAS(0.2,7.0,27.77,D,G)
        CALL FILTER(DAT,NN,D,G,1)
        WRITE(7,12) NN
  12    FORMAT(I4)
        DO 98 I=1,NN
        S=I
        WRITE(7,101) S,DAT(I)
 101    FORMAT(2E12.5)
  98    CONTINUE
      C
      C   IN THIS PROGRAM WE ARE ASSUMING A P VELOCITY OF 6.5 KM/SEC
      C   AND THE PROGRAM ASK FOR THE S-P TIME, SHEAR WAVE VELOCITY
      C     VS (OR P WAVE VELOCITY VP) AND ATTENUATION Q.
      C
        WRITE(5,802)
  802   FORMAT(' S-P, VS OR VP & Q ')
        READ(5,FREE,END=64) SP,VS,Q
        HDIS=8.66*SP
        DTI=1./20
        M=2048
        LH=M/2+1
        DELF=1./(FLOAT(M)*DTI)
        DO 45 I=2,LH
        J=I-1
  45    FF(J)=(I-1)*DELF
        CALL CONDI(DAT,NN,DATC,M)
        DO 11 I=1,M
  11    C(I)=CMPLX(DATC(I),0.0)
      C
```

```
                      $R *FORTG T=5S
      C
      C **************** PROGRAM LEE2N *******************
      C
      C    THIS PROGRAM READ AND PLOT THE RESMAC DATA
      C
      C
            INTEGER ILFTL,ILFTR,ILSTL,ILSTR,IARR(50)
            DIMENSION D(6)
            INTEGER*2 IB(512),IB2(512)
            INTEGER *4 ISAM(40000)
            INTEGER SHFTR,SHFTL,ALL,ALL1,ALL2
            INTEGER ILF(100),ILS(100),IL,IR,IMA,IMAN,IEXP,LNUM
            INTEGER*2 LX,IS(512)
            INTEGER*4 A(10000)
            LOGICAL*1 FREE(1)/'*'/
            DATA YES/'Y'/,ANO/'N'/
            REAL PI/3.141592654/
            CALL PLOTS
            GO TO 1000
      5     CALL SKIP(0,-2,6)
      C
      C  HERE THE COMPUTER TELL YOU IN WHICH FILE YOU ARE
      C
            CALL FTNCMD('$DISPLAY *T*',13)
            WRITE(6,12)
        12  FORMAT(' DO YOU WANT TO QUIT ? Y/N')
            READ(5,13) DE
            IF(DE.EQ.YES) GO TO 63
      C
      C     SKIP ONE FILE AFTER THE FILE IN WHICH THE
      C    "POINTER" IS POSITIONED; OTHERWISE STOP
      C
      1000  WRITE(6,10)
        10  FORMAT('DO YOU WANT THE NEXT FILE ? Y/N')
            READ(5,13) DE
            IF(DE.EQ.ANO) GO TO 63
            IWF=1
            CALL SKIP(IWF,0,6)
      C
      C        READ FIRST BLOCK
      C
            CALL READ(IB,LX,0,LNUM,6)
            DO 1 I=1,46
            ALL1=IB(I)
            ILFTL=SHFTL(ALL1,16)
            ILF(2*I-1)=SHFTR(ILFTL,24)
            ILFTR=SHFTL(ALL1,24)
      1     ILF(2*I)=SHFTR(ILFTR,24)
            WRITE(6,300)
      300   FORMAT(' YEAR MONTH DAY HOUR MIN SEC ')
            WRITE(6,200) (ILF(I),I=2,7)
            WRITE(6,400)
        400 FORMAT(' NUM OF STA THAT DETECTED THE EVENT')
            WRITE(6,499) ILF(38)
        499 FORMAT(15X,I4)
            WRITE(6,500)
        500 FORMAT(' STATIONS THAT DETECTED THE EVENT ',/,
           &'    0=CRX 1=ACX 2=MEX 4=IIT 5=IIC 6=IIP')
            DO 2 I=40,45
        2   ILF(I)=ILF(I)/2
            WRITE(6,200) (ILF(I),I=40,45)
        200 FORMAT(1X,6I4)
      C
      C       READ SECOND BLOCK
      C
            CALL READ(IB2,LX,0,LNUM,6)
            DO 3 I=1,7
            ALL2=IB2(I)
            ILSTL=SHFTL(ALL2,16)
            ILS(2*I-1)=SHFTR(ILSTL,24)
            ILSTR=SHFTL(ALL2,24)
      3     ILS(2*I)=SHFTR(ILSTR,24)
            WRITE(6,600)
      C
      C
      C   THIS IS IMPORTANT BECAUSE IT TELL YOU HOW MANY BLOCKS IN EACH
      C   STATION WERE RECORDED. FOR EXAMPLE IF 6 STATIONS RECORDED AN
      C   EVENT YOU CAN GET
      C
      C         ARRAY IN BLOCKS OF THE STATIONS
      C           3  48  93  0  138  183 228
      C
      C                    THIS  MEAN
      C
      C     CHANEL             BLOCKS            STATION
      C       0                3   -  48           CRX
      C       1                49  -  93           ACX
      C       2                94  -  138          MEX
      C       4                139 -  183          IIT
      C       5                184 -  228          IIC
      C       6                229 -  END OF FILE  IIP
      C
      C      THEREFORE IF YOU WANT STAION 4 (IIT) THEN
      C           YOU NEED TO SKIP 138 BLOCKS AND
      C              THEN YOU ARE AT THE BIGINING
      C                   OF IIT
      C
```

```
  500 FORMAT(' ARRAY IN BLOCKS OF THE STATIONS ')
      DO 4 I=34,40
      ALL2=IB2(I)
      ILSTL=SHFTL(ALL2,16)
      ILS(2*I-1)=SHFTR(ILSTL,24)
      ILSTR=SHFTL(ALL2,24)
      ILSTR=SHFTR(ILSTR,24)
      ILS(2*I)=SHFTL(ILSTR,8)
    4 IARR(I)=ILS(2*I-1)+ILS(2*I)
      WRITE(6,99) (IARR(I),I=34,40)
   99 FORMAT(1X,7I5)
      CRX=IARR(35)-IARR(34)+1
      CRXS=IARR(34)
      CRXE=IARR(35)
C
C HERE IT TELL YOU HOW MANY BLOCKS HAS EACH STATION, IN WHICH
C           BLOCK START AND IN WICH BLOCK END
C
      WRITE(6,601) CRX,CRXS,CRXE
601   FORMAT('# OF BLOCKS IN CRX=',F6.3,' START=',F6.3,' END=',F6.3)
      ACX=IARR(36)-IARR(35)+1
      ACXS=IARR(35)+1
      ACXE=IARR(36)
      WRITE(6,602)ACX,ACXS,ACXE
602   FORMAT('# OF BLOCKS IN ACX=',F6.3,' START=',F6.3,' END=',F6.3)
      RMEX=IARR(38)-IARR(36)+1
      RMEXS=IARR(36)+1
      RMEXE=IARR(38)
      WRITE(6,603)RMEX,RMEXS,RMEXE
603   FORMAT('# OF BLOCKS IN MEX=',F6.3,' START=',F6.3,' END=',F6.3)
      RIIT=IARR(39)-IARR(38)+1
      RIITS=IARR(38)+1
      RIITE=IARR(39)
      WRITE(6,604)RIIT,RIITS,RIITE
604   FORMAT('# OF BLOCKS IN IIT=',F6.3,' START=',F6.3,' END=',F6.3)
      RIIC=IARR(40)-IARR(39)+1
      RIICS=IARR(39)+1
      RIICE=IARR(40)
      WRITE(6,605)RIIC,RIICS,RIICE
605   FORMAT('# OF BLOCKS IN IIC=',F6.3,' START=',F6.3,' END=',F6.3)
      RIIP=5
      RIIPS=IARR(40)+1
      RIIPE=5
      WRITE(6,606)RIIP,RIIPS,RIIPE
606   FORMAT('# OF BLOCKS IN IIP=',F6.2,' START=',F6.1,' END=',F6.1)
C
C     ASK FOR THE NUMBER OF BLOCKS TO BE READ
C
      WRITE(6,501)
501   FORMAT(/,' HOW MANY BLOCKS DO YOU WANT TO READ ?')
      READ(5,FREE,END=64) NBLCKS
C
C     CALCULATE THE NUMBER OF SAMPLES. EACH BLOCK HAS 256 SAMPLES
C     THAT IS EQUIVALENT TO 8 SECONDS (32 SAMPLES PER SECOND)
C
      NSEC=NBLCKS*8
      N=256*NBLCKS
      WRITE(6,3000) NBLCKS,NSEC
3000  FORMAT(I4,' BLOCKS IS EQUIVALENT TO ',I4,' SECONDS')
2001  WRITE(6,2000)
2000  FORMAT('HOW MANY BLOCKS DO YOU WANT TO SKIP ?')
      READ(5,FREE,END=64)ISTA
      CALL SKIP(0,ISTA,8)
      CALL GETSAM(N,NBLCKS,ISAM,A)
      IREW=ISTA+NBLCKS
C
C HERE THE TAPE IS REWINDED SO THAT YOU CAN SKIP WHATEVER
C   BLOCKS YOU WANT IN ORDER TO READ OTHER STATIONS
C
      CALL SKIP(0,-IREW,8)
      CALL FTNCMD('$DISPLAY *T*',12)
C
C     THE DATA IS STORED IN "ISAM"
C
      CALL PLTTRC(ISAM,N)
      WRITE(6,11)
11    FORMAT('DO YOU WANT TO PLOT OTHER STATION ? Y/N')
      READ(5,13)DES
      IF(DES.EQ.ANO) GO TO 9
      WRITE(6,500)
      WRITE(6,200) (ILF(I),I=40,45)
      WRITE(6,500)
      WRITE(6,99) (IARR(I),I=34,40)
      WRITE(6,601) CRX,CRXS,CRXE
      WRITE(6,602)ACX,ACXS,ACXE
      WRITE(6,603)RMEX,RMEXS,RMEXE
      WRITE(6,604)RIIT,RIITS,RIITE
      WRITE(6,605)RIIC,RIICS,RIICE
      WRITE(6,606)RIIP,RIIPS,RIIPE
      GO TO 2001
   13 FORMAT(A1)
   63 CALL PLOT(0.,0.,999)
   64 STOP
      END
END OF FILE
```

```
C
C  **************** PROGRAM KADATA S *****************
C
C    WRITTEN BY CECILIO J. REBOLLAR ON SUMMER 1979
C
C THIS PROGRAM CALCULATE THE BODY WAVE SPECTRA OF S WAVES
C OF THE EVENTS RECORDED BY E. KANASEWHICH. THESE EVENTS
C ARE STORED IN THE TAPE G06025 VOL=ROCKY1  THE PROGRAM
C READ THE NECESARY INFORMATION FROM THE FILE EV.S.1 &.
C
C     NBLKS   NUMBER OF BLOCKS TO BE READ
C     NN      NUMBER OF SAMPLES
C     Q       ATENUATION
C     STRT    STARTING POINT OF THE SAMPLING INTERVAL
C     SP      S-P TIME
C     VS      S-WAVE VELOCITY
C     DSNAME  DATA SET NAME
C
C               OUTPUT FILES
C
C     -Z   SPECTRA OF VERTICAL COMPONENT
C     -N   SPECTRA NORTH-SOUTH COMPONENT OR TRANSVERSE
C     -E   SPECTRA EAST-WEST   COMPONENT OR RADIAL
C     -ZSL SAMPLE INTERVAL OF Z N-S & E-W COMPONENTS
C
C
      COMMON /PLTLOG/WIDTH,SCP,SCT
      REAL*4 Z(1020),NS(1020),EW(1020),T(1020),ZC(1024),SNC(1024)
     1,WEC(1024),FF(512),AZ(512),AS(512),AW(512)
      INTEGER POSN(8)/'SCON',' =T','= P','DSN=',4*'    '/
      LOGICAL*1 DSNAME(13)
      EQUIVALENCE(POSN(5),DSNAME(1))
      COMPLEX CZC(513),CSNC(513),CWEC(513)
      DIMENSION D(8)
      INTEGER Q,STRT,IWK(9)
      DATA ANO/'N'/
      REAL PI/3.141592654/
      REAL*4 Z1(1024),NS1(1024),EW1(1024),MINNS1,MAXNS1,MINEW1
     1,MAXEW1
      INTEGER UNIT/4/,BLANK/'    '/
      INTEGER*2 LEN
      LOGICAL*1 FREE(1)/'*'/,LOGX,LOGY
C
C             HERE WE START
C
      DTI=1/100.
      WRITE(6,1)
 1    FORMAT('ENTER THE NUMBER OF EVENTS TO BE SKIPPED',
      ' NUMBER TO BE RUN')
      READ(5,FREE,END=64) NSKIP,NEVNTS
      IF(NSKIP.EQ.0) GO TO 100
      DO 2 I=1,NSKIP
 2    READ(12,3) NBLKS,NN,Q,STRT,SP,VS,DSNAME
 3    FORMAT(I2,3I4,2F5.2,13A1)
 100  DO 4 III=1,NEVNTS
C
C  READ IN THE NECESSARY INFORMATION:NUMBER OF BLOCKS, NUMBER OF
C       SAMPLES, STARTING POINT, S-P TIME, S VELOCITY
C                   AND DATA SET NAME
C
         READ(12,3) NBLKS,NN,Q,STRT,SP,VS,DSNAME
C
C  SET THE TAPE TO THE APROPIATE DATA SET NAME
C
         CALL FTNCMD(POSN,28)
          CALL GETDAT(Z1,NS1,EW1,N,NBLKS)
C
C  FIND MAXIMUN OF NS AND EW COMPONENTS IN ORDER TO CALCULATE
C                  LOCAL MAGNITUDE
C
      WRITE(6,400)
400   FORMAT('DO YOU WANT MAX AMPLITUDE OF NS & EW COMPONENT')
      READ(5,201) DE
      IF(DE.EQ.ANO) GO TO 402
      CALL USMNMX(NS1,N,1,MINNS1,MAXNS1)
       CALL USMNMX(EW1,N,1,MINEW1,MAXEW1)
      WRITE(6,401) MAXNS1,MAXEW1
401   FORMAT('NS MAX=',F12.4,' EW MAX=',F12.4,/)
C
C HERE THE PROGRAM ASK IF YOU WANT TO CALCULATE THE SPECTRA
C
      WRITE(6,403)
403   FORMAT('DO YOU WANT TO CALCULATE THE SPECTRA ? Y/N')
      READ(5,201) DE
      IF(DE.EQ.ANO) GO TO 64
402   JJ=0
      NEND=STRT+NN
      DO 20 JK=STRT,NEND
      JJ=JJ+1
      Z(JJ)=Z1(JK)
      NS(JJ)=NS1(JK)
  20  EW(JJ)=EW1(JK)
      DO 21 KK=1,NN
 21   T(KK)=KK
      WRITE(13,101) NN
      WRITE(13,102) (T(II),Z(II),II=1,NN)
      WRITE(13,101) NN
      WRITE(13,102) (T(II),NS(II),II=1,NN)
      WRITE(13,101) NN
      WRITE(13,102) (T(II),EW(II),II=1,NN)
C
C IF YOU KNOW THE AZIMUTH YOU CAN ROTATE YOUR SIGNALS
C
       WRITE(6,300)
 300   FORMAT('DO YOU WANT TO ROTATE THE SEISMOGRAMS ?')
       READ(5,201) DE
       IF(DE.EQ.ANO) GO TO 304
       WRITE(6,302)
 302   FORMAT('GIVE THE AZIMUTH !!')
       READ(5,FREE,END=64) AZIM
       CALL ROTATE(EW,NS,NN,AZIM)
      C
      C  NOW EW = RADIAL COMPONENT & NS = TRANSVERSE COMPONENT
      C                AZIM = AZIMUTH
      C        ALL THREE COMPONENTS ARE FILTERED
      C
      304   CALL BNDPAS(1.0,45.0,10.0,D,G)
             CALL FILTER(Z,NN,D,G,1)
              CALL FILTER(NS,NN,D,G,1)
               CALL FILTER(EW,NN,D,G,1)
      C
      C            HERE WE START THE CALCULATION OF
      C     THE SPECTRUM AND WE ASSUME A VP OF 8.0 KM/SEC
      C
                          HDIS=8.2*SP
      C
      C    HERE WE ARE GENERATING A VECTOR IN FREQUENCIES FF
      C
               M=256
               MM=M/2
               LH=M/2+1
               DELF=1./(M*DT1)
               DO 10 I=2,LH
               J=I-1
           10  FF(J)=J*DELF
      C
      C    REMOVE THE TREND, AVERAGE, ADD ZEROES TO AN EVEN
      C    NUMBER "M" AND SMOOTH THE SIGNAL AT THE ENDS WITH
      C            A COSBELL  (SEE KANASEWICH BOOK)
      C
               CALL CONDI(Z,NN,ZC,M)
                CALL CONDI(SN,NN,SNC,M)
                 CALL CONDI(EW,NN,WEC,M)
      C
      C    SET THE DATA FOR THE USE OF THE FFT FFTRC FROM THE IMLS
      C                            LIBRARY
      C
               CALL FFTRC(ZC,M,CZC,IWK,WK)
                CALL FFTRC(SNC,M,CSNC,IWK,WK)
                 CALL FFTRC(WEC,M,CWEC,IWK,WK)
               DO 11 I=1,LH
               AZ(I)=REAL(CZC(I))
               AS(I)=REAL(CSNC(I))
           11  AW(I)=REAL(CWEC(I))
               LL=LH+1
               DO 12 I=LL,M
               J=I-LH+1
               AZ(I)=AIMAG(CZC(J))
               AS(I)=AIMAG(CSNC(J))
           12  AW(I)=AIMAG(CWEC(J))
               LOG2N=8
               CALL AMPPHZ(LOG2N,AZ,1,PDCZ,PFNZ)
                CALL AMPPHZ(LOG2N,AS,1,PDCS,PFNS)
                 CALL AMPPHZ(LOG2N,AW,1,PDCW,PFNW)
      C
      C       YOU CAN SMOOTH YOUR SPECTRUM IF YOU WANT
      C              (SEE KANASEWICH 900K)
              WRITE(6,200)
      200     FORMAT('DO YOU WANT TO SMOOTH THE SPECTRA')
              READ(5,201) DES
      201     FORMAT(A1)
              IF(DES.EQ.ANO) GO TO 202
              WRITE(5,14)
         14   FORMAT('WE NEED THE WINDOW .N FREQUENCY DOMAIN FOR DANIEL '')
              READ(5,FREE,END=64) FWIND
               CALL DANIEL(AZ,M,FWIND,10.0)
                CALL DANIEL(AS,M,FWIND,10.0)
                 CALL DANIEL(AW,M,FWIND,10.0)
      C
      C THE SPRENGNETHER INTRUMENT WAS WORKING WITH A GAIN FROM 60 TO
```

```
      C 120 DB IN  6 DB STEPS. THE GAIN WAS SET UP TO 66 DB. HENCE
      C WE NEED TO MULTIPLY THE OUTPUT BY 2**9 IN ORDER TO RECOVER
      C                          THE SIGNAL
      C
      202      DO 13 I=2,MM
               V=AMAGN(FF(I))
               ATENUA=EXP((PI*HDIS*FF(I))/(Q*VS))
               AZ(I)=((AZ(I)*ATENUA)/V)*(2**9)
               AS(I)=((AS(I)*ATENUA)/V)*(2**9)
               AW(I)=((AW(I)*ATENUA)/V)*(2**9)
               AZ(I)=ALOG10(AZ(I))
               AS(I)=ALOG10(AS(I))
               AW(I)=ALOG10(AW(I))
               FF(I)=ALOG10(FF(I))
          13   CONTINUE
               MMM=85
               WRITE(9,101) MMM
               WRITE(9,102) (FF(I),AZ(I),I=6,90)
               WRITE(10,101) MMM
               WRITE(10,102) (FF(I),AS(I),I=6,90)
               WRITE(11,101) MMM
               WRITE(11,102) (FF(I),AW(I),I=6,90)
         101   FORMAT(I4)
         102   FORMAT(2G12.5)
               WRITE(6,5) DSNAME
        5      FORMAT('I FINISHED WITH ',13A1)
        4      CONTINUE
         64    STOP
               END
END OF FILE
```

```
$R *FORTG T=6
C
C ***************    PROGRAM  RDANIEL    ***************
C
C THIS PROGRAM CALCULATE THE SPECTRA OF EARTHQUAKES FROM THE
C ROCKY MOUNTAIN HOUSE EARTHQUAKE SWARM RECORDED AT EDMONTON
C USING A DANIEL-SPECTRAL ESTIMATE FROM
C THE PERIODROGRAM, USING A SUBROUTINE BY D. GANLEY.
C THE SEISMOGRAMS ARE IN THE TAPE GO6067 VOL=MANO67
C AND THE PROGRAM READ ALL THE INFORMATION FROM
C                  THE FILE "ROCKYF"
C
      DIMENSION Z(6000),SN(6000),WE(6000),VB(6000)
      REAL*4 FF(1024),ZC(1024),SNC(1024),WEC(1024),AZ(1024),SVC(1024)
     1,AIZ(1024),AS(1024),ASI(1024),AW(1024),AWI(1024),SV(1024)
     2,AMPZ(1024),AMPE(1024),AMPW(1024),T(1024),AZIM,WR(6)
      COMPLEX CZC(1025),CSNC(1025),CWEC(1025),CSVC(1025)
      REAL*4 AV(512)
      INTEGER Q,NN,IWK(6)
      DIMENSION D(6)
      REAL PI/3.141592654/
      INTEGER RC/4/,
     .CONRES(27),DSNAME(5),BLANK/'    '/,LP/'  LP'/,CLP/'CLIP'/,CLIP
     .,POSN(7)/'POSN',5*'    '/
      INTEGER MOUNTC(6)
      DATA YES/'Y'/,ANO/'N'/
      INTEGER TAPE/'TAPE'/
      LOGICAL*1 FREE(1)/'*'/
C
      EQUIVALENCE (DSNAME(1), POSN(3))
      EQUIVALENCE (MOUNTC(1), CLIP), (MOUNTC(2), DSNAME)
C
      INTEGER*2 CONLEN/28/, MNTLEN/24/
C
C              READ IN THE NECESSARY INFORMATION:
C     LONG OR SHORT PERIOD DATA ?, NUMBER OF SAMPLES, ATENUATION
C           STARTING POINT IN SEC, S-P, S-WAVE VELOCITY
C                        &  DATA SET NAME
C
 1015 FORMAT(' ENTER THE NUMBER OF EVENTS TO BE SKIPPED, NUMBER',
     .' TO BE RUN')
      WRITE(6,1015)
      READ(5,FREE)NSKIP,NEVNTS
      DO 1010 I=1,NSKIP
 1010 READ(12,97,END=64) LPD,NN,Q,STRT,SP,VS,DSNAME
      DO 1011 JJJJ=1,NEVNTS
      READ(12,97,END=64) LPD,NN,Q,STRT,SP,VS,DSNAME
   97 FORMAT(A4,2I4,2F8.0,F5.2,5A4)
C
C  IS THE DATA LONG PERIOD DATA ? IF NOT, THERE ARE 18 POINTS PER
C           SEC. OTHERWISE, THERE ARE 3 PER SEC
C
       DTI=1./18.
       IF(LPD.EQ.LP) DTI=1./3.
       IST=STRT/DTI
C
C   SET THE TAPE TO THE APPROPIATE DATA SET NAME.
C
       CALL CNTRL(POSN,CONLEN,4,CONRES,&990,&995,&999)
C
C     READ IN THE DATA ACORDING TO WHETER WE WANT LONG
C              PERIOD OR SHORT PERIOD
C
       IF(LPD.NE.LP) CALL GETDAT(Z,SN,WE,VB,NN,4,IST)
       IF(LPD.EQ.LP) CALL GTDTLP(Z,SN,WE,VB,NN,4,IST)
       DO 9 I=1,NN
    9  T(I)=I
       WRITE(6,101) NN
       WRITE(6,102) (T(I),Z(I),I=1,NN)
C
C     WE ARE FILTERING BELOW F1=0.5 HZ AND ABOVE
C                   F2=7.0 HZ
C
       WRITE(6,200)
  200  FORMAT('DO YOU WANT TO ROTATE THE SEISMOGRAMS ?')
       READ(5,201) DE
  201  FORMAT(A1)
       IF(DE.EQ.ANO) GO TO 204
       WRITE(6,202)
  202  FORMAT('GIVE THE AZIMUTH !!')
       READ(5,FREE,END=64) AZIM
       CALL ROTATE(WE,SN,NN,AZIM)
C
C  NOW WE = RADIAL COMPONENT & SN = TRANSVERSE COMPONENT
C        AZIM = AZIMUTH, SV(KK) IS PURE SV WAVE
C
       DO 15 KK=1,NN
   15  SV(KK)=SQRT(Z(KK)**2+WE(KK)**2)
  204  CALL BNDPAS(0.5,9.0,55.55,D,G)
       CALL FILTER(Z,NN,D,G,1)
       CALL FILTER(SN,NN,D,G,1)
       CALL FILTER(WE,NN,D,G,1)
C      CALL FILTER(SV,NN,D,G,1)
C
C           HERE WE START THE CALCULATION OF
C     THE SPECTRUM AND WE ASSUME A VP OF 6.2 KM/SEC
C
C      HDIS=8.37*SP
       HDIS=325.
C
C   HERE WE ARE GENERATING A VECTOR IN FREQUENCIES FF
C
       M=1024
       MM=M/2
       LH=M/2+1
       DELF=1./(M*DTI)
      DO 10 I=3,LH
      J=I-1
   10 FF(J)=(I-1)*DELF
C
C   REMOVE THE TREND, AVERAGE, ADD ZEROES TO AN EVEN
C   NUMBER "M" AND SMOOTH THE SIGNAL AT THE ENDS WITH
C                  A COSBELL
C
      CALL CONDI(Z,NN,ZC,M)
      CALL CONDI(SN,NN,SNC,M)
      CALL CONDI(WE,NN,WEC,M)
C     CALL CONDI(SV,NN,SVC,M)
C
C   SET THE DATA FOR THE USE OF THE FFT FFTRC FROM THE IMLS
C                       LIBRARY
C
      CALL FFTRC(ZC,M,CZC,IWK,WK)
      CALL FFTRC(SNC,M,CSNC,IWK,WK)
      CALL FFTRC(WEC,M,CWEC,IWK,WK)
C     CALL FFTRC(SVC,M,CSVC,IWK,WK)
      DO 11 I=1,LH
      AZ(I)=REAL(CZC(I))
      AS(I)=REAL(CSNC(I))
   11 AW(I)=REAL(CWEC(I))
C 11   AV(I)=REAL(CSVC(I))
      LL=LH+1
      DO 12 I=LL,M
      J=I-LH+1
      AZ(I)=AIMAG(CZC(J))
      AS(I)=AIMAG(CSNC(J))
   12 AW(I)=AIMAG(CWEC(J))
C     AV(I)=AIMAG(CSVC(J))
      LOG2N=10
      CALL AMPPHI(LOG2N,AZ,1,POCZ,PFNZ)
      CALL AMPPHI(LOG2N,AS,1,POCS,PFNS)
      CALL AMPPHI(LOG2N,AW,1,POCW,PFNW)
C     CALL AMPPHI(LOG2N,AV,1,POCV,PFNV)
     WRITE(5,14)
   14 FORMAT('WE NEED THE WINDOW IN FREQUENCY DOMAIN FOR DANIEL !')
     READ(5,FREE,END=64) FWIND
      CALL DANIEL(AZ,M,FWIND,55.55)
      CALL DANIEL(AS,M,FWIND,55.55)
      CALL DANIEL(AW,M,FWIND,55.55)
C     CALL DANIEL(AV,M,FWIND,55.55)
      DO 13 I=2,MM
      V=AMAGN(FF(I))
      ATENUA=EXP((PI*MDIS*FF(I))/(Q*VS))
      AZ(I)=(AZ(I)*ATENUA)/V
      AS(I)=(AS(I)*ATENUA)/V
      AW(I)=(AW(I)*ATENUA)/V
C     AV(I)=(AV(I)*ATENUA)/V
      AZ(I)=ALOG10(AZ(I))
      AS(I)=ALOG10(AS(I))
      AW(I)=ALOG10(AW(I))
C     AV(I)=ALOG10(AV(I))
      FF(I)=ALOG10(FF(I))
   13 CONTINUE
      MP=157
      MWILL=200
      WRITE(9,101) MWILL
      WRITE(9,102) (FF(I),AZ(I),I=120,320)
      WRITE(10,101) MP
      WRITE(10,102) (FF(I),AS(I),I=19,175)
      WRITE(11,101) MP
 1011 WRITE(11,102) (FF(I),AW(I),I=18,175)
C     WRITE(12,101) MP
C1011  WRITE(12,102) (FF(I),AV(I),I=18,175)
  101 FORMAT(I4)
  102 FORMAT(2G12.5)
      GO TO 64
  999 RC=RC+4
  995 RC=RC+4
  990 CONTINUE
      WRITE(6,991) RC,CONREG
  991 FORMAT('0*** RETURN CODE FROM CNTRL =',I2,/,
     * ' INFORMATION: ',27A4)
   64 STOP
      END
END OF FILE
```

```
C
C **********Get long period data from Charlie tapes********************
C
      SUBROUTINE GTDTLP(Z,SN,WE,VB,N,IU,IST)
C
C This picks up long period data from CHARLIE tapes
C
C Also picks up the signal into VB (refer to GETDAT for
C explanation of where time signal is located).
C
      DIMENSION Z(N), SN(N), WE(N), VB(N)
      INTEGER*2 IE(2700), LX
      K=((N+IST)/900)+1
      M=-IST
      DO 10 I=1,K
     *   CALL READ(IE,LX,0,LNR,IU)
         DO 10 J=1,2700,3
               M=M+1
                IF(M.LE.0)GO TO 10
                IF(M.GT.N)GO TO 11
                ITEMP =  ( IE(J) - ((IE(J)/4) * 4) ) / 2
                VB(M) = IABS(ITEMP)
                Z(M)=IE(J)
                SN(M)=IE(J+1)
                WE(M)=IE(J+2)
10    CONTINUE
      GO TO 12
   11 M=M-1
   12 CONTINUE
  101 FORMAT(' ',I5,/(3G15.5))
      RETURN
C     DEBUG SUBTRACE
       END
END OF FILE
```

```
C     ***********************************************************
C     *                                                         *
C     *                 Get short period data                   *
C     *                                                         *
C     ***********************************************************
      SUBROUTINE GETDAT(Z,SN,WE,VB,N,IU,IST,*)
C
C This picks up short period data from CHARLIE tapes
C
C Array VB contains the time signal.  This time signal is found
C in bit 14 of the data, where bit 0 is the leftmost bit, and
C bit 15 is the rightmost bit of a 16-bit integer (integer*2).
C
C
      DIMENSION Z(N), SN(N), WE(N), VB(N)
      INTEGER*2 IE(2700), LX
      K=((N+IST)/900)+1
      M=-IST
      DO 10 I=1,K
         CALL READ(IE,LX,0,LNR,IU,&12,&12,&120)
         DO 10 J=1,2700,15
            DO 10 KK=1,5
               M=M+1
                IF(M.LE.0)GO TO 10
                IF(M.GT.N)GO TO 11
                IPNT = J + KK - 1
                ITEMP =  ( IE(IPNT) - ((IE(IPNT)/4) * 4) ) / 2
                VB(M) = IABS(ITEMP)
                Z(M) = IE(IPNT)
                SN(M) = IE(J+KK+5)
                WE(M) = IE(J+KK+11)
   10 CONTINUE
      GO TO 12
   11 M=M-1
   12 CONTINUE
      RETURN
  120 RETURN 1
      END
END OF FILE
```

```
      SUBROUTINE BNDPAS(F1,F2,DELT,D,G)
C
C          SUBROUTINE BY DAVE GANLEY ON MARCH 5, 1977.
C
C          THE PURPOSE OF THIS SUBROUTINE IS TO DESIGN AND APPLY A
C     RECURSIVE BUTTERWORTH BAND PASS FILTER (KANASEWICH, TIME SERIES
C     ANALYSIS IN GEOPHYSICS, UNIVERSITY OF ALBERTA PRESS, 1975; SHANKS,
C     JOHN L, RECURSION FILTERS FOR DIGITAL PROCESSING, GEOPHYSICS, V32,
C     PP 33-51,, 1967).  IN ORDER TO DESIGN THE FILTER A CALL MUST BE
C     MADE TO  BNDPAS AND THEN THE FILTER MAY BE APPLIED BY CALLS TO
C     FILTER.  THE FILTER WILL HAVE 4 POLES IN THE S PLANE AND IS
C     APPLIED IN FORWARD AND REVERSE DIRECTIONS SO AS TO HAVE ZERO
C     PHASE SHIFT.  THE GAIN AT THE TWO FREQUENCIES SPECIFIED AS
C     CUTOFF FREQUENCIES WILL BE -6DB AND THE ROLLOFF WILL BE ABOUT
C     36 DB PER OCTAVE.  A BILINEAR Z TRANSFORM IS USED IN DESIGNING
C     THE FILTER TO PREVENT ALIASING PROBLEMS.
C
      COMPLEX P(4),S(8),Z1,Z2
      DIMENSION D(8),X(1),XC(3),XD(3),XE(3)
      DATA ISW/0/,TWOPI/6.2831853/
C
C     THIS SECTION CALCULATES THE FILTER AND MUST BE CALLED BEFORE
C     FILTER IS CALLED
C
C        F1 = LOW FREQUENCY CUTOFF (6 DB DOWN)
C        F2 = HIGH FREQUENCY CUTOFF (6 DB DOWN)
C        DELT = SAMPLE INTERVAL IN MILLISECONDS
C        D = WILL CONTAIN 8 Z DOMAIN COEFICIENTS OF RECURSIVE FILTE
C        G = WILL CONTAIN THE GAIN OF THE FILTER
C
C     WRITE (6,1) F1,F2,DELT
    1 FORMAT ('1 BANDPASS FILTER DESIGN FOR A BAND FROM ',F8.3,' TO ',F8
     ..3,' HERTZ.',//' SAMPLE INTERVAL IS ',F5.2,' MILLISECONDS.')
      DT=DELT/1000.0
      TDT=2.0/DT
      FDT=4.0/DT
      ISW=1
      P(1)=CMPLX(-.3826834,.9238795)
      P(2)=CMPLX(-.3826834,-.9238795)
      P(3)=CMPLX(-.9238795,.3826834)
      P(4)=CMPLX(-.9238795,-.3826834)
      W1=TWOPI*F1
      W2=TWOPI*F2
      W1=TDT*TAN(W1/TDT)
      W2=TDT*TAN(W2/TDT)
      HWID=(W2-W1)/2.0
      WW=W1*W2
      DO 19 I=1,4
      Z1=P(I)*HWID
      Z2=Z1*Z1-WW
      Z2=CSQRT(Z2)
      S(I)=Z1+Z2
   19 S(I+4)=Z1-Z2
C     WRITE (6,2) S
    2 FORMAT ('-S PLANE POLES ARE AT:',/' ',8(/' ',E12.6,' + I ',E12.6))
      G=.5/HWID
      G=G*G
      G=G*G
      DO 29 I=1,7,2
      B=-2.0*REAL(S(I))
      Z1=S(I)*S(I+1)
      C=REAL(Z1)
      A=TDT+B+C/TDT
      G=G*A
      D(I)=(C*DT-FDT)/A
   29 D(I+1)=(A-2.0*B)/A
      G=G*G
C     WRITE (6,3)
    3 FORMAT ('-FILTER IS (1-Z**2)**4 / B1*B2*B3*B4')
C     WRITE (6,4) D
    4 FORMAT (4(/' B(I) = 1 + ',E12.6,' Z + ',E12.6,' Z**2'))
C     WRITE (6,5) G
    5 FORMAT ('-FILTER GAIN IS ',E12.6)
      RETURN
      ENTRY FILTER(X,N,D,G,IG)
C
C     X = DATA VECTOR OF LENGTH N CONTAINING DATA TO BE FILTERED
C     D = FILTER COEFFICIENTS CALCULATED BY BNDPAS
C     G = FILTER GAIN
C     IG = 1 MEANS TO REMOVE THE FILTER GAIN SO THAT THE GAIN IS UNITY
C
      IF (ISW.EQ.1) GO TO 31
C     WRITE (6,6)
    6 FORMAT ('1BNDPAS MUST BE CALLED BEFORE FILTER')
      CALL EXIT
C
C     APPLY FILTER IN FORWARD DIRECTION
C
   31 XM2=X(1)
      XM1=X(2)
      XM=X(3)
      XC(1)=XM2
      XC(2)=XM1-D(1)*XC(1)
      XC(3)=XM-XM2-D(1)*XC(2)-D(2)*XC(1)
      XD(1)=XC(1)
      XD(2)=XC(2)-D(3)*XD(1)
      XD(3)=XC(3)-XC(1)-D(3)*XD(2)-D(4)*XD(1)
      XE(1)=XD(1)
      XE(2)=XD(2)-D(5)*XE(1)
      XE(3)=XD(3)-XD(1)-D(5)*XE(2)-D(6)*XE(1)
      X(1)=XE(1)
      X(2)=XE(2)-D(7)*X(1)
      X(3)=XE(3)-XE(1)-D(7)*X(2)-D(8)*X(1)
      DO 39 I=4,N
      XM2=XM1
      XM1=XM
      XM=X(I)
      K=I-((I-1)/3)*3
      GO TO (34,35,36),K
   34 M=1
      M1=3
      M2=2
      GO TO 37
   35 M=2
      M1=1
      M2=3
      GO TO 37
   36 M=3
      M1=2
      M2=1
```

```
       37 XC(M)=XM-XM2-D(1)*XC(M1)-D(2)*XC(M2)
          XD(M)=XC(M)-XC(M2)-D(3)*XD(M1)-D(4)*XD(M2)
          XE(M)=XD(M)-XD(M2)-D(5)*XE(M1)-D(6)*XE(M2)
       38 X(I)=XE(M)-XE(M2)-D(7)*X(I-1)-D(8)*X(I-2)
     C
     C    FILTER IN REVERSE DIRECTION
     C
          XM2=X(N)
          XM1=X(N-1)
          XM=X(N-2)
          XC(1)=XM2
          XC(2)=XM1-D(1)*XC(1)
          XC(3)=XM-XM2-D(1)*XC(2)-D(2)*XC(1)
          XD(1)=XC(1)
          XD(2)=XC(2)-D(3)*XD(1)
          XD(3)=XC(3)-XC(1)-D(3)*XD(2)-D(4)*XD(1)
          XE(1)=XD(1)
          XE(2)=XD(2)-D(5)*XE(1)
          XE(3)=XD(3)-XD(1)-D(5)*XE(2)-D(6)*XE(1)
          X(N)=XE(1)
          X(N-1)=XE(2)-D(7)*X(1)
          X(N-2)=XE(3)-XE(1)-D(7)*X(2)-D(8)*X(1)
          DO 48 I=4,N
          XM2=XM1
          XM1=XM
          J=N-I+1
          XM=X(J)
          K=I-((I-1)/3)*3
          GO TO (44,45,46),K
       44 M=1
          M1=3
          M2=2
          GO TO 47
       45 M=2
          M1=1
          M2=3
          GO TO 47
       46 M=3
          M1=2
          M2=1
       47 XC(M)=XM-XM2-D(1)*XC(M1)-D(2)*XC(M2)
          XD(M)=XC(M)-XC(M2)-D(3)*XD(M1)-D(4)*XD(M2)
          XE(M)=XD(M)-XD(M2)-D(5)*XE(M1)-D(6)*XE(M2)
       48 X(J)=XE(M)-XE(M2)-D(7)*X(J+1)-D(8)*X(J+2)
          IF (IC.NE.1) RETURN
          DO 58 I=1,N
       58 X(I)=X(I)/C
          RETURN
          END
END OF FILE
```

```
                 SUBROUTINE PLTTRC(IV,N)
     C
     C   WRITTEN BY CECILIO J. REBOLLAR SUMMER 1979
     C
     C THIS SUBROUTINE PLOT A SINGLE TRACE i. e. A SISMOGRAM
     C
            INTEGER*4 IV(N)
            REAL*4 FL(5000)
            DIMENSION ITITL(7)
            DATA ITITL/7*'    '/
            WRITE(6,100)
     100    FORMAT('ENTER TITLE (28 CHARS OR LESS)')
            READ(5,101) ITITL
     101    FORMAT(7A4)
            CALL PLOT(2.,0.,-3)
            CALL SYMBOL(-1.,0.,0.25,ITITL,90.0,28)
            DO 2 I=1,N
       2    FL(I)=IV(I)
            CALL USMNMX(FL,N,1,FMIN,FMAX)
            Y=0.
            X=IV(1)/FMAX
            CALL PLOT(X,Y,3)
            DO 1 I=2,N
            Y=Y+.0027
            X=IV(I)/FMAX
       1    CALL PLOT(X,Y,2)
           RETURN
           END
```

```
      SUBROUTINE AMPPHI(LOG2N,X,IC,PDC,PFN)
C
C*************************************************************
C
C    WRITTEN BY DAVE GANLEY ON MAY 18, 1977
C
C      THIS SUBROUTINE CALCULATES AMPLITUDE AND/OR PHASE
C    SPECTRA FROM THE REAL AND IMAGINARY PARTS OF A
C    FREQUENCY SPECTRUM OR VICE VERSA. THE INPUT (OUTPUT)
C    ARRAY X IS OF LENGTH 2**LOG2N WITH THE REAL PARTS OF
C    THE FOURIER COEFFICIENTS FOR FREQUENCIES ZERO TO
C    NYQUIST IN THE FIRST N/2+1 POSITIONS OF X. THE
C    IMAGINARY PARTS OF THE COEFFICIENTS ARE IN POSITIONS
C    N/2+2 TO N AND ARE NOT STORED FOR DC OR NYQUIST FREQUENCY
C    (WHERE THEY ARE ZERO). THE OUTPUT (INPUT) ARRAY HAS
C    AMPLITUDES IN THE FIRST N/2+1 POSITIONS AND PHASES
C    (IN DEGREES) IN THE LAST N/2-1 POSITIONS. PHASES
C    FOR DC AND NYQUIST FREQUENCIES ARE RETURNED (SPECIFIED)
C    IN PDC AND PFN.
C
C    IC=1  INPUT IS FOURIER COEFFICIENTS.
C          OUTPUT IS AMPLITUDE AND PHASE.
C      =2  INPUT IS FOURIER COEFFICIENTS.
C          OUTPUT IS AMPLITUDE ONLY.
C      =3  INPUT IS FOURIER COEFFICIENTS.
C          OUTPUT IS PHASE ONLY.
C      =-1 INPUT AMPLITUDE AND PHASE.
C          OUTPUT IS FOURIER COEFFICIENTS.
C
C**********************************************************
C
C
      DIMENSION X(1)
      M=1
      IF(LOG2N.LT.1) RETURN
      DO 5 I=2,LOG2N
   5  M=2*M
      N=2*M
      MP1=M+1
      IF(IC.LT.1) GO TO 400
      GO TO (100,200,300),IC
C
C  CALCULATE AMPLITUDE AND PHASE SPECTRUM
C
  100 IF(X(1).GE.0.0) GO TO 105
      X(1)=-X(1)
      PDC=180.0
      GO TO 110
  105 PDC=0.0
  110 IF(X(MP1).GE.0.0) GO TO 115
      X(MP1)=-X(MP1)
      PFN=180.0
      GO TO 120
  115 PFN=0.0
  120 IF(LOG2N.EQ.1) RETURN
      DO 125 I=2,M
      A=X(I)
      B=X(I+M)
      X(I)=SQRT(A*A+B*B)
  125 X(I+M)=57.29578*ATAN2(B,A)
      RETURN
C
C         CALCULATE AMPLITUDE SPECTRUM ONLY
C
  200 IF(X(1).LT.0.0) X(1)=-X(1)
      IF(X(MP1).LT.0.0) X(MP1)=-X(MP1)
      IF(LOG2N.EQ.1) RETURN
      DO 205 I=2,M
      A=X(I)
      B=X(I+M)
  205 X(I)=SQRT(A*A+B*B)
      RETURN
C
C      CALCULATE PHASE SPECTRUM ONLY
C
 300  IF(X(1).LT.0.0) GO TO 305
      PDC=0.0
      GO TO 310
 305  PDC=180.0
 310  IF(X(MP1).LT.0.0) GO TO 315
      PFN=0.0
      GO TO 320
 315  PFN=180.0
 320  IF(LOG2N.EQ.1) RETURN
      DO 325 I=2,M
      A=X(I)
      B=X(I+M)
 325  X(I+M)=57.29578*ATAN2(B,A)
      RETURN
C
C      CALCULATE FOURIER COEFFICIENTS FROM AMPLITUDE AND PHASE
C
 400  X(1)=X(1)*COS(PDC/57.29578)
      X(MP1)=X(MP1)*COS(PFN/57.29578)
      IF(LOG2N.EQ.1) RETURN
      DO 405 I=2,M
      A=X(I)
      B=X(I+M)/57.29578
      X(I)=A*COS(B)
 405  X(I+M)=A*SIN(B)
      RETURN
      END
END OF FILE
```

```
      SUBROUTINE DANIEL(X,N,FWIND,DT)
C
C     SUBROUTINE BY DAVE GANLEY DECEMBER 12, 1977.
C
C     THIS SUBROUTINE CALCULATES A DANIEL-LIKE SPECTRAL
C     STIMATE FROM THE PERIODOGRAM. THIS IS DONE BY
C     AVERAGING ALL FREQUENCIES WITHIN A WINDOW CENTERED
C     ABOUT THE DESIRED FREQUENCY. SINCE REAL AND
C     IMAGINARY COEFFICIENTS (OR AMPLITUDE AND PHASE VALUES)
C     ARE AVERAGED THIS IS NOT A DANIELL POWER SPECTRAL
C     STIMATE. ALSO NOTE THAT AT FREQUENCIES WITHIN HALF
C     OF THE WINDOW WIDTH OF DC OR NYQUIST FREQUENCIES THE
C     ESTIMATES ARE CALCULATED BY AVERAGING OVER FEWER
C     VALUES.
C
C     INPUTS:
C        X = INPUT FOURIER TRANSFORM AS OUTPUT BY FFTRC OR
C            AMPPHI. ON OUTPUT X CONTAINS THE SMOOTHED
C            SPECTRAL ESTIMATE IN THE SAME FORMAT.
C       N = LENGTH OF THE X (N IS 2**M WHERE M IS AN INTEGER)
C       FWIND = WINDOW WIDTH IN FREQUENCY DOMAIN (HERTZ)
C       DT = SAMPLE INTERVAL. OF ORIGINAL TIME SERIES (MSEC)
C
       DIMENSION X(N)
       DIMENSION Y(512)
       IF (N.LE.512) GO TO 10
      WRITE(6,1)
    1 FORMAT(' N CANNOT EXCEED 512 IN SUBROUTINE DANIEL')
      STOP 64
   10 N2=N/2
       N22=N2+2
       NP2=N+2
       DF=500.0/(N*DT)
       M2=FWIND/(2.0*DF)+.5
       M21=M2+1
       M=2*M2+1
       XM=M
       XM1=M-1
       FWIND=2.0*M2*DF
       WRITE(6,2) M,FWIND
    2  FORMAT(' ',I3,' POINTS USED IN DANIEL WINDOW '
     @,'WHICH IS A WIDTH OF ',F6.2,' HERTZ')
       IF (M2.EQ.0) RETURN
       DO 19 I=1,N
   19  Y(I)=X(I)
       KE=0
       DO 49 I=1,M2
       II=N22-I
       L=I-M2
       LL=II+M2
       JE=M21-I
       I21=2*I-1
       II21=N22-I21
       L21=I21+N2
       LL21=NP2-I21
       XF=XM-JE
       XF1=XF-1.0
       IF(I.EQ.1) GO TO 30
       KE=I-1
       DO 29 K=1,KE
       X(I)=X(I)+Y(I+K)+Y(I-K)
       X(II)=X(II)+Y(II+K)+Y(II-K)
       X(L)=X(L)+Y(L+K)
       X(LL)=X(LL)+Y(LL-K)
       IF(K.EQ.KE) GO TO 29
       X(L)=X(L)+Y(L-K)
       X(LL)=X(LL)+Y(LL+K)
   29  CONTINUE
   30  DO 39 J=1,JE
       X(I)=X(I)+Y(I21+J)
       X(II)=X(II)+Y(II21-J)
       IF(I.EQ.1) GO TO 39
       X(L)=X(L)+Y(L21+J)
       X(LL)=X(LL)+Y(LL21-J)
   39  CONTINUE
       X(I)=X(I)/XF
       X(II)=X(II)/XF
       IF(I.EQ.1) GO TO 49
       X(L)=X(L)/XF1
       X(LL)=X(LL)/XF1
   49  CONTINUE
       IE=N22-M21
       IF(M21.GT.IE) RETURN
       L=M21+M2
       DO 59 I=1,M2
       X(M21)=X(M21)+Y(M21+I)+Y(M21-I)
       IF(M.GT.N2.AND.I.EQ.M2) GO TO 59
       X(L)=X(L)+Y(L+I)
       IF (I.EQ.M2) GO TO 59
       X(L)=X(L)+Y(L-I)
   59  CONTINUE
       X(M21)=X(M21)/XM
       X(L)=X(I)/XM1
       IF (M.GT.N2) X(L)=X(L)*XM1/(XM1-1.0)
       IF(IE.EQ.M21) RETURN
       L=IE+N2
       DO 69 I=1,M2
       X(IE)=X(IE)+Y(IE+I)+Y(IE-I)
       X(L)=X(L)+Y(L-I)
       IF(I.NE.M2) X(L)=X(L)+Y(L+I)
   69  CONTINUE
       X(IE)=X(IE)/XM
       X(L)=X(L)/XM1
       IE=IE-1
       IS=M21+1
       IF(IS.GT.IE) RETURN
       DO 89 I=IS,IE
       L=I+N2
       DO 79 J=1,M2
       X(I)=X(I)+Y(I+J)+Y(I-J)
       X(L)=X(L)+Y(L+J)+Y(L-J)
   79  CONTINUE
       X(I)=X(I)/XM
       X(L)=X(L)/XM
   89  CONTINUE
       RETURN
       END
END OF FILE
```

```
      SUBROUTINE GETDAY(Z,NS,EW,N,NBLKS)
C
C THIS SUBROUTINE WAS WRITTEN BY CHARLIE MCCLOUGHAN
C
C READ THE DATA RECORDEC IN THE SPREGNTHER DR-100
C
      REAL Z(1020),NS(1020),EW(1020)
      INTEGER LNR
      INTEGER*2 ID(510),LN,IS(3,1020)
      NBLKSS=NBLKS*170
      M=0
      DO 2 I=1,NBLKS
      CALL READ(ID,LN,0,LNR,4)
      DO 2 K=1,510,3
      N=0
      M=M+1
      KK=K+2
      DO 3 L=K,KK
      N=N+1
3     IS(N,M)=ID(L)
2     CONTINUE
      N=0
      DO 4 I=1,NBLKSS
      IFL=0
      DO 5 K=1,3
      IT=IS(K,I)
      IT=IABS(IT)
      IF(IT.LT.2047) GO TO 5
      IFL=IFL+1
5     CONTINUE
      IF(IFL.NE.3) GO TO 6
      GO TO 4
6     N=N+1
      Z(N)=IS(1,I)
      NS(N)=IS(2,I)
      EW(N)=IS(3,I)
4     CONTINUE
      RETURN
      END
END OF FILE
```

```
      SUBROUTINE GETSAM(N,NBCS,ISAM,A)
C
C   THIS SUBROUTINE DECOD THE MAGNETICS TAPES OF RESMAC
C
      INTEGER SHFTR,SHFTL,ALL,IL,IR,IMA,IMAN,IEXP,LNUM
      INTEGER*2 IS(512),IE(40000)
      REAL ISAM(40000),A(10000)
      INTEGER*2 LX
      INTEGER ISUB,N
      ISUB=0
      DO 3 I=1,NBCS
      CALL READ(IS,LX,0,LNUM,8)
      DO 2 J=1,256
      ISUB=ISUB+1
      IE(ISUB)=IS(J)
2     CONTINUE
3     CONTINUE
      DO 1 I=1,N
      ALL=IE(I)
      IL=SHFTL(ALL,16)
      IL=SHFTR(IL,24)
      IR=SHFTL(ALL,24)
      IR=SHFTR(IR,24)
      IR=SHFTL(IR,8)
      IMA=IL+IR
      IMAN=IMA/4
      IEXP=SHFTL(IMA,30)
      IEXP=SHFTR(IEXP,30)
      ISAM(I)=(IMAN-2048)*4**IEXP
      A(I)=I
1     CONTINUE
      RETURN
      END
END OF FILE
```

```
      SUBROUTINE CONCI(TS,NTS,TS1,N)
C
C   THIS SUB REMOVE THE TREND(LINEAR), THE AVERAGE, ADD ZEROS TO
C     AN EVEN NUMBER AND SMOOTH THE SIGNAL AT THE ENDS WITH A
C        COSBELL SEE KANASEWICH'S BOOK PAGE 98.
C               IT CALL SUB KOSBELL
C
       REAL TS(512),TS1(512)
       TREND=(TS(NTS)-TS(1))/(NTS-1)
       DO 7 I=1,NTS
 7     TS(I)=TS(I)-TREND*(I-1)
       SUM=0.0
       DO 5 I=1,NTS
 5     SUM=SUM+TS(I)
       SUM=SUM/NTS
       DO 6 I=1,NTS
 6     TS(I)=TS(I)-SUM
       CALL KOSBEL(TS,NTS,NTS/50)
       NZERO=(N-NTS)/2
       DO 9 I=1,N
       TS1(I)=0.0
       INZERO=NZERO+NTS
       IF(I.GT.NZERO.AND.I.LT.INZERO) TS1(I)=TS(I-NZERO)
 9     CONTINUE
       RETURN
       END
END OF FILE
```

```
        SUBROUTINE ROTATE(WE,SN,NN,AZIM)
C
C       WRITTEN BY CECILIO J. REBOLLAR SUMMER 1979
C
C       THIS SUBROUTINE ROTATE EW AND NS COMPONENTS IN ORDER
C       TO GET THE RADIAL SND TRANSVERSE COMPONENTS OF THE
C                     SEISMOGRAM
C       WE=RADIAL COMPONENT   SN=TRANSVERSE COMPONENT
C                AS THE OUTPUT
C
      REAL*4 WE(8000),SN(8000),AZ
      REAL SAZ,CAZ
      CONV=57.295779
      SAZ=SIN(AZIM/CONV)
      CAZ=COS(AZIM/CONV)
      DO 1 I=1,NN
      WE(I)=WE(I)*SAZ+SN(I)*CAZ
      SN(I)=SN(I)*SAZ-WE(I)*CAZ
 1    CONTINUE
      RETURN
      END
END OF FILE
```

```
      SUBROUTINE KOSBEL(TS,NI,M)
C     WRITTEN BY CECILIO J. REBOLLAR SUMMER 1979
C
C SMOOTH THE SIGNAL WITH A COSBELL (SEE KANASEWICH BOOK)
C
      REAL TS(512),PI/3.14159/
      LPM=NI/2
      IF(2*LPM.NE.NI) GO TO 2
      GO TO 3
 2    NI=NI+1
      TS(NI)=0.0
      LPM=NI/2
 3    L=LPM-M
      DO 1 I=1,NI
      CBEL=1.0
      NN=I-LPM
      IF(I.LE.M) CBEL=(1.+COS(PI*(NN+L)/M))/2
      IF(I.GT.2*L+M) CBEL=(1.+COS(PI*(NN-L)/M))/2
 1    TS(I)=TS(I)*CBEL
      RETURN
      END
END OF FILE
```

```
C  FAST FOURIER TRANSFORM SEE CLEARBOUT BOOK PAGE 12
C
      CALL FORK(M,C,1.)
      MM=M/2
      C(M+1)=C(1)
      DO 301 I=2,MM
      AR(I)=REAL(C(I))
      AI(I)=AIMAG(C(I))
      AMPOUT(I)=SQRT(AR(I)*AR(I)+AI(I)*AI(I))
  301 CONTINUE
      DO 401 I=2,MM
      V=AMAGN(FF(I))
      ATENUA=EXP((PI*HDIS*FF(I))/(Q*VQ))
      AMP(I)=AMPOUT(I)*ATENUA
      AMPOUT(I)=(AMPOUT(I)*ATENUA)/V
  401 CONTINUE
      DO 501 I=2,MM
      AMPLOG(I)=ALOG10(AMPOUT(I))
 501  FFLOG(I)=ALOG10(FF(I))
      NUMM=MM-700
      NUMM=NUMM-20
      NUMMM=NUMM-10
      WRITE(9,12) NUMMM
      WRITE(9,101) (FFLOG(I),AMPLOG(I),I=10,NUMM)
      WRITE(11,12) NUMMM
      WRITE(11,101) (FF(I),AMP(I),I=10,NUMM)
      WRITE(12,12) NUMMM
      WRITE(12,101) (FF(I),AMPOUT(I),I=10,NUMM)
  100 FORMAT(1X,10I10)
  84  STOP
      END
END OF FILE
```

```
      SUBROUTINE GETSAM(N,NBCS,ISAM,A)
C
C   THIS SUBROUTINE DECOD THE MAGNETICS TAPES OF RESMAC
C        WRITEN BY CECILIO J. REBOLLAR
C
      INTEGER SHFTR,SHFTL,ALL,IL,IR,IMA,IMAN,IEXP,LNUM
      INTEGER*2 IS(512),IE(40000)
      REAL ISAM(40000),A(10000)
      INTEGER*2 LX
      INTEGER ISUB,N
      ISUB=0
      DO 3 I=1,NBCX
      CALL READ(IS,LX,0,LNUM,8)
      DO 2 J=1,256
      ISUB=ISUB+1
      IE(ISUB)=IS(J)
    2 CONTINUE
    3 CONTINUE
      DO 1 I=1,N
      ALL=IE(I)
      IL=SHFTL(ALL,16)
      IL=SHFTR(IL,24)
      IR=SHFTL(ALL,24)
      IR=SHFTR(IR,24)
      IR=SHFTL(IR,8)
      IMA=IL+IR
      IMAN=IMA/4
      IEXP=SHFTL(IMA,30)
      IEXP=SHFTR(IEXP,30)
      ISAM(I)=(IMAN-2048)*4**IEXP
      A(I)=I
    1 CONTINUE
      RETURN
      END
END OF FILE
```

```
      FUNCTION AMAGN(FRE)
C
C THIS SUBROUTINE CALCULATE THE INTRUMENT RESPONCE OF
C    CERRILLO STATION THE AUTPUT IS IN COUNTS/CM
C       WRITEN BY CECILIO J REBOLLAR
C
      REAL PI/3.141592654/
      AMP=2.52E+13
      W=2*PI*FRE
      WF=2*PI*10.0
      HF=0.707
      HO=0.7
      WO=2*PI*1.
      TEM=((WF**2-W**2)**2-(2*HF*WF*W)**2)**2
      TEM=TEM+(4.*(WF**2-W**2)**2*(2*HF*WF*W)**2)
      TEM=(W**3)*SQRT(TEM)
      TEMO=SQRT((WO**2-W**2)**2+(2*HO*WO*W)**2)
      TEMO=TEMO*(((WF**2-W**2)**2+(2*HF*WF*W)**2)**2)
      AMAGN=(AMP*TEM)/TEMO
      RETURN
      END
END OF FILE
```